Dissertation

Solvent Motion in Quaternary Reverse Micelles

Submitted by

Elizabeth M. Corbeil

Department of Chemistry

In partial fulfillment of the requirements

For the degree of Doctor of Philosophy

Colorado State University

Fort Collins, Colorado

Summer 2004

COLORADO STATE UNIVERSITY

March 31, 2003

WE HEREBY RECOMMEND THAT THE DISSERTATION PREPARED UNDER OUR SUPERVISION BY ELIZABETH M. CORBEIL ENTITLED **SOLVENT MOTION IN QUATERNARY REVERSE MICELLES** BE ACCEPTED AS FULFILLING IN PART REQUIREMENTS FOR THE DEGREE OF DOCTOR OF PHILOSOPHY.

Committee on Graduate Work

Advisor

Department Head

Abstract of Dissertation

Solvent Motion in Quaternary Reverse Micelles

The solvation response in CTAB and SDS reverse micelles has been investigated via ultrafast time-resolved fluorescence spectroscopy. These measurements represent the first determination of solvation reorganization on the subpicsecond timescale in quaternary micellar systems. These experiments provide insight on the solvent motion in quaternary reverse micelles and are compared to bulk water relaxation on a femtosecond timescale.

The solvent response in CTAB and SDS reverse micelles was measured as a function of hydration. Solvent reorganization was found to be independent of hydration. In all of the systems investigated, two solvent relaxation components are observed, specifically an inertial component on the femtosecond timescale as well as a diffusive component on the order of hundreds of picoseconds. These relaxation components were attributed to collective motion of the interface.

To explore the role of the cosurfactant, we explored solvent motion in ternary and quaternary AOT reverse micelles. The addition of alkanol significantly slows down solvent motion in the micellar systems. The solvent response in quaternary AOT

reverse micelles also had a diffusive component that was similar to that found in CTAB and SDS reverse micelles.

Elizabeth M. Corbeil
Department of Chemistry
Colorado State University
Fort Collins, Colorado 80523
Summer 2004

Acknowledgements

I would like to thank my brother, Dave, for letting me live with him, eat all his food, clean his house, cook for him, grocery shop for him, and pet his dog, Farer. It was a true honor that I hope never to repeat except of course petting Farer. I would like to thank Steven for providing an interesting outlook on life and providing amusing stories that made me laugh. Thank you to all of my friends for keeping me sane. Finally, I would also like to thank my parents for supporting me during this time and all the time it took to get here. I love you Mom and Dad!

Table of Contents

List of Figures

List of Tables

Chapter 1

Introduction

I. Microemulsions.

A. Introduction. Aggressively shaking oil and water results in a cloudy mixture that will eventually separate into two distinct phases. By adding a surfactant to the system, the interfacial tension between the oil and water phases will decrease, enabling the water and oil to be dispersed in each other. Depending on the proportions of each of the components either water-in-oil, w/o, or oil-in-water, o/w, microemulsions are formed as shown in Fig. 1.1.[1-5] These microemulsions can remain stable for a considerable length of time, are homogeneous, optically isotropic, and have a low viscosity.

The spontaneous nature of microemulsion formation indicates that the free energy change of formation is negative in accordance with the thermodynamic requirement:

$$-\Delta G = \gamma_{o/w} \Delta A \qquad (1.1)$$

where $\gamma_{o/w}$ is the interfacial tension between the oil and water phases and ΔA is the change in surface area due to microemulsion formation.[2] The interfacial tension between the

(a)

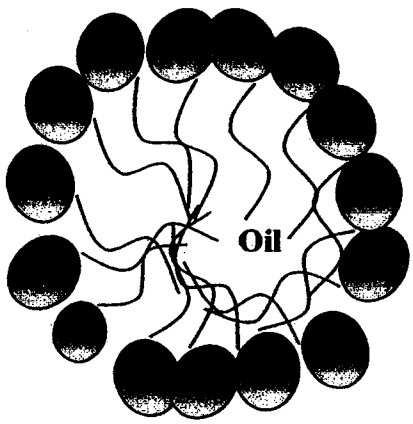

(b)

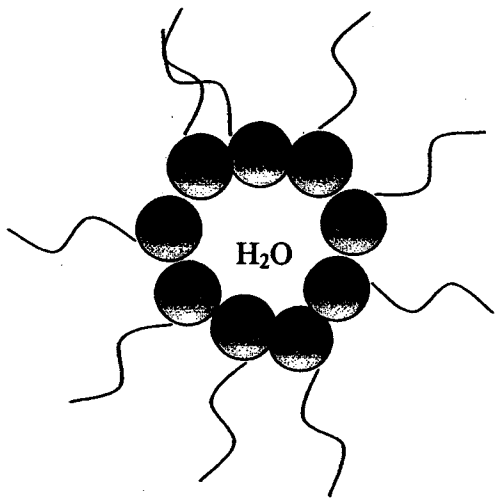

Figure 1.1. Schematic of (a) micelle and (b) reverse micelle.

phases decreases with the formation of microemulsions and thermodynamically stable w/o or o/w dispersions are created.

Four distinct systems can be created as described by Winsor by changing the proportions of the oil, surfactant, and water as well as the temperature of the system.[6] Winsor type I depicts a system that has two distinct phases: a microemulsion phase in equilibrium with an oil phase. Winsor type II describes a microemulsion phase in equilibrium with a water phase. Winsor type III systems have three phases: water, oil, and microemulsions all in equilibrium with each other. Finally, Winsor type IV systems consist of a system where oil, water and surfactant are homogeneously mixed.

There are three primary reasons to study microemulsions. First, microemulsions have enormous solubilizing power for oil or water.[7] Thus, it is possible to prepare microemuslions made of 45% oil, 45% water, and 10% surfactant. This is important for environmental remediation applications: a mixture of 10% surfactant and 45% water should have the capability of solubilizing 45% oil. This would be useful in cleaning up oil spills. Secondly, the interfacial tensions measured between water saturated microemuslions and excess water is extremely low, 10^{-4} mN/m.[8] The third reason is that microemulsions constitute a new

liquid phase with original properties. This has attracted many liquid state theoreticians and experimentalists.

B. Reverse Micelles. Reverse micelles are a specific type of microemulsion. In these self-assembled structures, the polar head group of the surfactant molecule points inward while the nonpolar surfactant tails point out into the oil phase.[1-5,9,10] Experimental studies such as dynamic light scattering, small angle neutron scattering, small angle X-ray scattering, cryo-transmission electron microscopy, fluorescence spectroscopy, NMR, and viscosity have all been used to characterize both the water pool in reverse micelles as well as the interface of reverse micelles.[11-18]

Although double chained surfactants such as aerosol-OT (AOT) are able to form ternary reverse micelles, single chain surfactants such as cetyltrimethyl ammonium bromide (CTAB, Figure 1.2) and sodium dodecyl sulfate (SDS, Figure 1.2) both form reverse micelles with the aid of a cosurfactant such as alkanol.[19-30] As shown in Fig 1.3, the cosurfactant intercalates between the surfactant headgroups thus minimizing the repulsive forces between the polar headgroups. This allows the formation of reverse micelles.

Several studies have been done to investigate the addition of alkanol to reverse micelles. Most of these studies focus on the effect of increasing the alkanol chain length on water droplet size,

(a)

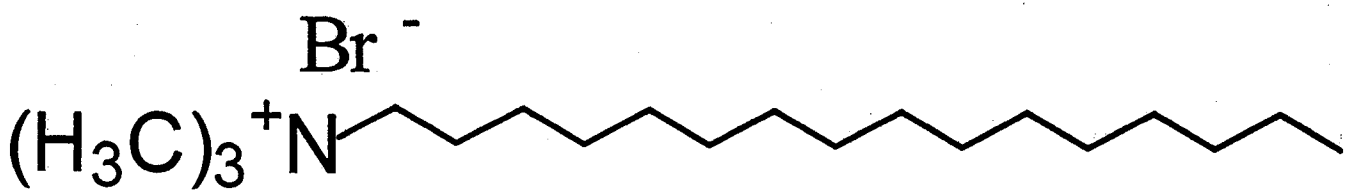

(b)

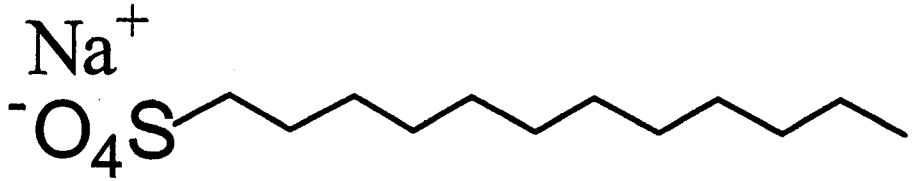

Figure 1.2. Structures of (a) CTAB and (b) SDS.

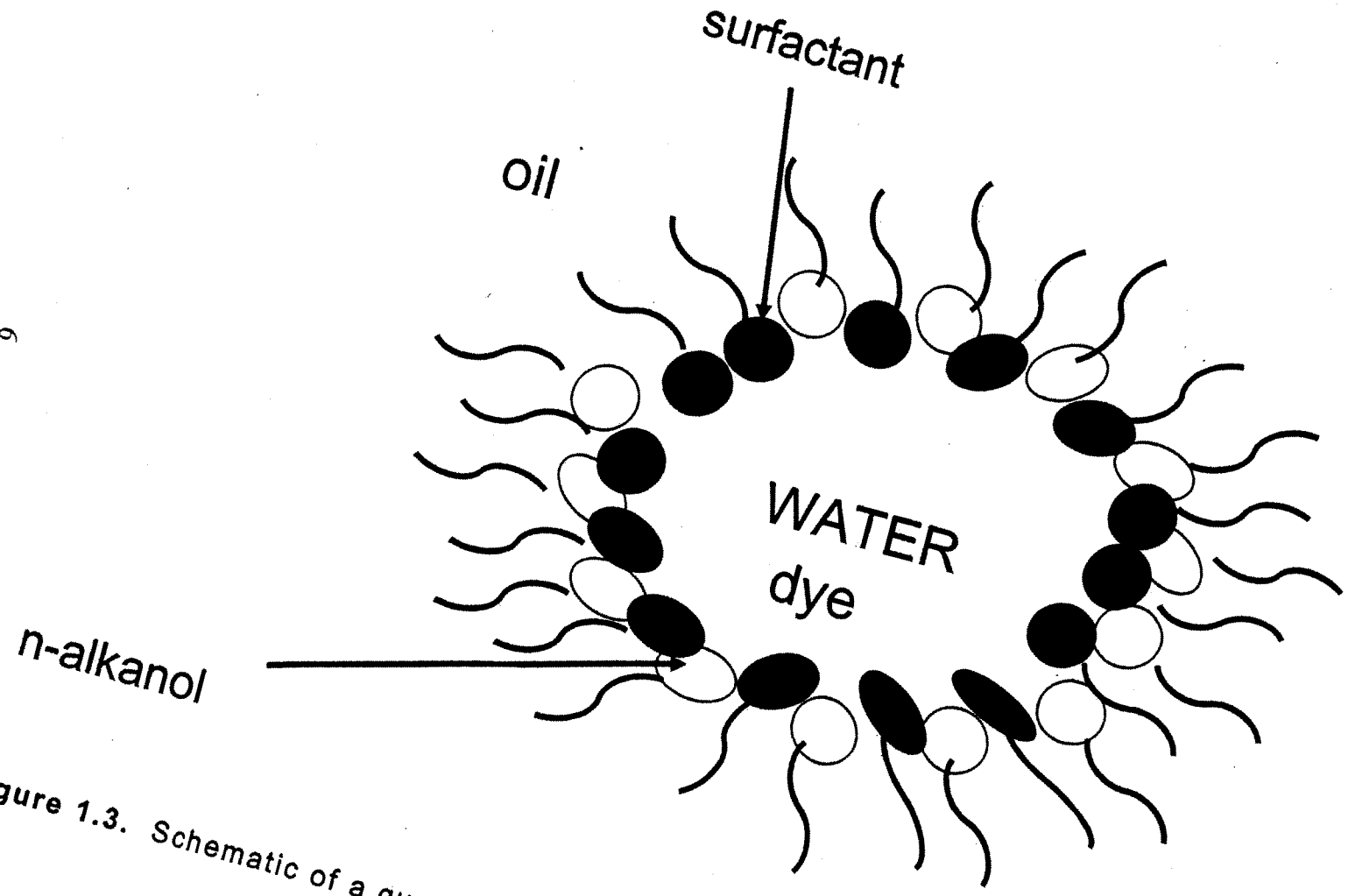

Figure 1.3. Schematic of a quaternary reverse micelle.

dynamics of droplet collisions with exchange, microemulsion electrical conductivity, and water solubility in reverse micelles.[31-38] These studies have shown that there is dependence between chain length and the interfacial properties found in reverse micelles. For short chain alkanols there is an increase in the fluidity of the interface thus allowing faster reactions at the interface as well as allowing the reverse micelle to solubilize more water. As the alkanol chain length increased, studies found an increase of alkanol at the interface thus creating a more rigid interface. Although all of these studies have investigated the microviscosity at the interface, no studies have investigated solvent motion at the interface.

C. Microenvironment in Reverse Micelles. Compared to bulk solvents, reverse micelles have unique properties due to the existence of different microenvironments found in reverse micelles.[31,36,37,39-51] Water found in reverse micelles has shown reduced activity, reduced polarity, and reduced translational diffusion in comparison to bulk water.[1,7,13,17,18,52-55] Furthermore, ^{1}H NMR has shown two or three distinguishable types of water in reverse micelles.[12,17] These are water bound to the headgroups, water bound to the hydrated ionic groups and bulk-like water. IR studies done by Liveri et al. have also shown these three types of water.[18] Theoretical calculations have also shown that there are

three distinct types of water in reverse micelles as shown in Fig. 1.4 (figure created by J. Faeder).[56] Faeder and Ladanyi also discovered that by increasing the size of the reverse micelle, the relative amounts of water in each region also increased.

Dynamical measurements have also been used to probe the microenvironment of solute molecules in reverse micelles.[25,27,57-60] these studies have all shown that micellar water is more restricted than bulk water. Hasegawa et al. measured the microviscosity inside AOT reverse micelles.[42] Their results indicated that the microviscosities remained independent of w_0 when w_0>10. Altamirano et al.. investigated the fluorescence quenching of pyrene derivatives in AOT reverse micelles.[61] They found that the fluorescence quenching increased as w_0 increased for probes located in the water pool, whereas fluorescence quenching at the interface was much lower than that of water. This was attributed to the high microviscosity of the interface. Sarker et al.. measured nanosecond components of the water solvation motion.[62] These results indicated that water in AOT reverse micelles moves more slowly than bulk water. However, the time resolution of these studies did not allow them to observe motion that occurs on the picosecond or sub-picosecond timescale.

Time resolved fluorescence studies have also shown that motion in reverse micelles is restricted compared to bulk solvent

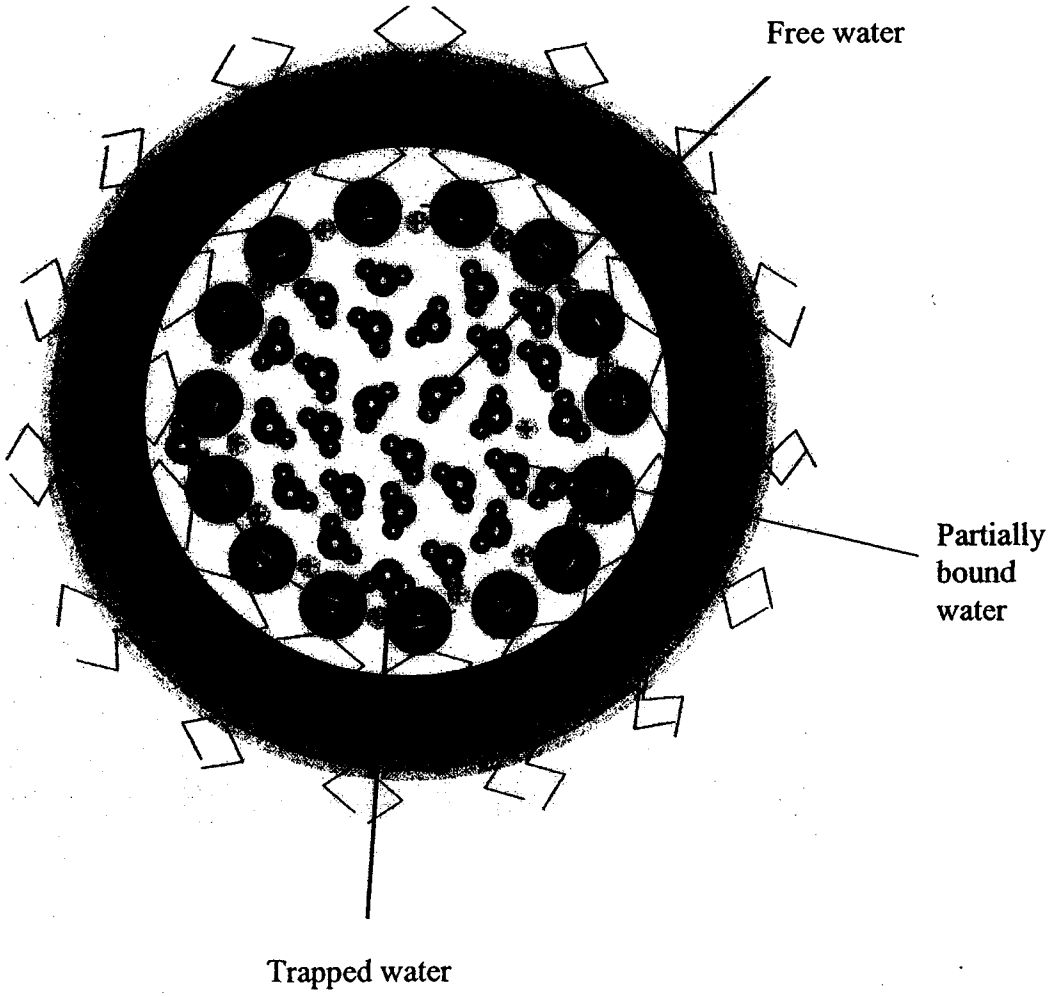

Figure 1.4. Types of water in reverse micelles (figure created by J. Faeder).[56]

motion. Specifically, in AOT reverse micelles, solvent motion has been investigated as a function of hydration, counterion interactions.[63,64] These studies determined that solvent motion increased as the concentration of water increased. Also, the solvent motion in AOT microemuslions is affected by the counterion. AOT reverse micelles solubilizing formamide rather than water have also shown restricted motion compared to bulk motion in formamide.[65] Solvent motion in nonionic reverse micelles has also been investigated. In studies with Brij-30/cyclohexane and Triton X-100/cyclohexane reverse micelles the polar solvation dynamics are slower and show additional slow relaxation modes not observed in bulk water.[66] Finally, polar solvation dynamics in lecithin reverse micelles as well as at the interface of lecithin reverse micelles has been investigated.[50,48] These studies once again showed that the solvent response in restricted environments is slower than bulk solvent.

D. Applications. Both micelles and reverse micelles have numerous applications in everyday life. People use microemulsions to wash their hair, brush their teeth and clean their clothes. They also depend on microemulsions to lubricate moving parts in vehicles. Industry relies on microemulsions for numerous applications. In the oil industry they are used for tertiary oil recovery, improved fuel burning and decrease of

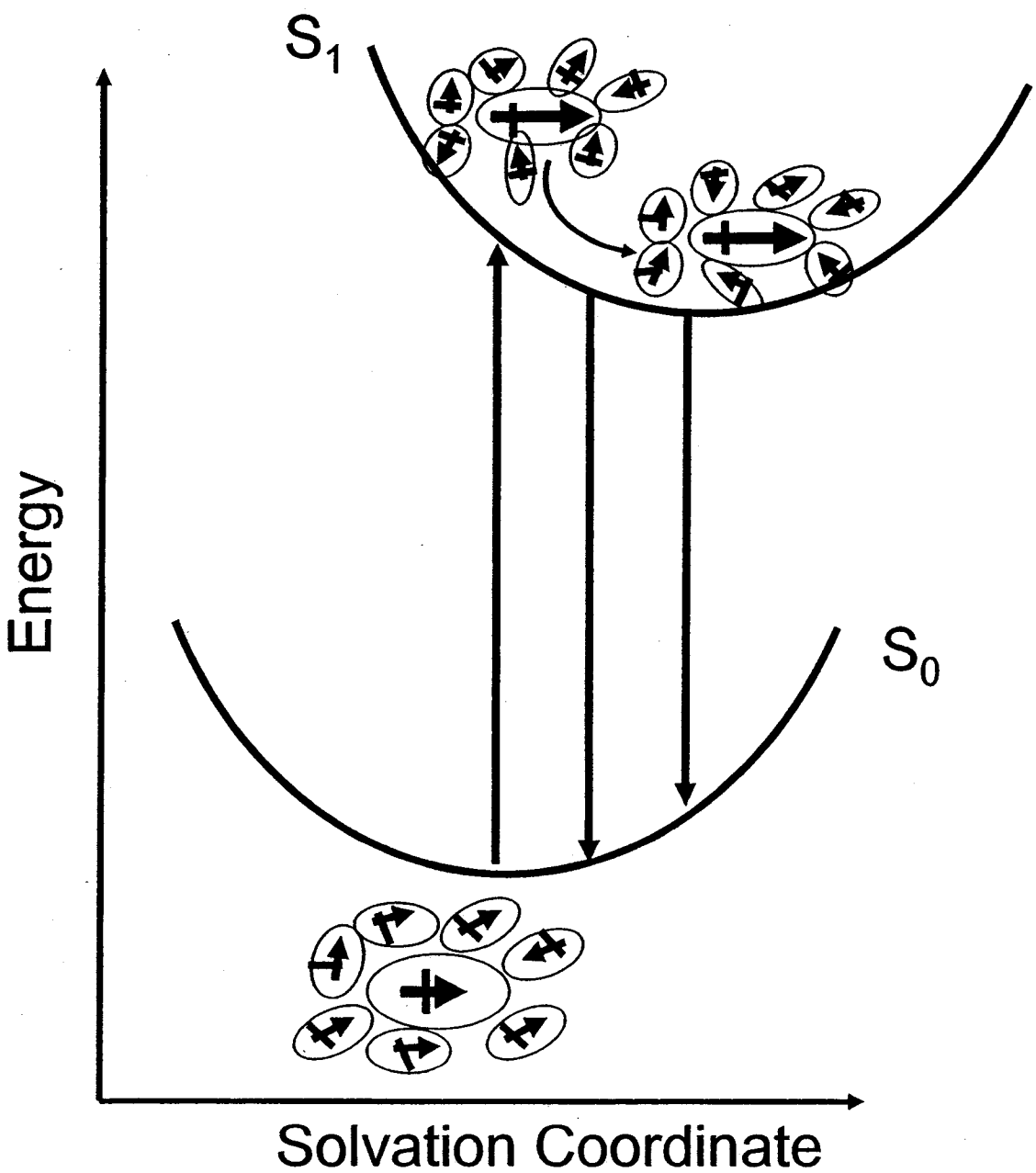

Figure 1.5. Schematic of time dependent fluorescence.

pollution, and for petrochemistry. In the textile industry, microemulsions are used for detergency, fabric dyeing, and fabric surface treatment. In the metal industry they are used for lubrication, surface coating and cleaning, preparation of metal catalysts. Microemuslions are used in the chemical industry for polymerization, photochemistry, and chemical reactivity control. The pharmaceutical industry uses microemulsions for drug solubilization as well as artificial blood

II. Polar Solvation Dynamics.

Polar solvation dynamics investigates the question of what happens to a solvent molecule when the solute molecule undergoes a change in its electronic configuration.[67,68] There are several possible ways this process can occur. For example, a charge can be created on a previously neutral solute, the magnitude of the dipole can change, or the direction of the dipole can change.[68] We will consider an increase of the dipole moment on a solute molecule. Optical excitation of an equilibrated ground state probe produces a nonequilibrium configuration of the solvent molecules about the excited state probe as shown in Fig. 1.5. The solvent molecules will reorganize to this change in energy thus lowering the free energy of the system. The relaxation of the probe is accompanied by time-dependent fluorescence spectral shifts towards lower frequencies, which can be analyzed to

quantify the dynamics of solvation via the solvent response function (SRF):

$$C(t) = \frac{\nu(t) - \nu(\infty)}{\nu(0) - \nu(t)}. \qquad (1.2)$$

Here, $\nu(0)$, $\nu(t)$, and $\nu(\infty)$ represent the frequency of the intensity maximum of the fluorescence spectrum immediately after excitation, at some time t after excitation and at a time sufficiently long enough to ensure that the excited state solvent configuration is in equilibrium.

The molecular dynamics exhibited in the SRF reflect the different motions that are required to produce the final polarized environment of the solute from the ground state configuration of the solvent surrounding the solute.[68] The polarization of the final state can be divided into several degrees of freedom, each of which occurs on a different time scale. First, the solvent's electronic degrees of freedom become polarized in the presence of the ionic field. This response is instantaneous with respect to experimental observation. The second type of motion is nuclear distortion, which occurs on the vibrational time scale (10^{-15} seconds) and has a small contribution to the overall polarization. Rotational motion of the solvent molecules has a large contribution to the overall polarization of the sample. Rotational dynamics can be broken down into two different types: large amplitude rotations that are diffusive in nature which occur on the

picosecond time scale, and faster, small amplitude non-diffusive motion such as librational modes. This type of motion occurs on the femtosecond time scale. The final type of motion that largely contributes to the overall polarization is translational motion. Translational motion is broken down into diffusive motion that occurs in the picosecond regime and non-diffusive motion that occurs in the femtosecond regime.

III. Goals.

While there is an enormous amount of information about the microenvironment in quaternary reverse micelles[47,61,69-74], relatively little is known about the solvent motion in these systems. NMR and time-resolved fluorescence quenching studies with the time resolution of several picoseconds have investigated solvent motion in both the water pool and interface.[24,31,75] In the following chapters, we will explore solvation dynamics in quaternary reverse micelles using time resolved fluorescence upconversion.

In this work we explored several different aspects of quaternary reverse micelles. First, we explored the role water loading has on solvent reorganization in quaternary reverse micelles. The effects of cationic and anionic surfactants were also investigated in Chapter 3. To fully understand the role of

alkanol, the solvent motion in ternary and quaternary AOT micellar systems was also investigated.

The ultimate goal of our research is to provide a better understanding of solvent motion in quaternary reverse micelles. This will lead to better understanding of reactions that occur in these reverse micelles as well as at the interface of these reverse micelles. Many new techniques such as nanoparticles synthesis, environmental cleanup, electron transfer processes, and separation science utilize quaternary reverse micelles.[19-21,76-78] Therefore, the motion of water in quaternary reverse micelles will play a role in numerous branches of science. The importance of this is far reaching. Since reverse micelles are used in numerous aspects of industry from microreactors to part lubrication it is important to fully understand the microenvironment in reverse micelles.

References:

(1)Paul, B. K.; Moulik, S. P. *Journal of Dispersion Science and Technology* **1997**, *18*, 301-367.

(2)Zana, R. *Heterogeneous Chemistry Reviews* **1994**, *1*, 145-157.

(3)*Microemulsion Systems*; Marcel Dekker: New York, 1987.

(4)*Surfactants in Solution*; Plenum: New York, 1987.

(5)*Physics of Complex and Supermolecular Fluids*; Wiley Interscience: New York, 1987.

(6)Winsor, P. A. *Transition Faraday Society* **1948**, *44*, 376.

(7)Shinoda, K.; Kunieda, H.; Arai, T.; Saijo, H. *Journal of Physical Chemistry* **1984**, *88*, 5126.

(8)Chan, K. S.; Shah, D. O. *Journal of Dispersion Science and Technology* **1980**, *1*, 55.

(9)De Gennes, P. G.; Taupin, C. J. *Journal of Physical Chemistry* **1982**, *86*, 2294.

(10)Luisi, P. L.; Giomini, M.; Pileni, M. P.; Robinson, B. H. *Biochem Biophysica Acta* **1988**, *947*, 209.

(11)Fletcher, P. D. I.; Robinson, B. H.; Tabony, J. J. *Journal of the Chemical Society Faraday Transactions* **1986**, *82*, 2311.

(12)Kawai, T.; Hamada, K.; Shinoda, K.; Kon-no, K. *Bulletin of the Chemical Society of Japan* **1992**, *65*, 2715.

(13)Fulton, J. L. *Journal of Physical Chemistry* **1991**, *85*, 458.

(14)Belletete, M.; Durocher, G. *Journal of Colloid and Interface Science* **1990**, *134*, 289.

(15)Hauser, H.; Haering, G.; Pande, A.; Luisi, P. L. *Journal of Physical Chemistry* **1989**, *93*, 7869.

(16)Giammona, G.; Goffredi, F. *Journal of Colloid and Interface Science* **1992**, *154*, 411.

(17)Jain, T. K.; Varshney, M.; Maitra, A. N. *Journal of Physical Chemistry* **1989**, *93*, 7409.

(18)Aliotta, E.; Migliardo, P.; Donato, D. I.; Liveri, V. T.; Bardez, E.; Larrey, B. *Progress in Colloid and Polymer Science* **1992**, *89*, 1.

(19)Adhikari, S.; Joshi, R.; Gopinathan, C. *Journal of Colloid and Interface Science* **1997**, *191*, 268-271.

(20)Cuccovia, I. M.; Dias, L. G.; Maximiano, F. A.; Chaimovich, H. *Langmuir* **2001**, *17*, 1060-1068.

(21)Curri, M. L.; Agostiano, A.; Manna, L.; Monica, M. D.; Catalano, M.; Chiavarone, L.; Spagnolo, V.; Lugara, M. *Journal of Physical Chemistry B* **2000**, *104*, 8391-8397.

(22)Das, P. K.; Srilakshmi, G. V.; Chaudhuri, A. *Langmuir* **1999**, *15*, 981-987.

(23)Das, P. K.; Chaudhuri, A. *Langmuir* **2000**, *16*, 76-80.

(24)El Seoud, O. A. *Journal of Molecular Liquid* **1997**, *72*, 85-103.

(25)Lu, Q.; Chen, H.; Li, K.; Shi, Y. *Biochemical Engineering Journal* **1998**, *1*, 45-52.

(26)Luisi, P. L.; Straub, B. E., Eds. *Reverse Micelles: Biological and Technological Relevance of Amphiphilic Structures in Apolar Media*; Plenum Press: New York, 1984.

(27)Marhuenda-Egea, F. C.; Piera-Velazquez, S.; Cadenas, C.; Cadenas, E. *Biocatalysis and Biotransformation* **2000**, *18*, 201-222.

(28)Rodenas, E.; Perez-Benito, E. *Journal of Physical Chemistry* **1991**, *95*, 4552-4556.

(29)Rodgers, M. A. J. *Journal of Physical Chemistry* **1981**, *85*, 3372-3374.

(30)Sengupta, B.; Guharay, J.; Sengupta, P. K. *Spectrochimica Acta, Part A* **2000**, *56A*, 1433-1441.

(31)Bellocq, A. M.; Biaia, J.; Clin, B.; Lalanne, P.; Lemanceau, B. *Journal of Colloid and Interface Science* **1979**, *70*, 524-536.

(32)Colafemmina, G.; Palazzo, G.; Balestrieri, E.; Giomini, M.; Ceglie, A. *Progress in Colloid and Polymer Science* **1997**, *105*, 281-289.

(33)Digout, L. G.; Bren, K.; Palepu, R.; Moulik, S. P. *Colloid Polymer Science* **2001**, *279*, 655-663.

(34)Lang, J.; Lalem, N.; Zana, R. *Journal of Physical Chemistry* **1991**, *95*, 9533-9541.

(35)Li, X.; Lin, E.; Zhao, G.; Xiao, T. *Journal of Colloid and Interface Science* **1996**, *184*, 20-30.

(36)Sergeyev, V. G.; Mikhailenko, S. V.; Pyshkina, O. A.; Yaninsky, I. V.; Yoshikawa, K. *Journal of the American Chemical Society* **1999**, *121*, 1780-1785.

(37)Wang, W.; Weber, M. E.; Vera, J. H. *Journal of Colloid and Interface Science* **1994**, *168*, 422-427.

(38)Yao, J.; Romsted, L. S. *Colloid and Surfaces* **1997**, *123-124*, 89-105.

(39)Kegel, W. K.; Lekkerkerker, H. N. W. *Colloid and Surfaces A: Physicochemical and Engineering Aspects* **1993**, *76*, 241-248.

(40)Rabie, H. R.; Vera, J. H. *Langmuir* **1996**, *12*, 3580-3584.

(41)Hasegawa, M.; Sugimura, T.; Shindo, Y.; Kitahara, A. *Colloid Surfuces A- Physicochemical Engineering Aspects* **1996**, *109*, 305-318.

(42)Hasegawa, R.; Sugimura, T.; Suzaki, Y.; Shindo, Y.; Kitahara, A. *Journal of Physical Chemistry* **1994**, *98*, 2120-2124.

(43)Pant, D.; Levinger, N. E. *Journal of Physical Chemistry B* **1999**, *103*, 7846-7852.

(44)Pant, D.; Levinger, N. E. *Langmuir* **2000**, *16*, 10123-10130.

(45)Nazario, L. M. M.; Crespo, J.; Holzwarth, J. F.; Hatton, T. A. *Langmuir* **2000**, *16*, 5892-5899.

(46)Ray, S.; Moulik, S. P.*Journal of Colloid and Interface Science* **1995**, *173*, 28-33.

(47)Silber, J. J.; Biasutti, A.; Abuin, E.; Lissi, E. *Advances in Colloid and Interface Science* **1999**, *82*, 189-252.

(48)Willard, D. M.; Levinger, N. E. *Journal of Physical Chemistry B* **2000**, *104*, 11075-11080.

(49)Willard, D. M.; Levinger, N. E. *Biophysical Journal* **2000**, *submitted*.

(50)Willard, D. M.; Riter, R. E.; Levinger, N. E. *Journal of the American Chemical Society* **1998**, *120*, 4151-4160.

(51)Ueda, M.; Kimura, A.; Wakida, T.; Yoshimura, Y.; Schelly, Z. A. *Journal of Colloid and Interface Science* **1994**, *163*, 515-516.

(52)Fletcher, P. D. I.; Robinson, B. H. *Journal of the Chemical Society Faraday Transactions* **1984**, *80*, 2417.

(53)Lo'pez-Quintela, M. A.; Cassado, J. *Journal of Themal Biology* **1989**, *139*, 129.

(54)O'Connor, C. J.; Lomax, T. D.; Ramage, R. E. *Advanced Colloid and Interface Science* **1984**, *20*, 21.

(55)Thomas, J. K. *Chemical Reviews* **1980**, *80*, 285.

(56)Faeder, J.; Ladanyi, B. M. *Journal of Physical Chemistry B* **2000**, *104*, 1033-1046.

(57)Fan, K.-K.; Ouyang, P.; Wu, X.; Lu, Z. *Journal of Chemical Technology and Biotechnology* **2001**, *76*, 27-34.

(58)Garcia-Rio, L.; Leis, J. R.; Reigosa, C. *Journal of Physical Chemistry B* **1997**, *101*, 5514-5520.

(59)Lin, J.; Zhou, W. L.; O'Connor, C. J. *Clusters Nanostruct. Interfaces, [Proc. Int. Symp.]* **2000**, 405-410.

(60)Liou, J.-Y.; Huang, T.-M.; Chang, G.-G. *Journal of the Chemical Society, Perkins Transactions 2* **1999**, 2171-2176.

(61)Altamirano, M. S.; Borsarelli, C. D.; Cosa, J. J.; Previtali, C. M. *Journal of Colloid and Interface Science* **1998**, *205*, 390-396.

(62)Sarkar, N.; Das, K.; Datta, A.; Das, S.; Bhattacharyya, K. *Journal of Physical Chemistry* **1996**, *100*, 10523.

(63)Pant, D.; Riter, R. E.; Levinger, N. E. *Journal of Chemical Physics* **1998**, *109*, 9995-10003.

(64)Riter, R. E.; Undiks, E. P.; Levinger, N. E. *Journal of the American Chemical Society* **1998**, *120*, 6062-6067.

(65)Riter, R. E.; Undiks, E. P.; Kimmel, J. R.; Levinger, N. E. *Journal of Physical Chemistry B.* **1998**, *102*, 7931-7938.

(66)Pant, D.; Levinger, N. E. *Langmuir* **2000**, *16*, 10123-10130.

(67)Maroncelli, M.; MacInnis, J.; Flemming, G. R. *Science* **1989**, *243*, 1674.

(68)Barbara, P. F.; Jarzeba, W. In *Advances in Photochemistry*; Vo'man, D. H. H., George S.; Gollnick, Klaus, Ed.; John Wiley and Sons, Inc., 1990; Vol. 15.

(69)Akhter, M. S.; Al-Alawi, S., M. *Colloids and Surfaces A* **2000**, *164*, 247-255.

(70)Antalek, B.; Williams, A. J.; Texter, J.; Feldman, Y.; Garti, N. *Colloid Surfaces A-Physicochemical Engineering Aspects* **1997**, *128*, 1-11.

(71)Browne, E. P.; Hatton, T. A. *NASA Conference Publishing* **1996**, *3338*, 667-672.

(72)Chiang, C. L. *Biotechnology Techniques* **1999**, *13*, 453-457.

(73)Freeman, K. S.; Tan, N. C. B.; Trevino, S. F.; Kline, S.; McGown, L. B.; Kiserow, D. J. *Langmuir* **2001**, *17*, 3912-3916.

(74)Garcia-Rio, L.; Herves, P.; Mejuto, J. C.; Perez-Juste, J.; Rodriguez-Dafonte, P. *Journal of Colloid and Interface Science* **2000**, *225*, 259-264.

(75)Abuin, E.; Lissl, E. *Journal of Physical Chemistry* **1983**, *87*, 5166-5172.

(76)Brichkin, S. B.; Razumov, V. F.; Spirin, M. G. *Colloid Journal* **2000**, *62*, 8-12.

(77)Carpenter, E. E.; Sangregorio, C.; O'Connor, C. J. *IEEE Transactions on Magnetics* **1999**, *35*, 3496-3498.

(78)Carpenter, E. E.; Kumbhar, A.; Wiemann, J. A.; Srikanth, H.; Wiggins, J.; Zhou, W.; O'Connor, C. *Journal of Material Science and Engineering, A* **2000**, *A286*, 81-86.

Chapter 2

Experimental Methods

Until recently, the time resolution available in fluorescence spectroscopy was not fast enough to observe solvation dynamics on the femtosecond time scale.[1-9] In order to observe solvation dynamics in liquids, the samples were either cooled so the observable dynamics were on the picosecond timescale, or solvation dynamics measurements were restricted to hydrogen bonded solvents.[10] With advances in ultrafast laser spectroscopy, specifically ultrafast time-resolved fluorescence upconversion, scientists have achieved the subpicosecond time resolution necessary to measure solvation dynamics in nonassociated liquids. Barbara et al. have measured the solvation dynamics in various liquids using several different Coumarin probes.[10] Maroncelli and coworkers have also investigated solvation dynamics in various liquids using Coumarin 153.[1-3]

I. Laser Spectroscopy

A. Time Resolved Fluorescence Upconversion. To determine the time shifting fluorescence, we have used fluorescence upconversion. The premise for fluorescence upconversion is to gate a long time process such as fluorescence with a short gate pulse. This results in a higher time resolution than would be obtained by just monitoring the fluorescence pulse. For our experiments, this involves using a femtosecond gate pulse to investigate the time dependence of the fluorescence spectrum at several different wavelengths (Figure 2.1).

The femtosecond fluorescence upconversion spectrometer is similar to the apparatus developed by Fleming et al. [11] A schematic of the apparatus is shown in Figure 2.2. A Ti:Sapphire oscillator (Clark, NJA-3) is pumped by all the lines of an argon ion laser (Coherent, Innova) at 5 W. The oscillator is passively mode locked resulting in 80 fs, 5 nJ pulses with a repetition rate of 100 MHz. The beam is collimated and focused onto a 0.5 mm barium borate crystal (BBO, Type I, Casix). The BBO crystal produces second harmonic light centered at ~400 nm. The frequency-doubled beam is separated from the fundamental beam using a dielectric beam splitter (CVI). The frequency doubled light is passed through a half wave plate (Meadowlark, 400 nm center wavelength), and focused onto a 1 mm path length flow cell (NSG,

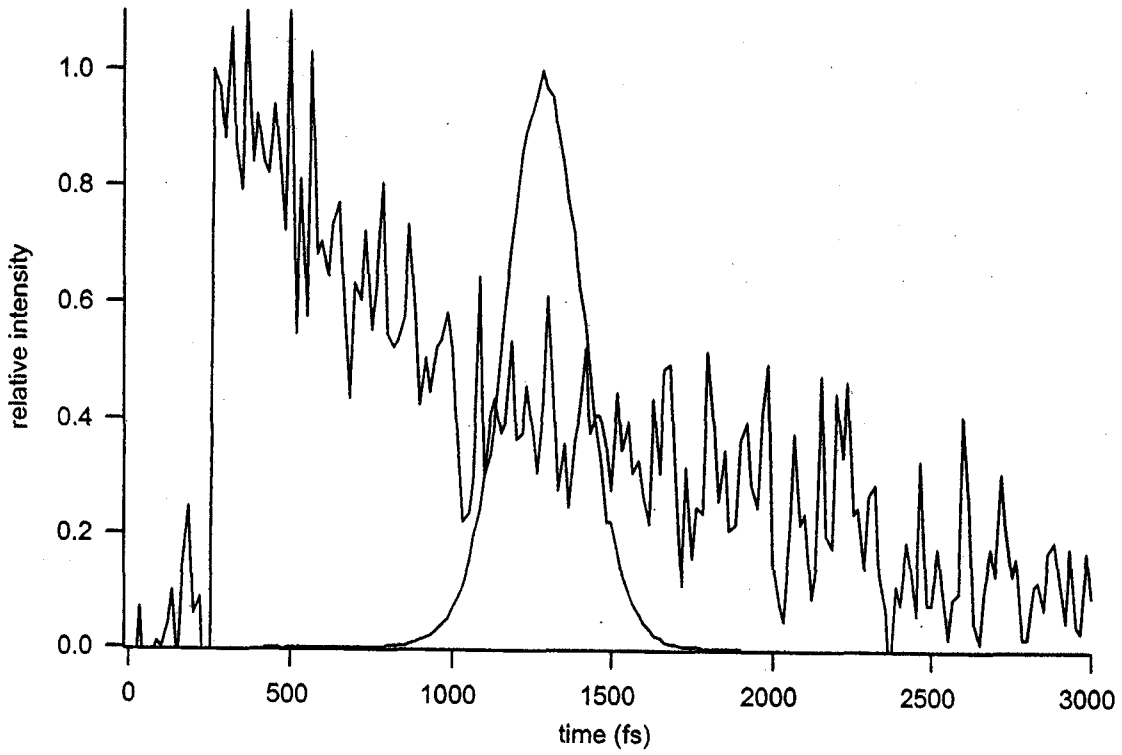

Figure 2.1. Time-resolved fluorescence transient at 440 nm with a short gate pulse.

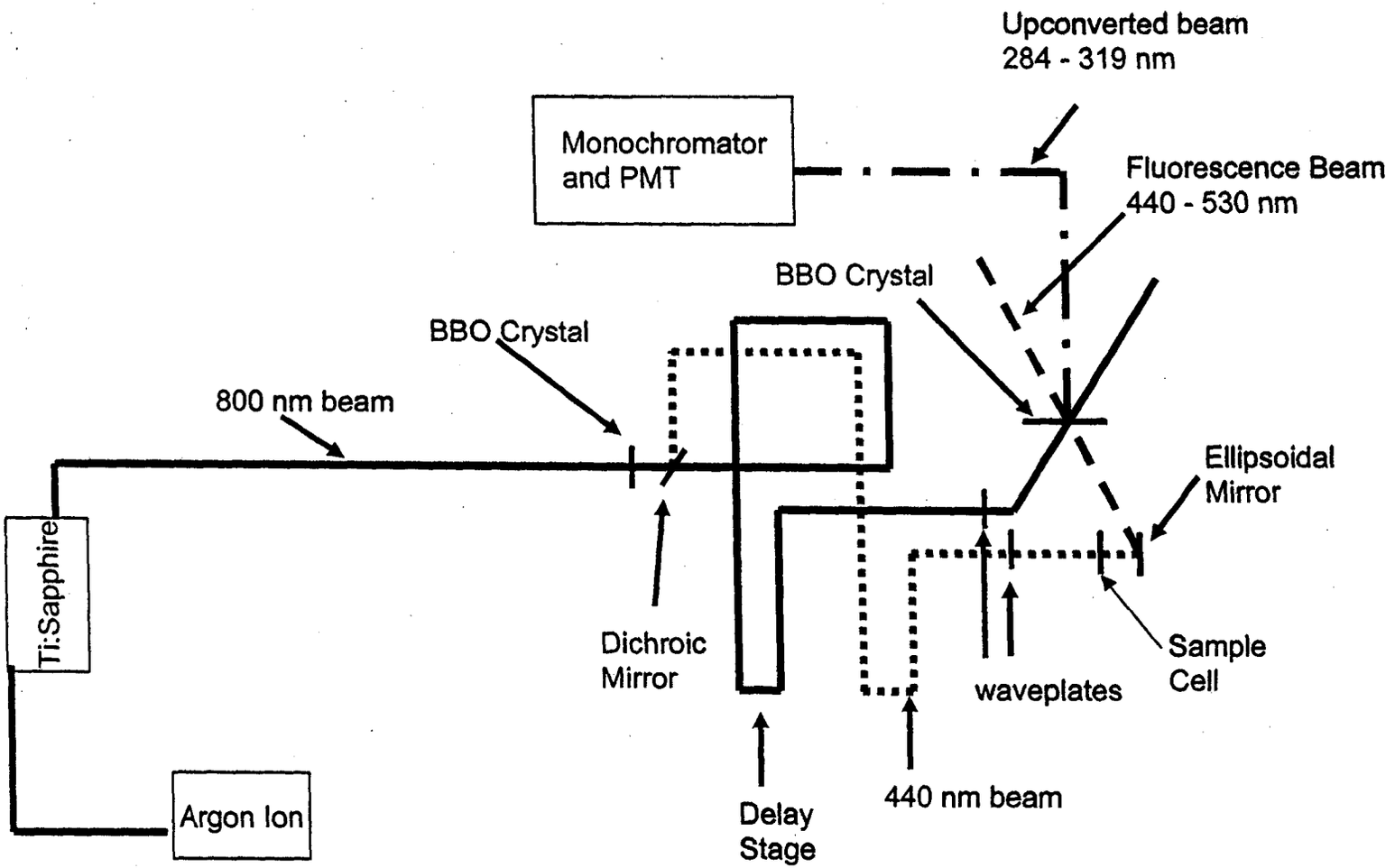

Figure 2.2. A schematic of the time-resolved fluorescence upconversion instrument.

Type 48, Code H). The sample is circulated through the flow cell using a peristaltic pump (Masterflex, Model 7553-70). A small portion of the fluorescence is collected at 180 degrees with respect to the excitation beam and focused onto a second 0.5 mm BBO crystal (Type I, Casix) using an ellipsoidal mirror. The fluorescence is upconverted with the fundamental pulses that is sent through an optical delay line utilizing a motor delay stage (American Precision, Parker-Daedl delay stage). All solvation dynamics measurements are made with the excitation beam at 54.7° with respect to the gate beam. The upconverted light is collimated by a 10 cm lens, isolated from the gate and frequency doubled beams with an iris and focused with a 12.8 cm lens through a UV- transmitting filter (340 nm, Opto-Sigma) into a 0.33 m single monochromator equipped with a 2400 grooves/mm grating blazed at 400 nm. The instrument response is determined from the cross correlation of the excitation and gate pulses in the BBO crystal. The upconverted photons are detected using a photomultiplier tube (Hamamatsu, R1527P) and sent to a single photon counter (Stanford Research Systems, SR400). A personal computer using LabVIEW (National Instruments) collects the photon counter signal as a function of the optical delay between the excitation and gate pulses.

The solvent response in quaternary AOT reverse micelles and the solvent response in CTAB reverse micelles made with varying chain length alkanols employed a new laser system for fluorescence upconversion. Briefly, the excitation source is a mode-locked Ti:Sapphire oscillator (KM Labs) pumped by a Verdi (Coherent) at 5 W. The Ti:Sapphire laser produces an output pulse with a 60 fs duration (fwhm assuming a Gaussian pulse shape) at an 80 MHz repetition rate. The spectrum of the pulse was centered at 800 nm. The rest of the experimental setup was the same as described above.

B. Time Correlated Single Photon Counting.

Fluorescence lifetimes were measured with time correlated single photon counting (TCSPC) as described by O'Connor.[12] This was done by marking the decay at the peak of the fluorescence spectrum. Briefly, a Ti:sapphire regenerative amplifier (Coherent RegA) produced pulses centered at 866 nm with a 200 KHz repetition rate and 650 nJ/pulse. The light was frequency doubled to promote C343 to its first excited state. The subsequent fluorescence relaxation was collected through a subtractive double monochromator. Single photons impinging on a microchannel plate detector (Hamamatsu, MCP-PMT) were detected and digitized using an analog-to-digital converter (Oxford, ADC) and served as the start pulse for a time-to-

amplitude converter (Oxford, TAC). A small fraction of the excitation light was split off and directed to a fast photodiode (ThorLabs). This served as the stop pulse for the TAC. Signals from the TAC were fed into a multichannel analyzer (Oxford, MCA) whose output is monitored by a computer. Decay traces were collected until sufficient signal-to-noise was achieved to allow adequate data analysis.

C. Time-Resolved Fluorescence Anisotropy. We have used time-resolved fluorescence anisotropy to determine the location of the dye molecule in the reverse micellar water pool. Time-resolved fluorescence anisotropy measures the degree and rate of rotation of the probe molecule. To determine the anisotropy, the probe molecule, C343, is excited by parallel or perpendicular light with respect to the gate beam. The fluorescence is then mixed with the residual gate pulse as in our fluorescence-upconversion experiment. The anisotropy, r(t), was calculated as follows

$$r(t) = \frac{I_{II} - I_{\perp}}{I_{II} + 2I_{\perp}} \qquad (2.1)$$

where I_{II} is the intensity of the signal with the excitation beam parallel to the gate beam and $I_{\perp}$ is the intensity of the signal with the excitation beam perpendicular to the gate beam. The rotation of the dye coupled to the micelle should yield a substantially

longer rotational correlation time than free dye. From a simple Debye-Stokes-Einstein analysis

$$\tau_{rot} = \frac{V_m \eta}{k_b T} \tag{2.2}$$

where V_m is the micellar volume, his the viscosity of the supporting nonpolar phase, k_b is the Boltzman constant, and T is the temperature, we estimate that the rotational correlation time is approximately 600 ns for a reverse micelle with w_0=5. Because we collect r(t) data only out to 500 ps, we cannot measure the micellar rotation but we can see if the dye rotation is hindered. The anisotropy measurements were collected in the same manner as the time-resolved fluorescence upconversion measurements.

II. Dynamic Light Scattering.

We used dynamic light scattering (DLS, DynaPro-801MSTC40, Protein Solutions) to ensure that we were forming reverse micelles. This technique utilizes a beam of monochromatic light that is sent through the sample. When a single particle is illuminated by the beam of light, the light is scattered in all directions. The fluctuation of the intensity of the scattered light by the microemulsions is analyzed and from this one can determine the hydrodynamic radius of the particle. [14]

The hydrodynamic radius of the particle is determined from the translational diffusion coefficient, DT, of the particles in solution.[14] Assuming Brownian motion of the particles, DT is

converted to the hydrodynamic radius, RH, via the Stokes-Einstein equation:

$$RH = \frac{k_b T}{6\pi\eta D_T} \qquad (2.3)$$

where k_b is the Boltzman constant, T is the absolute temperature in Kelvin, and η is the solvent viscosity.

III. Data Analysis.

A. Spectral Reconstruction. The data collected in the time-resolved fluorescence upconversion consist of a set of fluorescence decays collected at a series of wavelengths spanning the steady-state emission spectrum. Initially these decays were collected with three different time resolutions. Short scans were collected with 17 fs steps for either 2 or 5 ps, medium scans were collected with 200 fs steps for 60 ps, and long scans were collected with 2.5 ps steps for 500 or 750 ps. For all of the AOT studies as well as the CTAB/n-alkanol chainlength studies, scans were collected with high, medium, and low resolution in one scan, that is, 17 fs steps for the first 2 ps, followed by 200 fs steps for 45 ps, followed 2.5 ps steps for 450 ps for a total of a 500 ps scan. Data were collected at 8-10 different wavelengths to monitor the entire fluorescence spectrum. All of the scans were initially fit in RFGraph (Fayer Group, Stanford) to deconvolve the instrument response function. A single, bi- or tri exponential with offsets were required to fit both the medium and long scans.

In order to reconstruct the shifting fluorescence spectrum, the long fluorescence transient was normalized to the value of the steady state fluorescence at that wavelength. The medium scan is then normalized to the long run. When this process has been completed for each wavelength, it possible to generate the time resolved fluorescence spectrum as shown in Figure 2.3.

Individual fluorescence spectra are fit to the lognormal lineshape as shown below:

$$F(\nu) = h\exp(-\ln(2) + (\ln(1 + (2\gamma(\nu - \nu_t)/\Delta))/\gamma)^2) \qquad (2.4)$$

where h is the height of the fluorescence peak, γ is the is the asymmetry parameter, ν_t is the peak frequency, and Δ is the width parameter. From this equation, we can obtain ν_t and thus we can calculate the SRF from Equation 1.2 where $\nu(0)$ is obtained from time zero analysis and $\nu(\infty)$ is obtained from fitting the steady state fluorescence to the lognormal function (Equation 2.4). The particular time components of the SRF are determined by fitting the Equation 1.2 to either a single, bi- or tri exponential.

B. Time Zero Analysis. An important problem in determining the SRF is that it is difficult to determine the position of the time zero spectrum, $\nu(0)$. Previously, SRF values have been obtained using the assumption that $\nu(0)$ can be derived by extrapolating the observed spectra back to time equals zero. However, the $\nu(0)$ spectrum obtained in this manner will depend

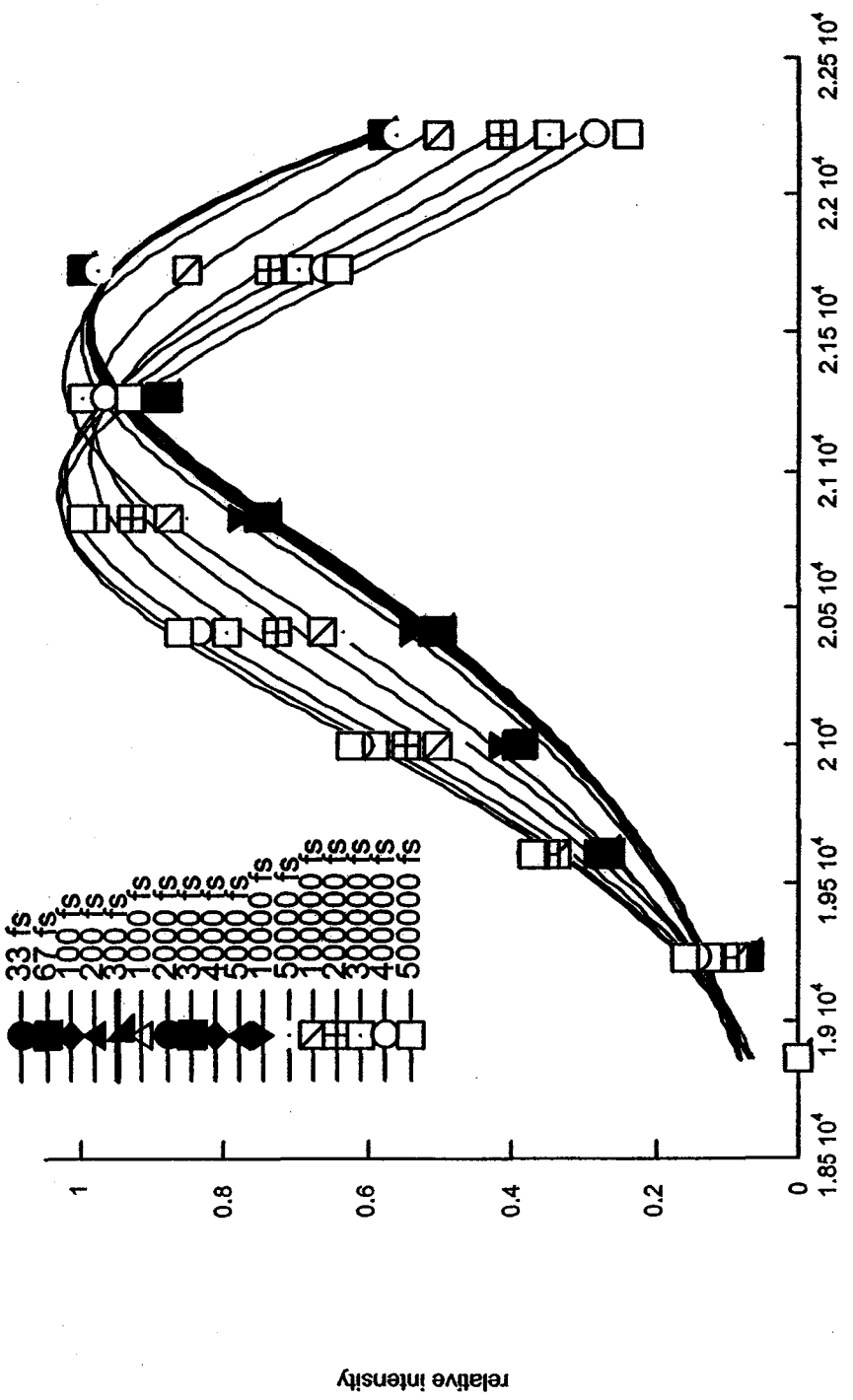

Figure 2.3. Time resolved spectra for CTAB/1-heptanol/cyclohexane/water $w_0=10$.

significantly on the time resolution employed. Hence, early experiments often missed the inertial component of the SRF or gave results that were somewhat misleading.[3,7]

The discovery that 70% of the relaxation can occur during the ultrafast inertial relaxation made it necessary to be able to accurately calculate $\nu(0)$ and thus be able to accurately calculate the SRF. In systems containing water this is especially true since miscalculating $\nu(0)$ will result in missing a large part of the relaxation. It is therefore necessary to approximate the time zero spectrum as described by Fee and Maroncelli.[15] It is based on the principle that different probe molecules experience different local solvation environments. If it is assumed that all the probe molecules fit the same absorption line shape function $g(\nu)$, that the spectrum is shifted due to its interaction with the solvent (δ), and that δ has a distribution described by $p(\delta)$ then the absorption spectrum is given as

$$A_p(\nu) \propto \nu \int g(\nu - \delta) p(\delta) d\delta. \qquad (2.5)$$

$p(\delta)$ is assumed to be a Gaussian function

$$p(\delta) = (2\pi\sigma)^{-\frac{1}{2}} \exp\left[-\frac{(\delta - \delta_0)^2}{2\sigma^2} \right] \qquad (2.6)$$

where δ_0 is the average shift due to the polar solvent and σ is the variance of the distribution.

The emission line shape can be described by

$$F_p(\nu, t=0; \nu_{ex}) \propto \nu^3 \nu_{ex} \times \int g(\nu_{ex} - \delta) p(\delta) f(\nu - \delta) k_{rad}(\delta) d\delta \qquad (2.7)$$

where k_{rad} is the radiative rate constant which Maroncelli et al. have shown to have negligible effects on time zero analysis and thus has been ignored for our analysis.[15] ν_{ex} is the excitation frequency and the integral term is the convolution of the solvent distribution transferred to the excited state $g(\nu_{ex} - \nu)p(\delta)$ and the fluorescence intensity function $f(\nu-\delta)k_{rad}$.

The functions $g(\nu)$, $f(\nu)$, and $p(\delta)$ have to be calculated to determine the time zero fluorescence spectrum. The nonpolar steady state absorption (A_{np}) and fluorescence (F_{np}) spectra are used to calculate $g(\nu)$ and $f(\nu)$ respectively. Thus

$$g(\nu) \propto \nu^{-1} A_{np}(\nu) \qquad (2.8)$$

and

$$f(\nu) \propto \nu^{-3} F_{np}(\nu). \qquad (2.9)$$

By utilizing these functions for polar solvents, one assumes that the nonpolar spectra are purely homogeneously broadened independent of the solvent. While neither statement is completely true, the effects of polar interactions dominate in determining the spectral shifts and widths and such an approximation is acceptable.

To actually calculate the time zero emission spectrum, one first has to collect the steady state absorption and emission spectra of the dye molecule in a nonpolar solution. From the

nonpolar reference spectra, f(ν) and g(ν) are calculated using Equations 2.8 and 2.9 respectively. Then, σ and δ are determined from fitting the p(δ) to the polar absorption spectrum convolved with g(ν). After this is completed, the time zero spectrum is calculated using equation 2.7.

IV. Coumarin 343.

Ideal probe molecules are rigid molecules with a large dipole change between the ground state and the first excited state.[10] They should exhibit solvent dependent fluorescence Stokes shift that reflects solute/solvent interactions instead of exhibiting vibronic activity from intramolecular modes.[10] Finally, the probe molecule needs to be soluble in a broad range of solvents.

Coumarin molecules fulfill the above requirements and as a result have been used in numerous solvation dynamic studies during the past decade.[1-10] For all of the solvation relaxation studies we have used Coumarin 343 (C343) as shown in Figure 2.4. The advantage of utilizing C343 in solvation relaxation studies in reverse micelles is that C343 is soluble in polar solvents and insoluble in nonpolar solvents. Hence, it is possible to probe the polar interior of reverse micelles with C343.

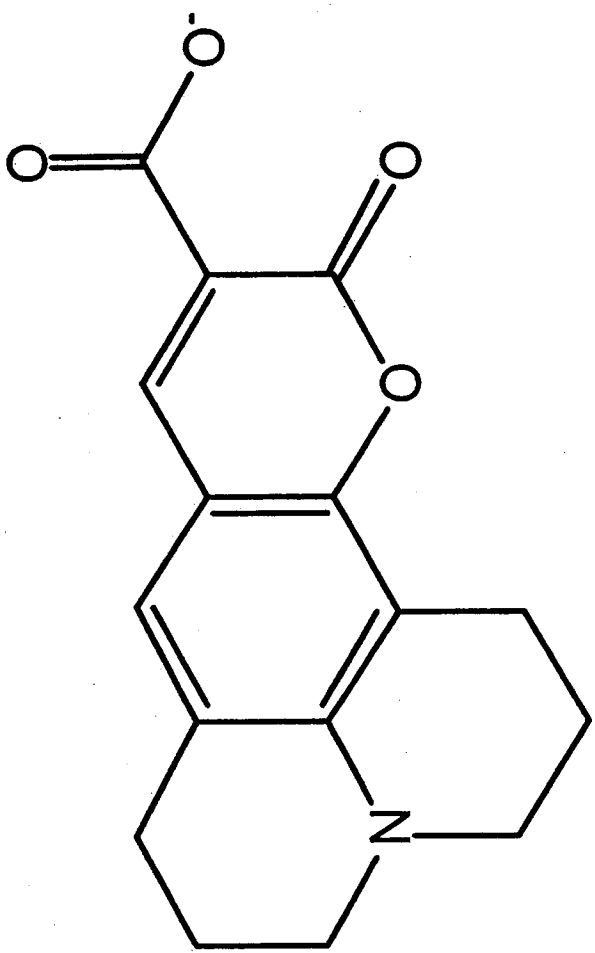

Figure 2.4. Coumarin 343 anion.

References:

(1)Horng, M. L.; Gardecki, J. A.; Maroncelli, M. *Journal of Physical Chemistry A* **1997**, *101*, 1030-1047.

(2)Horng, M. L.; Gardecki, J. A.; Papazyan, A.; Maroncelli, M. *Journal of Physical Chemistry* **1995**, *99*, 17311-17337.

(3)Jimenez, R.; Fleming, G. R.; Kumar, P. V.; Maroncelli, M. *Nature* **1994**, *369*, 471-473.

(4)Pant, D.; Levinger, N. E. *Chemical Physics Letters* **1998**, *292*, 200-206.

(5)Pant, D.; Levinger, N. E. *Journal of Physical Chemistry B* **1999**, *103*, 7846-7852.

(6)Pant, D.; Levinger, N. E. *Langmuir* **2000**, *16*, 10123-10130.

(7)Riter, R. E.; Undiks, E. P.; Levinger, N. E. *Journal of the American Chemical Society* **1998**, *120*, 6062-6067.

(8)Willard, D. M.; Levinger, N. E. *Biophysical Journal* **2000**, *submitted.*

(9)Willard, D. M.; Riter, R. E.; Levinger, N. E. *Journal of the American Chemical Society* **1998**, *120*, 4151-4160.

(10)Barbara, P. F.; Jarzeba, W. In *Advances in Photochemistry*; Volmar, D. H., Hammond, G. G., Gollnick, K., Eds.; John Wiley and Sons, 1990; Vol. 15, p 1.

(11)Castner Jr., E. W.; Maroncelli, M.; Fleming, G. R. *Journal of Chemical Physics* **1987**, *86*, 1090.

(12)O'Connor, D. V.; Phillips, D. *Time-Correlated Single-Photon Counting*, 1988.

(13)Debye, P. J. W. *Polar Molecules*; Chemical Catalog Co.: New York, 1929.

(14) http://www.proterion.com/ps_dynapro.html

(15)Fee, R. S.; Maroncelli, M. *Chemical Physics* **1994**, *183*, 235-247.

Chapter 3

Dynamics of Polar Solvation in Quaternary Microemulsions

Elizabeth M. Corbeil and Nancy E. Levinger

Published in Langmuir 2003, *19*, 7264.

Elizabeth M. Corbeil collected and analyzed all of the data presented in this chapter. She also wrote the manuscript.

Abstract

Steady-state spectroscopy and time-resolved solvation dynamics have been used to investigate the effects the addition of alkanol has on the location of Coumarin 343 (C343) in CTAB/1-pentanol/cyclohexane/water, CTAB/1-heptanol/cyclohexane/water and SDS/1-heptanol/cyclohexane/water reverse micelles. Steady-state spectroscopy showed that the probe molecule is not sensitive to alkanol chain lengths or water loading. Instead, C343 is sensitive to the surfactant used to form the reverse micelles. Solvation dynamics measurements utilizing ultrafast time-resolved fluorescence-upconversion spectroscopy revealed two solvation reorganization times regardless of the micellar system studied or hydration level. A hundreds of picosecond time component is attributed to collective motion of the interface. Time zero analysis

reveals a substantial relaxation component occurring on the femtosecond timescale.

I. Introduction

When surfactant molecules are dispersed in nonpolar solvents, reverse micelles can form.[1] In these self-assembled structures, the polar headgroup of the surfactant molecule points inward toward a pool of water that forms while the surfactant tails point out into the oil phase. Though Aerosol OT (AOT) is by far the most common surfactant used to form reverse micelles,[2] other microemulsion systems present effective environments for a range of chemistries. In particular, cetyltrimethylammonium bromide (CTAB) has been used as an alternative surfactant due to the positive charge on the headgroup. Unlike AOT, whose branched alkyl chains facilitate reverse micelle formation, single chained surfactants, such as CTAB and sodium dodecyl sulfate (SDS), do not form reverse micelles in alkanes in the absence of a cosurfactant. Generally, medium chain length primary alcohols, such as 1-butanol, 1-pentanol, or 1-hexanol, permit the formation of CTAB or SDS reverse micelles in alkane solvents.

Although reverse micelles from these quaternary microemulsions have not been investigated to the same degree as AOT reverse micelles, researchers have probed a range of properties in these reverse micellar systems.[3-12] For example, the size and shape characteristics of CTAB reverse micelles formed in alkanes with alcohol cosurfactants have been determined through

light scattering, pulsed field gradient NMR, near IR spectroscopy and conductivity.[4,12] Time-resolved fluorescence quenching studies have been used to determine the water core diameter as well as the aggregation number for CTAB reverse micelles.[3] Studies have also been performed to determine the interfacial thickness and the ion concentration at the interface.[3,10,11]

Due to confinement and interactions with the surfactant interface, the properties of water in reverse micelles can differ vastly from bulk water.[4,13,14] At the same time, the water solubilized in the cavity of the reverse micelle controls the size of the micelle, the shape of the micelle, and the surfactant packing. Because the water content is critical to their nature, reverse micelles are often characterized by w_0, which is defined as the ratio of water to surfactant,

$$w_0 = \frac{[H_2O]}{[Surfactant]}. \qquad (3.1)$$

The nature of the reverse micelles formed in quaternary microemulsions differs from ternary systems. Among others, a range of differing chemistries is possible leading to novel nanoparticles[11] and stabilization for enzymes.[12] The ability of CTAB and SDS reverse micelles to dissolve and compartmentalize polar reactants can significantly affect chemical reactivity, especially when reactions occur at the micellar interface.[13] For example, Menger et al.[38] showed that model mustard and nerve

agents were effectively hydrolyzed and oxidized in SDS/n-butanol/ microemulsions. Their utility as nanoreactors led us to explore the differences between dynamics in these reverse micelles created in quaternary microemulsions and those in ternary systems, such as AOT.

One effective method for characterizing the dynamical response in reverse micelles is polar solvation dynamics experiments.[13,39,40] Polar solvation dynamics measures the polar solvent response to an instantaneous change of the charge distribution in a probe molecule.[41,42] Solvation dynamics of a wide variety of bulk liquids have been well studied both experimentally and theoretically.[42] These studies have revealed two different types of solvent motion: an ultrafast time component attributed to an inertial solvent response (<100 fs), and a slower diffusive component (hundreds of femtoseconds to nanoseconds) attributed to the diffusive solvent motion in response to the probe's new charge distribution. Perhaps the most common method to measure solvation dynamics utilizes time-resolved fluorescence upconversion to monitor the time dependent emission spectrum of a fluorescent probe.[19] When the probe is excited, the solvent reorganizes to lower its free energy in response to the change in charge distribution and leading to an increasing red shift of its fluorescence over time. Measuring the

time dependence of the solute emission reveals the solvent's dynamics and is quantified by the solvation response function (SRF), C(t), defined as

$$C(t)\frac{\nu(t)-\nu(\infty)}{\nu(t)-\nu(0)} \qquad (3.2)$$

where $\nu(0)$, $\nu(t)$, $\nu(\infty)$ represent the frequency of fluorescence intensity maximum immediately after excitation, at some time *t* after excitation, and at a time sufficiently long enough to ensure the excited solvent configuration is at equilibrium. Thus, one can monitor the interior motion of the microemulsion over time.

While solvation dynamics in homogeneous solutions have been explored for more than the past decade, studies of solvation dynamics experiments in heterogeneous environments are relatively new.[13,39,40] We have explored solvation dynamics in a range of reverse micellar systems with sub picosecond time resolution. In all our studies, we have found that the dynamics within the reverse micelles differs significantly from that of bulk water.

In this paper, we report results from studies of solvation dynamics in quaternary CTAB/1-heptanol/cyclohexane/water, CTAB/1-pentanol/cyclohexane/water, and SDS/1-heptanol/cyclohexane/water reverse micelles. The solvent response function is nearly the same for all of the reverse micelles used in this investigation. This indicates that the

a computer. The time resolution of the spectrophotometer was 250 fs, which was measured via cross correlation of the fundamental and doubled fundamental pulses in the nonlinear BBO crystal. Scans were collected with high medium and low resolution, that is, 17 fs steps for 5.1 ps full scan length, 250 fs steps for 60 ps full scan length and 2.5 ps steps for 500 ps full scan length. Data were collected at 8 –10 different wavelengths to monitor the entire fluorescence spectrum.

The second method used to measure solvation dynamics was time correlation single photon counting (TCSPC) as described by O'Connor and Phillips.[45] A Ti:sapphire regenerative amplifier (Coherent RegA) produced pulses centered at 866 nm with a 200 KHz repetition rate and 650 nJ/pulse. The light was frequency doubled to promote C343 to its first excited state. The subsequent fluorescence relaxation was collected through a subtractive double monochromator. Single photons impinging on a microchannel plate detector (Hamamatsu, MCP-PMT) were detected and digitized using an analog-to-digital converter (Oxford ADC) and served as the start pulse for a time-to-amplitude converter (Oxford TAC). A small fraction of the excitation light was split off and directed to a fast photodiode (ThorLabs). This served as the stop pulse for the TAC. Signals from the TAC were fed into a multichannel analyzer (Oxford MCA) whose output is

The anionic laser dye Coumarin 343 (C343, Exciton) was used without further purification. The dye was added in excess to each of the samples and allowed to sit overnight. Then, the samples were sonicated for 1/2 hour and filtered to remove any excess dye. Absorption spectra were collected using a Hewlett Packard 8452A Diode Array Spectrophotometer and fluorescence spectra were collected using an ISA Fluorolog Fluorometer. From the absorption spectrum, we estimate that the concentration of dye in the sample was 75 μM, which corresponds to 1 dye molecule per every hundred micelles. This ensures that the measured spectroscopy and dynamics arise from individual dye molecules rather than from aggregates.

B. Time-Resolved Fluorescence Spectroscopy. The solvation dynamics in these reverse micellar systems were measured two different ways. The first method used to monitor solvent motion was femtosecond fluorescence-upconversion, which has been described in detail elsewhere.[13] Briefly, a mode locked Ti: Sapphire produced output pulses centered at 810 nm with 100 a MHz repetition rate and energy of 6.5 nJ/pulse. The output pulse was frequency doubled to promote C343 to its first excited state. We mixed the resulting fluorescence with the time delayed residual gate pulse in a nonlinear barium borate crystal (BBO). Signal was collected using a photon counter interfaced to

environment sensed by the dye in these reverse micelles is the same despite differences in the surfactant or cosurfactant used to make the reverse micelles.

II. Experimental Methods

A. ***Sample Preparation.*** Cyclohexane (Aldrich, ACS spectrophotometric grade), 1-heptanol (Fluka, 99% purity), and 1-pentanol (Fluka, 99% purity) were dried overnight with molecular sieves (EM Science, 3Å) to remove any water. High-purity water (Milli-Q filtered, 18 MΩ·cm) was obtained from a Milli-Q filtration system. To remove water, cetyltrimethylammonium bromide (CTAB, Aldrich, 98.6% purity) was recrystallized three times from 100% ethanol. Thermo gravimetric Analysis (TA Instruments) coupled with mass spectrometry (Balzers Instruments) revealed that the CTAB contained no water after recrystalization. To prepare reverse micelles, 0.1 M CTAB was added to cyclohexane. Either 1-heptanol or 1-pentanol was added to the solution to achieve a ROH:CTAB ratio of 5:1. Water was added to each sample to yield w_0 values of 5, 10 15, and 40. The samples were sonicated until they were homogeneous. SDS reverse micelles were prepared in a similar manner with the same alcohol to surfactant ratio that is ROH:SDS of 5:1. Reverse micellar radii were measured with Dynamic Light Scattering (DLS, DynaPro, Protein Solutions).

monitored by a computer. Decay traces were collected until sufficient signal-to-noise was achieved to allow adequate data analysis. Once again, we collected the fluorescence spectrum at 10 different wavelengths to ensure that we were monitoring the entire fluorescence spectrum. Fluorescence lifetimes were measured with TCSPC by marking the decay at the peak of the fluorescence spectrum.

C. Data Analysis. The spectral reconstruction method was used to determine the solvent response function (SRF) in the various reverse micellar samples. This method is described in detail elsewhere.[42] The resulting time-resolved fluorescence upconversion decays were normalized to the steady-state spectrum and fit to multi-exponential functions. Time-resolved fluorescence spectra were constructed from the multi-exponential fits. The resulting spectra were fit to a log-normal function to determine the peak maximum $\nu(t)$. The peak maximum was used to calculate the SRF (eqn. 3.2). $\nu(\infty)$ was determined from the peak maximum of the steady-state spectrum. $\nu(0)$ is a hypothetical emission spectrum that would be observed if a molecule were to be promoted to its first excited state and allowed to relax vibrationally and emit before any nuclear solvent motion has occurred; the method used to calculate $\nu(0)$ is described in detail elsewhere.[46]

III. Results and Discussion

A. ***Characterization.*** Characterization of the reverse micelles assists in the interpretation of the dynamical results. Our DLS measurements show that as w_0 increases, the hydrodynamic radius of the reverse micelles also increases (see Table 3.1). This suggests that water added to the system migrates to the micellar interiors causing them to swell. Other researchers working under similar conditions and with equivalent microemulsion solutions report that the CTAB and SDS reverse micelles swell with increasing water content.[4,47] They used small angle neutron scattering and cryo-TEM to show that the micelles adopt a spherical form. Because our samples are prepared with the same concentrations, we assume that our reverse micelles are also spherical.

In microheterogeneous solutions such as those studied here, a dye probe molecule has the potential to reside in a range of locations. By comparing the spectroscopy of the probe molecule in various solutions, we can determine if it is associated with the reverse micelles in solution. First, we measured the steady-state absorption and fluorescence of C343 in environments ranging from pure cyclohexane to pure water, including a mixture of cyclohexane, pentanol and water; the steady state absorption spectra of C343 in these environments is shown in Fig. 3.1. Because the steady-state fluorescence spectrum of C343 follows

the same trends as the absorption spectrum, trends shown in figures for absorption also apply to trends we see for fluorescence. It is clear from the steady state absorption spectra shown in Fig. 3.1, that the environment sensed by the dye in the reverse micellar solution differs from all the other solutions. Comparison of the C343 spectrum in bulk water and in a CTAB reverse micelle at w_0=40, a hydration level high enough to present a bulk-like water pool,[49] clearly demonstrates that the dye environment in the micelle is not that of bulk water. Neither is the environment like that in the ternary water/n-alcohol/cyclohexane solution or pure cyclohexane. Both peak maxima and spectral shapes differ sufficiently in the various environments thus we are confident that C343 partitions to the interior of the reverse micelles.

The steady-state spectra of C343 in CTAB reverse micelles display different trends than what we have seen for other micellar systems. The steady-state absorption spectra of C343 in CTAB/1-pentanol/cyclohexane/water and CTAB/1-heptanol/cyclohexane/water reverse micelles as well as the fluorescence spectra of CTAB/1-pentanol/cyclohexane/water reverse micelles are shown in Fig. 3.2. Although DLS shows that the hydrodynamic radius increases with increasing w_0, the peak and shape of the C343 steady state absorption stays the same

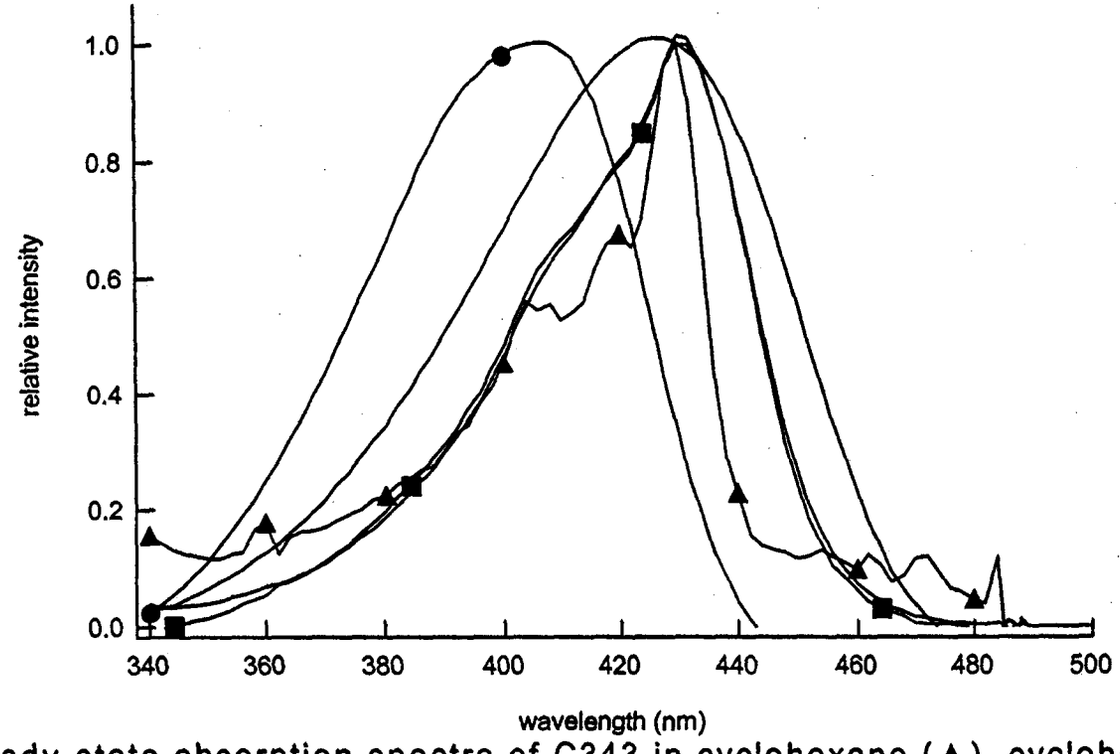

Figure 3.1. Steady-state absorption spectra of C343 in cyclohexane (▲), cyclohexane/1-pentanol (■), cyclohexane/1-pentanol/water (overlays cyclohexane/1-pentanol, CTAB/1-pentanol/cyclohexane/water w_0=40 (•), and water (solid line).

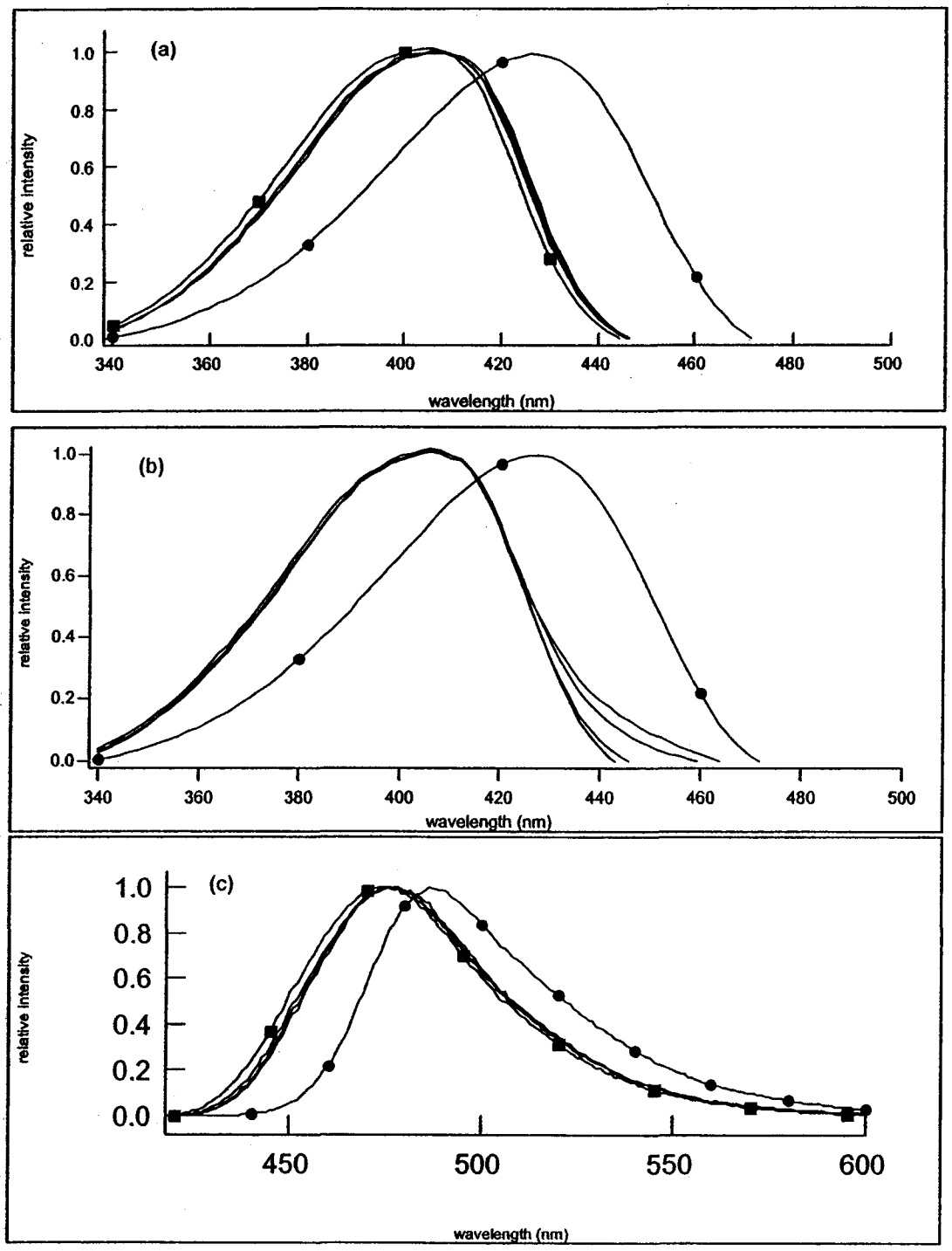

Figure 3.2. Steady-state spectra of C343 in reverse micelles and bulk water: (a) absorption spectra in CTAB/1-pentanol/cyclohexane/water w_0=5 (■), 10, 15, and 40 (overlay each other), and bulk water (•), (b) absorption spectra in CTAB/1-heptanol/cyclohexane/water w_0=5, 10, 15, and 40 (overlay each other), and bulk water (•) (c) fluorescence spectra in CTAB/1-pentanol/cyclohexane/water reverse micelles w_0=5 (■), 10, 15, and 40 (overlay each other), and bulk water (•).

regardless of water loading or cosurfactant alcohol. In previous studies of C343 in AOT reverse micelles,[13] lecithin reverse micelles[14,39] and reverse micelles made with nonionic surfactants,[50] the steady state absorption and emission spectra shifted toward the spectrum of C343 in pure H_2O with increasing water loading; the dye molecule's spectroscopy reflected the amount of water in the reverse micelles. In contrast, it appears that neither water loading nor the alcohol chain length of the 1-pentanol or 1-heptanol cosurfactant affects the C343 dye in these quaternary reverse micelles.

To explore the relative effect of cosurfactant versus surfactant on the observed spectroscopy and dynamics in reverse micelles, we compare our CTAB results with measurements in anionic SDS reverse micelles. If the C343 spectroscopy reflects direct interaction with the surfactant headgroup, its spectral characteristics should differ in SDS reverse micelles. Figure 3.3 contrasts the absorption spectrum of C343 in SDS reverse micelles with the spectrum in bulk water and in a representative CTAB reverse micelle, w_0=40. Similar to the case for the CTAB reverse micelles discussed above, the spectrum of C343 in the SDS reverse micelles with differing w_0 are so similar, they can be overlaid on each other; the C343 dye is again not sensitive to the hydration level in the reverse micelles. Comparison of the C343

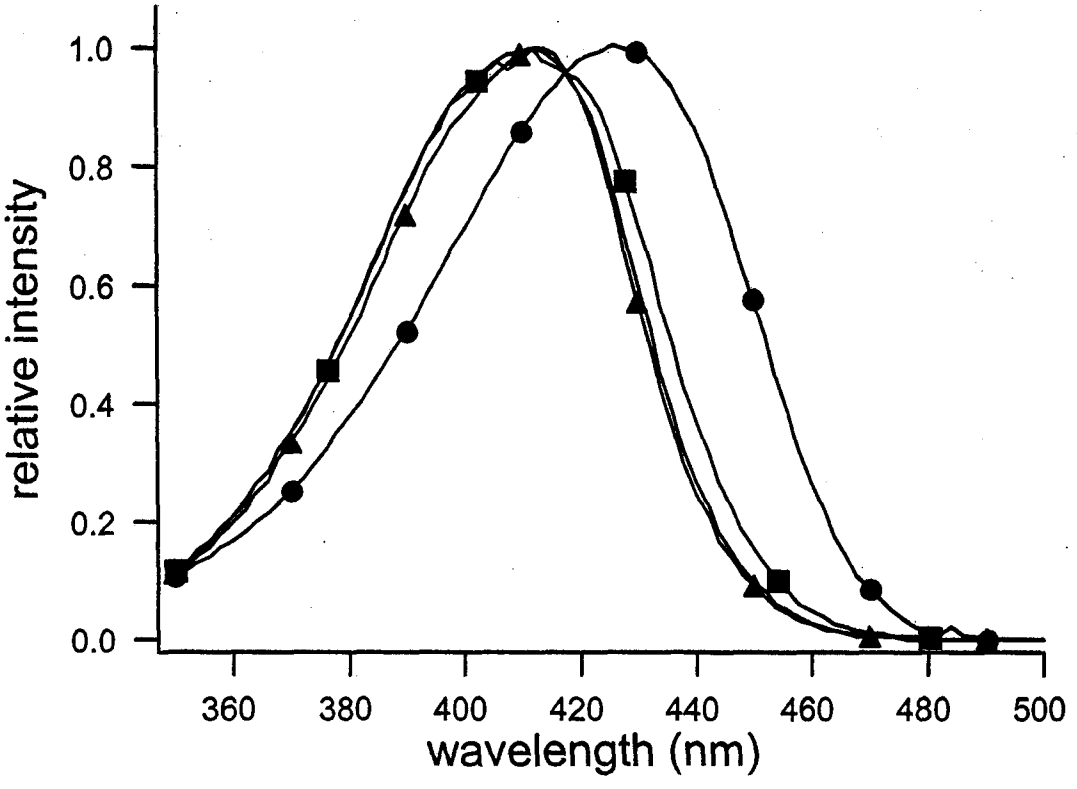

Figure 3.3. Steady-state absorption spectra of C343 in SDS/cyclohexane/1-heptanol/water w_0=10 (solid line), w_0 =15(▲), w_0=40 (■), and water (•).

absorption spectrum in CTAB and SDS microemulsions reveals a 6 nm shift in peak position. Thus, there are slight differences between the environments in the cationic versus anionic reverse micelles that may arise from direct surfactant/dye interactions in these quaternary reverse micelles.

The fluorescence lifetime of a dye molecule can often uncover information about interactions of the dye with its environment. Strong interactions of dyes with their surroundings frequently result in substantially reduced fluorescence lifetimes.[51] We have measured the C343 lifetime in a range of environments using TCSPC. We measure the fluorescence lifetime to be 3-4 ns regardless of solvent or environment. In the studies reported here, the lifetime in bulk water and in the reverse micelles used in this study are all approximately 3.8 ns. This suggests that interactions of the dye with its environment are relatively weak and are not sufficient to result in strong quenching.

From these studies, we conclude that C343 is strongly associated with the reverse micelles explored. Also, unlike other reverse micelles,[13,39,40] C343 appears to reside in a similar environment regardless of the amount of water in the water pool or the cosurfactant used to make the reverse micelles. We speculate that the dye molecule must reside embedded in the reverse micellar interface. From here, we investigate how this

environment in turn impacts the solvation dynamics that we measure and use the dynamical measurements to understand the system.

B. Solvation Dynamics. The solvation dynamics in CTAB and SDS reverse micellar systems can be gauged from the solvent response function (SRF, eqn. 3.2) for each; the SRF for CTAB reverse micelles created with 1-pentanol and 1-heptanol, and for SDS reverse micelles created with 1-heptanol with w_0=5, 10, 15 and 40 are shown in Fig. 3.4. The solvent relaxation times obtained from the spectral reconstruction analysis are given in Table 3.1. The measurable relaxation occurring on a time scale longer than 200 fs fit well to a bi-exponential decay. Interestingly, a substantial portion of the solvation response occurs on a timescale faster than we can measure; we attribute this to inertial motion.

Several features of the solvation dynamics in these systems interest us. First, unlike the other spherical micellar systems we have studied,[13,14,52] the time-resolved-fluorescence traces lack a decay component occurring on the hundreds of fs to ones of ps time scale, the time scale consistent with bulk water relaxation.[48] This is most easily seen in the raw time-resolved fluorescence data shown in Fig. 3.5 for CTAB/1-heptanol/cyclohexane/water w_0=5. For comparison, we include similar data collected for C343

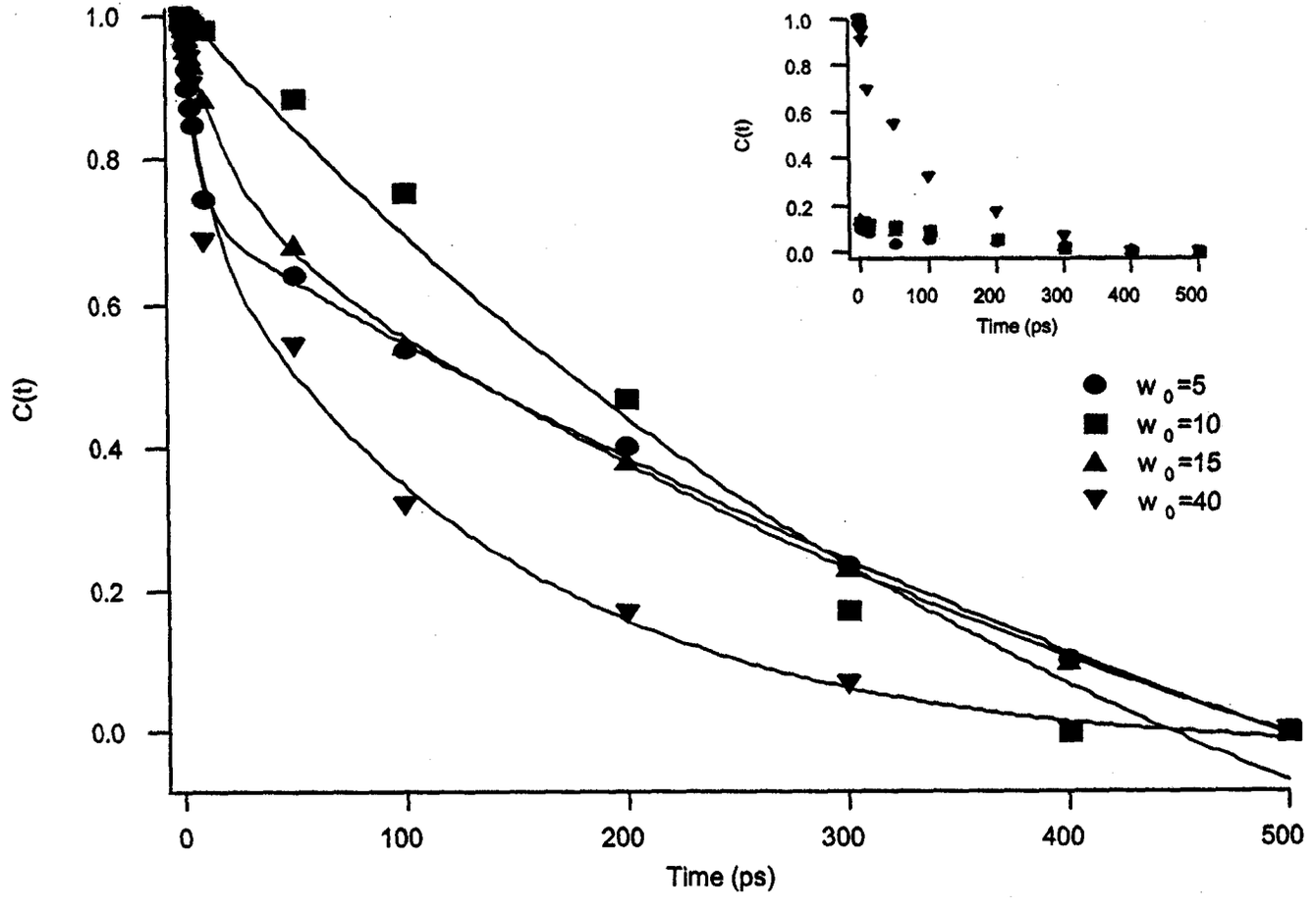

Figure 3.4a. Solvent correlation function, C(t), and multiexponential fits for CTAB/1-pentanol/cyclohexane/water reverse micelles. Inset. Solvent correlation function including point obtained from time zero analysis.

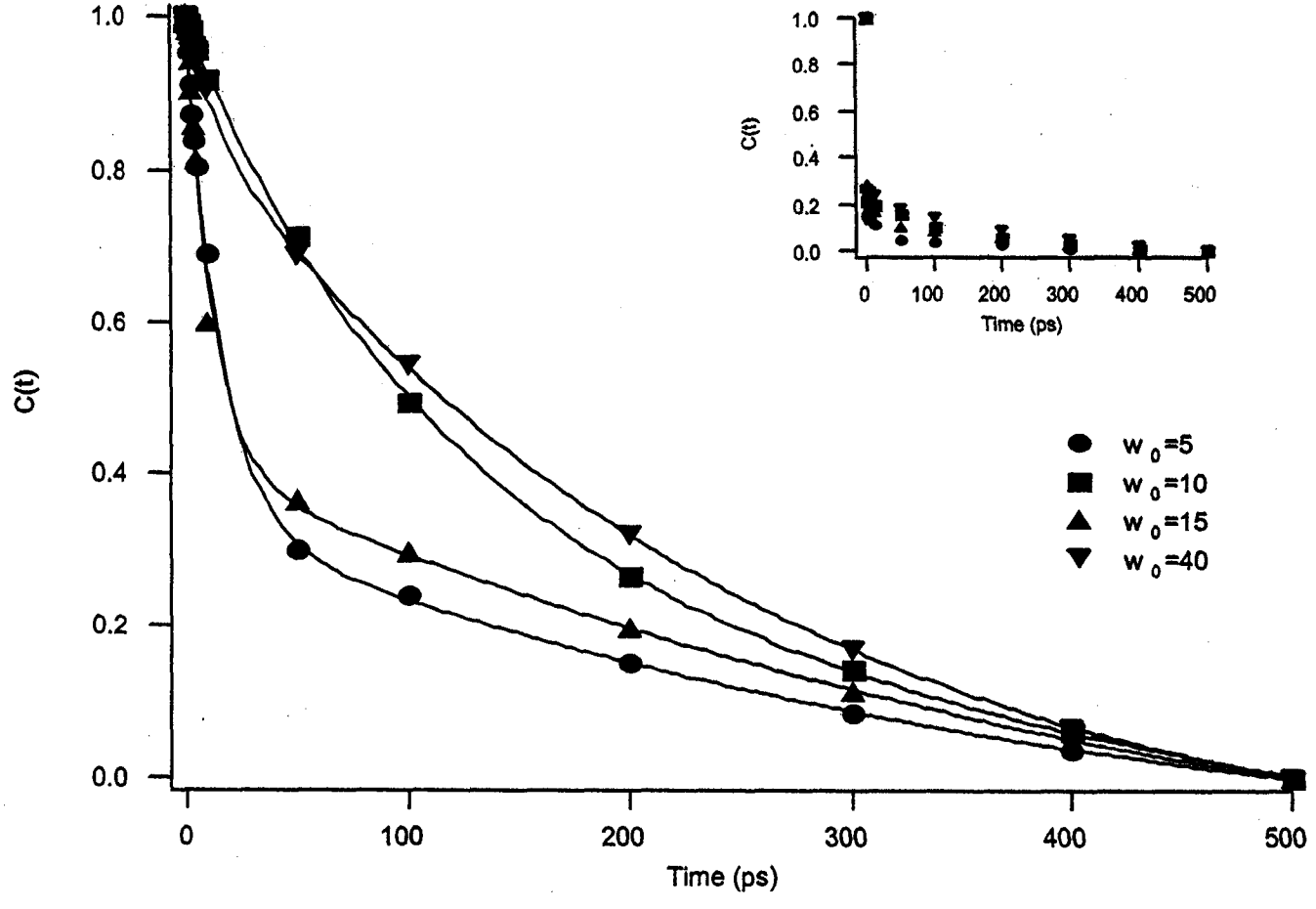

Figure 3.4b. Solvent correlation function, C(t), and multiexponential fits for CTAB/1-heptanol/cyclohexane/water reverse micelles. Inset. Solvent correlation function including point obtained from time zero analysis.

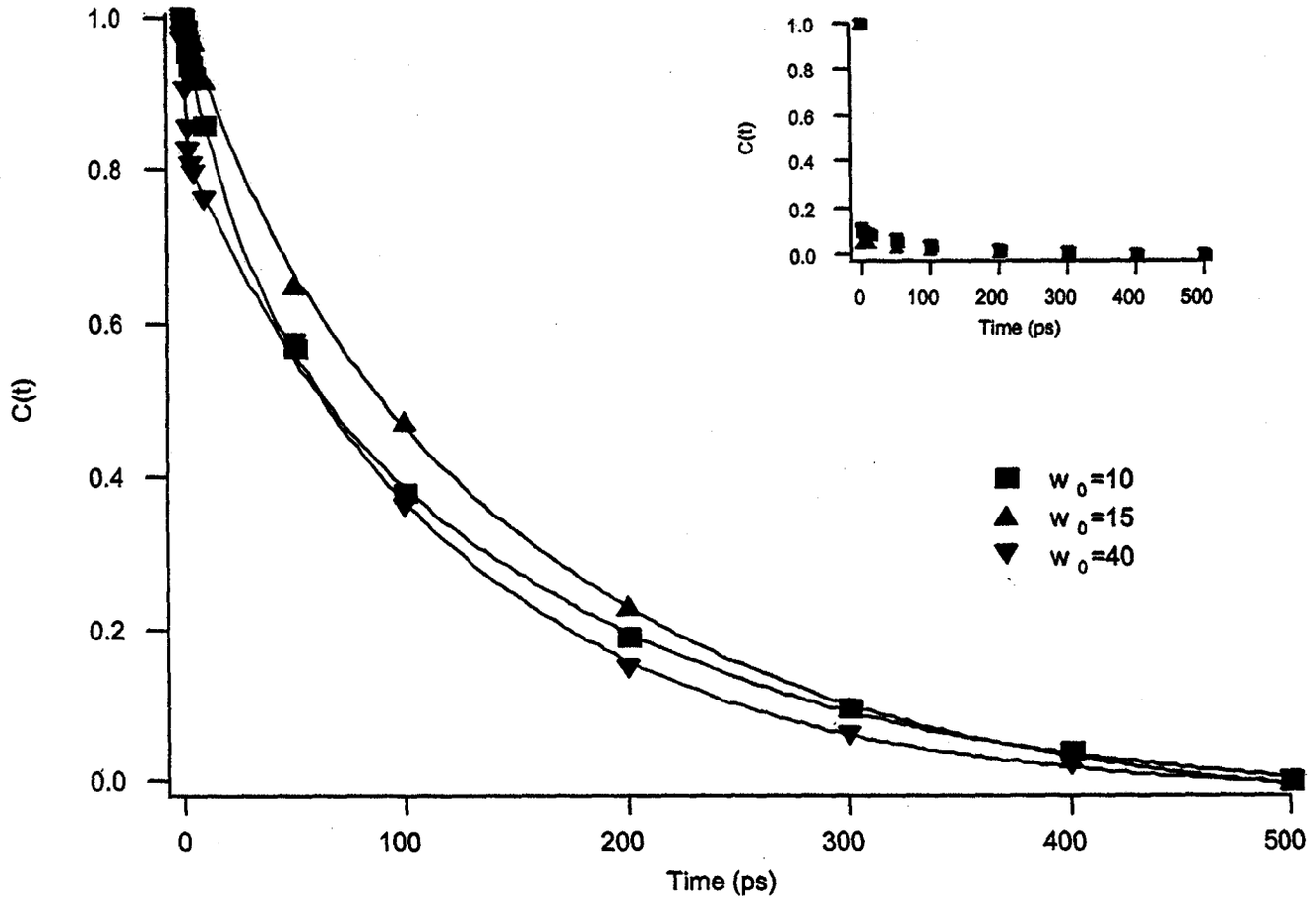

Figure 3.4c. Solvent correlation function, C(t), and multiexponential fits for SDS/1-heptanol/cyclohexane/water reverse micelles. Inset. Solvent correlation function including point obtained from time zero analysis.

sample	w_0	radius (nm)	stokes shift (cm^{-1})[c]	C(t)							
				A_1	τ_1 (ps)	A_2	τ_2 (ps)	A_3	τ_3 (ps)	A_4	τ_4 (ps)
bulk water[a]				0.3	0.2	0.7	0.6				
1-pentanol[b]				0.04	0.03	0.07	0.7	0.3	21.7	0.6	151
CTAB/1-heptanol											
	5	2.8	2564	0.1	15	0.06	189				
	10	4	2358	0.2	11	0.1	218				
	15	6.1	2127	0.2	11	0.1	202				
	40	12.2	2098	0.3	162						
CTAB/1-pentanol											
	5	2.4	2484	0.05	11	0.06	302				
	10	3.3	2464	0.1	207						
	15	3.2	2435	0.01	9	0.1	204				
	40	11.4	2098	0.2	9	0.8	123				
SDS/1-heptanol											
	10	3.7	2581	0.02	18	0.01	137				
	15	6.3	2735	0.002	20	0.05	133				
	40	11.6	2524	0.02	1	0.09	120				

[a] Joo, T., et al.[53]

[b] Horng, M. L., et al.[39]

[c] Stokes shift in the first 33 fs.

Table 3.1. Fit parameters of the ultrafast components of the solvent correlation functions for water in various micellar environments.

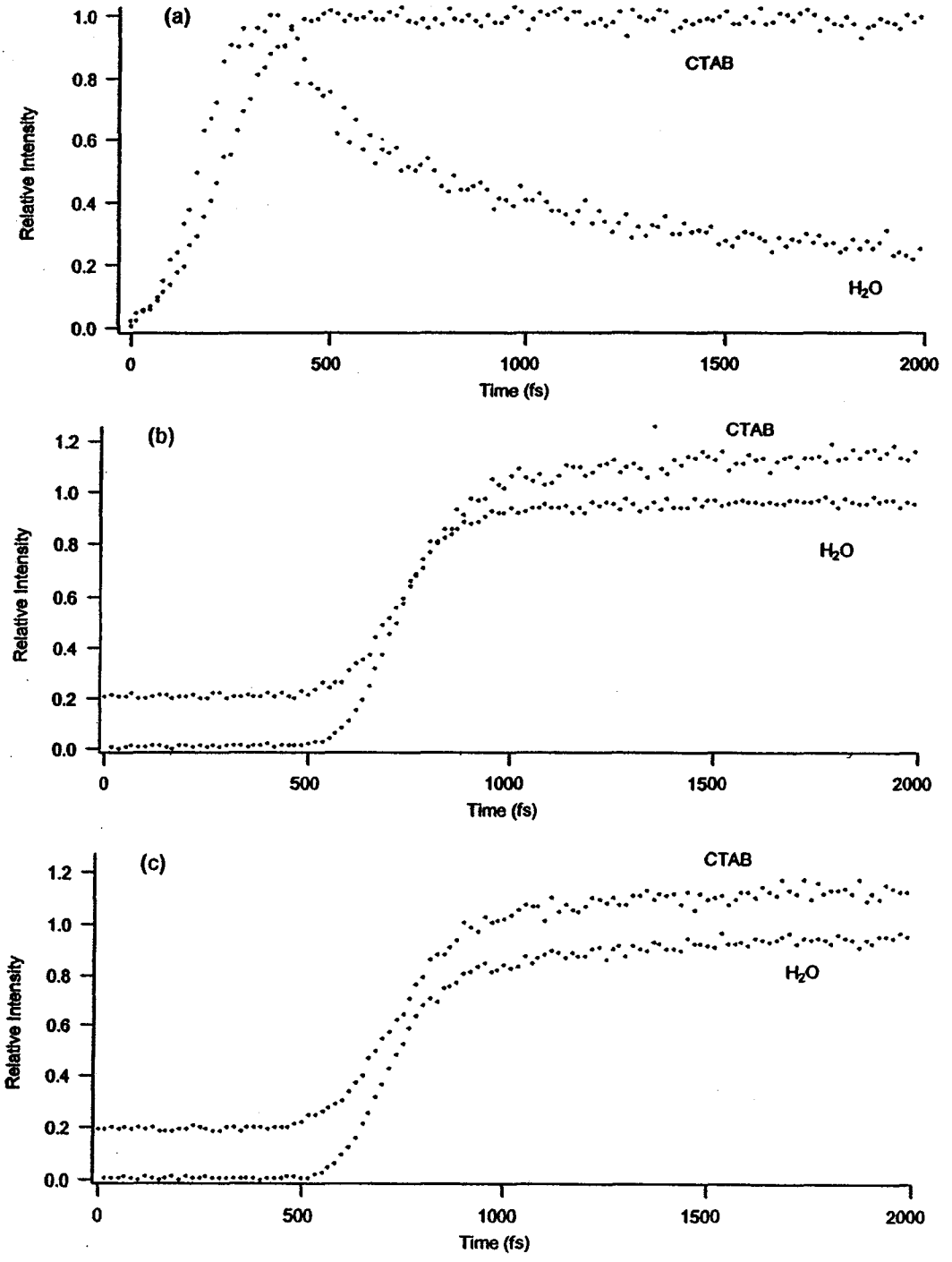

Figure 3.5. Femtosecond fluorescence-upconversion transients of C343 in CTAB/1-heptanol/cyclohexane/water w_0=10 reverse micelles and bulk water at (a) 460 nm, (b)500 nm, and (c) 520 nm. The CTAB transients are offset.

in an aqueous solution.[13] In water, the fluorescence signals at shorter wavelengths decay quickly while those at long wavelengths display a rise consistent with a time dependent fluorescent Stokes shift occurring on the timescale of the trace. In the CTAB sample, the transients neither rise nor fall on the 2 ps time scale shown. At all hydration levels that we have explored for these systems, there should be sufficient water present in the micellar core to display bulk-like water relaxation. Indeed, in all other solvation dynamics studies we have performed on similarly sized reverse micelles with spherical form, a bulk-like water pool was evident and the solvation dynamics showed a time component consistent with bulk water motion.

While the data presented here lack a diffusive relaxation component occurring on the 100's of fs to ps timescale, analysis using the predicted time-zero spectrum[46] indicates a significant inertial response on a sub 100 fs timescale. It appears that there is a substantial inertial component to the dynamics occurring on a timescale significantly shorter than we can measure. Pure water displays an inertial component comprising greater than 50% of its solvent response.[48] A large inertial component is also observed in AOT reverse micelles[28] and a large very short (9 fs) component has been observed in photon echo experiments for lecithin vesicles.[55]

In our previous solvation dynamics studies on reverse micelles, such as the anionic AOT reverse micelles, the dye molecule migrated into the free water pool as the hydrodynamic radius of the reverse micelle increases. Our DLS measurements and literature reports confirm that the hydrodynamic radius of the reverse micelles in the quaternary microemulsions studied here increases as w_0 increases. However, steady-state and the solvation dynamics results suggest that C343 remains in the same location regardless of the hydrodynamic radius of the reverse micelle. In contrast, in AOT reverse micelles, lecithin reverse micelles formed in benzene, and reverse micelles formed from alkylpolyethers, C_iE_j all spherical reverse micellar systems, the solvation dynamics depend strongly on w_0 and micelle radius. In these systems explored here, the C343 probe molecule appears insensitive to water loading; it reports on dynamics at the interface, not in the micellar interior.

CTAB/1-heptanol/cyclohexane/water reverse micelles show the similar trends to those of CTAB/1-pentanol/cyclohexane/water micellar systems. Both systems display a large inertial component from the time zero analysis, whose magnitude is larger than any previously reported values. Second, as the hydration level increases, the number of distinct decay components and their amplitudes remain constant. This indicates that, in addition

to being insensitive to dynamics in the micellar cores, the C343 probe molecule is also unaffected by the alcohol alkyl chain length. Finally, the relative relaxation dynamics for CTAB/1-pentanol and CTAB/1-heptanol reverse micelles are approximately the same regardless of hydration level. Taken together with steady-state spectroscopy, these results suggest that the n-alkanol impacts the location of the probe molecule and the observed interfacial solvation dynamics. However, the length of the alky chain length of the n-alkanol has little effect on the observed dynamics since 1-heptanol and 1-pentanol show approximately the same decay components.

The solvation dynamics of SDS reverse micelles respond with a slightly faster time than the solvation dynamics observed in CTAB micellar systems. As in the CTAB systems, there is a large inertial response in SDS reverse micellar samples. Also, like CTAB solutions, the time-resolved fluorescence traces for SDS reverse micelles, w_0=10, shown in Fig. 3.5 neither rise nor fall on the 2 ps time scale. However, a substantial inertial component is calculated in time-zero analysis. Furthermore, the inertial component is shorter in SDS w_0=5 systems than it is in CTAB systems. This suggests that the dye molecule interacts less strongly with the interface than it does in CTAB reverse micelles.

In contrast to the other reverse micellar studies, our results reveal some interesting points. First, the inertial component that we observe in CTAB and SDS micellar systems dominates the solvent response. No study in bulk solution matches this response. Joo et al. have observed a large inertial component in solvation dynamics in bulk alkanols.[56] However, in their studies the amplitude decreases with increasing chain length. We do not observe this trend in our studies. Instead, we observe approximately the same inertial component regardless of n-alkanol used in the micellar systems. This suggests that while the alkanol molecule is probably responsible for pulling the C343 probe molecule into the micelle interface, it does not solvate the probe completely. Alternatively, the interfacial environment makes it impossible for the cosurfactant to solvate the C343 probe in the same way as a bulk environment can, impacting the solvation responses. Jimenez et al. report that for neat water, 60% of the total solvent response occurs within the first 30 fs.[48] In their work, Jimenez et al. attribute the inertial component to small amplitude, underdamped motions of the solvent molecules in the confines of the instantaneous cage formed by surrounding molecules.[57] Within this model, the inertial response arises from librational motion of the solvent molecules in the first few hydration shells of the chromophore.[56-58] All our data point to the probe molecules

residing embedded in the interfacial region. Thus, it is unlikely that water surrounds the probe molecule or that the observed ultrafast inertial response corresponds only to water motion. However, it is likely that organization of the species that are responsible for solvation reside in the interfacial region

A second interesting result reveals that the relaxation processes do not follow a trend with increasing water content in the reverse micelles. This differs from what we have seen in other spherical reverse micelles, such as AOT,[13] lecithin in benzene,[14] and nonionic surfactants[52] where the relaxation processes speed up as w_0 increases. That we do not observe a trend in the solvation response as the water content and size of the reverse micelles increases supports the interpretation that the probe molecule resides at and samples the interfacial region. Interestingly, the OH stretching mode in IR spectra of CTAB reverse micelles in quaternary solutions shows no change as w_0 increases.[59] Thus it is conceivable that the presence of alcohol in the surface of these reverse micelles leads to significantly different behavior than other reverse micelles, that is, the water does not become bulk-like with increasing water content.

While, the relaxation rates measured do not follow a trend with w_0, they do differ between the CTAB and SDS samples. Specifically, the slow, diffusive relaxation times observed are

significantly faster for the SDS reverse micelles than they are for CTAB, see Table 3.1. This may reflect the location of the dye molecule in the interfacial region. Because the dye and the SDS headgroup are both anionic, we expect some Coulomb repulsion between them. In CTAB solutions, a strong cation-π affinity between the dye and the ammonium headgroup is possible,[60] as well as ion pairing of the C343 molecule with the ammonium headgroup through the C343 carboxylate group. These interactions do not exist for the SDS reverse micelles or for our prior AOT work due to electrostatic repulsion.[60] However, it is important to consider that the alkanol cosurfactant still appears to impact the solvation dynamics in the SDS reverse micelles. AOT reverse micelles also possess anionic headgroups and, in those micelles, the solvation dynamics get faster as the micelle water content increases.[13] The longest time component that we measure in CTAB reverse micelles agrees well with the long relaxation components of 1-pentanol.[42] However, if the slow component were entirely due to n-alkanol motion we should also observe the 21.7 ps relaxation component of 1-pentanol.[42] Yet because the alkanols are assembled into the reverse micellar interface, the organized surface structure may reduce or eliminate characteristic motion of the alcohols. It is also possible that the observed dynamics reflect the collective motion of the interface,

which includes motion of water bound to the surfactant or to the interface, the headgroup, and n-alkanol headgroup.

While the solvation dynamics do not display a trend with micelle hydration, the values do vary for the differing sizes. Several explanations could account for this. It is possible that the solvation dynamics that we measure corresponds to fluidity of the reverse micellar interface. Indeed, varying fluidity in reverse micelles has been hypothesized in other studies of quaternary reverse micelles.[35] Here, researchers observed a peak in the interfacial fluidity at an intermediate w_0 value where the fluidity increased with increasing micelle size and then decreased again as the micelles grew larger. We see a similar trend in our data. The fastest solvation times are observed for w_0=10 and 15; dynamics in smaller w_0=5 and larger w_0=40 are slower. The implications for these results are dramatic. Mixing among micelles and surface "stickiness" are key in the creation of nanoparticles from reverse micellar solutions containing different precursors. If micelles collide but do not stick, the micellar contents will never be exchanged and nanoparticles would never form. However, in experiments probing solvation dynamics in highly ionic solutions, e.g., 10 M aqueous Na acetate, the dynamics were significantly faster than what we observe in reverse micelles.[40,52] Thus it is unlikely that the slow dynamics

we observe arises from a bulk-like water pool with high ionic strength.

The effect the addition of n-alkanol has on the solvation dynamics in CTAB and SDS micellar systems is larger than we first anticipated. The alcohol appears key in driving the probe into the interface where the dynamics are dominated by an ultrafast component with a sub 75 fs time constant. The slow, diffusive component varies between micelles but shows no trend with hydration level. n-alkanol directly affects the water uptake in micellar systems.[67] The adsorption of n-pentanol to the interfacial film and the consequent decrease of n-alkanol in the organic phase along with the hydration of the surfactant headgroups are responsible for the solubility of water in the oil phase going from 0.1 M to 0.037 M. Hence, after the surfactant headgroups are solvated by water, a water pool is formed.

IV. Conclusion

Steady-state spectroscopy and time-resolved solvation dynamics have been used to investigate CTAB and SDS reverse micelles with an alkanol cosurfactant. Steady-state absorption and fluorescence spectra of C343 in CTAB and SDS reverse micelles show that the probe is not sensitive to water loading suggesting that the probe molecule remains in the same environment as w_0 increases. The steady-state absorption and fluorescence

spectroscopy of C343 in CTAB reverse micelles also indicate that C343 is not sensitive to the alkanol chain length. However, the steady-state absorption and fluorescence spectra of C343 is red-shifted in SDS reverse micelles from that of CTAB reverse micelles suggesting that the surfactant headgroup affects the location of the probe molecule. Time-resolved solvation dynamics studies show that the solvent reorganization in quaternary micellar systems is significantly slower than in ternary micellar systems indicating that the probe molecule is located at the micellar interface regardless of alkanol or surfactant. In addition, the solvation dynamics of these systems have a significant inertial component contributing to approximately 90% of the total solvent response. These studies indicate that the addition of alkanol affect both the steady-state spectroscopy as well as solvent reorganization in quaternary reverse micelles.

Acknowledgements: Results presented here resulted from support by the National Science Foundation under Grant Number 0075266.

References:

(1) Luisi, P. L.; Magid, L. J. *CRC Critical Reviews in Biochemistry* **1986**, *20*, 409.

(2) De, T.; Maitra, A. *Adv. Colloid Interface Science* **1995**, *59*, 95.

(3) Das, P. K.; Chaudhuri, A. *Langmuir* **1999**.

(4) Giustini, M.; Palazzo, G.; Colafemmina, G.; Della Monica, M.; Giomini, M.; Ceglie, A. *Journal of Physical Chemistry* **1996**, *100*, 3190-3198.

(5) Sengupta, B.; Guharay, J.; Sengupta, P. K. *Spectrochimica Acta, Part A* **2000**, *56A*, 1433-1441.

(6) Vinogradov, A. M.; Tatikolov, A. S.; Costa, S. M. B. *Physical Chemistry Chemical Physics* **2001**, *3*, 4325-4332.

(7) McNamara, G. L.; Hagen, J. P. *Book of Abstracts, 217th ACS National Meeting, Anaheim, Calif., March 21-25* **1999**, CHED-227.

(8) Gonzalez-Gaitano, G.; Valiente, M.; Tardajos, G.; Montalvo, G.; Rodenast, E. *Journal of Colloid and Interface Science* **1999**, *211*, 104-109.

(9) Garcia-Rio, L.; Leis, J. R.; Reigosa, C. *Journal of Physical Chemistry B* **1997**, *101*, 5514-5520.

(10) El Seoud, O. A. *Journal of Molecular Liquid* **1997**, *72*, 85-103.

(11) Cuccovia, I. M.; Dias, L. G.; Maximiano, F. A.; Chaimovich, H. *Langmuir* **2001**, *17*, 1060-1068.

(12) Palazzo, G.; Lopez, F.; Giustini, M.; Colafemmina, G.; Ceglie, A. *Journal of Physical Chemistry B* **2003**, *107*, 1924-1931.

(13) Riter, R. E.; Willard, D. M.; Levinger, N. E. *Journal of Physical Chemistry* **1998**, *102*, 2705-2714.

(14) Willard, D. M.; Levinger, N. E. *Journal of Physical Chemistry B* **2000**, *104*, 11075-11080.

(15) Carpenter, E. E.; Kumbhar, A.; Wiemann, J. A.; Srikanth, H.; Wiggins, J.; Zhou, W.; O'Connor, C. *Journal of Material Science and Engineering, A* **2000**, *A286*, 81-86.

(16) Curri, M. L.; Agostiano, A.; Manna, L.; Monica, M. D.; Catalano, M.; Chiavarone, L.; Spagnolo, V.; Lugara, M. *Journal of Physical Chemistry B* **2000**, *104*, 8391-8397.

(17) Hirai, T.; Okubo, H.; Komasawa, I. *Journal of Colloid and Interface Science* **2001**, *235*, 358-364.

(18) Lin, J.; Zhou, W.; O'Connor, C. *Journal of Material Letters* **2001**, *49*, 282-286.

(19) Lin, J.; Zhou, W. L.; O'Connor, C. J. *Clusters Nanostruct. Interfaces, [Proc. Int. Symp.]* **2000**, 405-410.

(20) Lin, J.; Zhou, W.; Kumbhar, A.; Wiemann, J.; Fang, J.; Carpenter, E. E.; O'Connor, C. J. *Journal of Solid State Chemistry* **2001**, *159*, 26-31.

(21) Smith, B. A.; Zhang, J. Z.; Joly, A.; Liu, J. *Physical Review B: Condensed Matter* **2000**, *62*, 2021-2028.

(22) Chen, D. H.; Wu, S. H. *Chemistry of Materials* **2000**, *12*, 1354-1360.

(23) Kumbhar, A.; Spinu, L.; Agnoli, F.; Wang, K. Y.; Zhou, W. L.; O'Connor, C. J. *IEEE Transactions on Magnetics* **2001**, *37*, 2216-2218.

(24) Syamala, P.; Rao, P. V. S.; Rao, G. G.; Venkateswarlu, G. *Oxidation Communications* **2002**, *25*, 555-565.

(25) Wu, Z. H.; Zhang, J.; Benfield, R. E.; Ding, Y. F.; Grandjean, D.; Zhang, Z. L.; Ju, X. *Journal of Physical Chemistry B* **2002**, *106*, 4569-4577.

(26) Zhu, H.; Fan, Y.-X.; Shi, N.; Zhou, J.-M. *Archives of Biochemistry and Biophysics* **1999**, *368*, 61-66.

(27) Zhang, T.; Liu, H.; Chen, J. *Chin. Journal of Chemical Engineering* **2001**, *9*, 314-318.

(28) Zhang, T.; Liu, H.; Chen, J. *Separation Science Technology* **2000**, *35*, 143-151.

(29) Zhang, T.; Liu, H.; Chen, J. *Biotechnology Progress* **1999**, *15*, 1078-1082.

(30) Zhang, T.; Liu, H.; Chen, J. *Biochemical Engineering Journal* **1999**, *4*, 17-21.

(31) Piera-Velazquez, S.; Marhuenda-Egea, F.; Cadenas, E. *Journal of Molecular Catalysis B: Enzymatic* **2001**, *13*, 49-55.

(32) Motlekar, N. A.; Bhagwat, S. S. *Journal of Chemical Technology and Biotechnology* **2001**, *76*, 643-649.

(33) Marhuenda-Egea, F. C.; Piera-Velazquez, S.; Cadenas, C.; Cadenas, E. *Journal of Molecular Catalysis B: Enzymatic* **2000**, *10*, 555-563.

(34) Marhuenda-Egea, F. C.; Piera-Velazquez, S.; Cadenas, C.; Cadenas, E. *Biocatalysis and Biotransformation* **2000**, *18*, 201-222.

(35) Menger, F. M.; Park, H. *Recueil des Travaux Chimiques des Pays-Bas* **1994**, *113*, 176-180.

(36) Gonzalez, A.; Murphy, J.; Holt, S. L. In *Inorganic Reactions in Organized Media*; Holt, S. L., Ed.; American Chemical Society: Washington D. C., 1982; pp 165-177.

(37) Akhter, M. S.; Al-Alawi, S., M. *Colloids and Surfaces A* **2000**, *164*, 247-255.

(38) Menger, F. M.; Elrington, A. R. *Journal of the American Chemical Society* **1990**, *112*, 8201-8203.

(39) Willard, D. M.; Riter, R. E.; Levinger, N. E. *Journal of the American Chemical Society* **1998**, *120*, 4151-4160.

(40) Riter, R. E.; Undiks, E. P.; Kimmel, J. R.; Levinger, N. E. *Journal of Physical Chemistry B* **1998**, *102*, 7931-7938.

(41) Barbara, P. F.; Jarzeba, W. In *Advances in Photochemistry*; Volmar, D. H., Hammond, G. G., Gollnick, K., Eds.; John Wiley and Sons, 1990; Vol. 15, p 1.

(42) Horng, M. L.; Gardecki, J. A.; Papazyan, A.; Maroncelli, M. *Journal of Physical Chemistry* **1995**, *99*, 17311-17337.

(43) Castner Jr., E. W.; Maroncelli, M.; Fleming, G. R. *Journal of Chemical Physics* **1987**, *86*, 1090-1097.

(44) Kahlow, M. A.; Jarzeba, W.; Kang, T. J.; Barbara, P. F. *Journal of Chemical Physics* **1989**, *90*, 151-158.

(45) O'Connor, D. V.; Phillips, D. *Time-Correlated Single-Photon Counting*, 1988.

(46) Fee, R. S.; Maroncelli, M. *Chemical Physics* **1994**, *183*, 235-247.

(47) Petit, C.; Bommarius, A. S.; Pileni, M.-P.; Hatton, T. A. *Journal of Physical Chemistry* **1992**, *96*, 4693-4658.

(48) Jimenez, R.; Fleming, G. R.; Kumar, P. V.; Maroncelli, M. *Nature* **1994**, *369*, 471-473.

(49) Faeder, J.; Ladanyi, B. M. *Journal of Physical Chemistry B* **2000**, *104*, 1033-1046.

(50) Pant, D.; Levinger, N. E. *Langmuir* **2000**, *16*, 10123-10130.

(51) Lakowicz, J. R. *Principles of Fluorescence Spectroscopy*; Plenum Press: New York, 1983.

(52) Pant, D.; Riter, R. E.; Levinger, N. E. *Journal of Chemical Physics* **1998**, *109*, 9995-10003.

(53) Corbeil, E. M.; Riter, R. E.; Levinger, N. E. *Journal of Physical Chemistry B.* **2003**, *submitted.*

(54) Levinger, N. E. In *We have recently reanalyzed out previously published solvation dynamics data for AOT reverse micelles using the time-zero prediction developed by Fee et. al. these data show a substantial inertial component to the solvation dynamics.*

(55) Bursing, H.; Ouw, D.; Kundu, S.; Vohringer, P. *Physical Chemistry Chemical Physics* **2001**, *3*, 2378-2387.

(56) Joo, T.; Jia, Y.; Yu, J.-Y.; Lang, M. J.; Fleming, G. R. *Journal of Chemical Physics* **1996**, *104*, 6089-6108.

(57) Maroncelli, M. *Journal of Chemical Physics* **1991**, *94*, 2084-2103.

(58) Bursing, H.; Ouw, D.; Kundu, S.; Vohringer, P. *Phys. Chem. Chem. Phys.* **2001**, *3*, 2378-2387.

(59) Mittleman, D. M.; Colvin, V. L. Private Communication.

(60) Karukstis, K. K.; Frazier, A. A.; Loftus, C. T.; Tuan, A. S. *Journal of Physical Chemistry B* **1998**, *102*, 8163-8169.

(61) Sergeyev, V. G.; Mikhailenko, S. V.; Pyshkina, O. A.; Yaninsky, I. V.; Yoshikawa, K. *Journal of the American Chemical Society* **1999**, *121*, 1780-1785.

(62) Abuin, E.; Lissl, E. *Journal of Physical Chemistry* **1983**, *87*, 5166-5172.

(63) Stratt, R. M.; Maroncelli, M. *Journal of Physical Chemistry* **1996**, *100*, 12981-12996.

(64) Varghese, V. A.; Upadhyay, S.; Srivastava, R. C. *Journal of Membrane Science* **1994**, *93*, 229-235.

(65) Yang, Y. C.; Baker, J. A.; Ward, J. R. *Chemical Reviews* **1992**, *92*, 1729-1743.

(66) Yang, Y.; Donegan, S.; Patel, R. C.; Ward, A. J. I. *Chemosphere* **1994**, *28*, 1967-1976.

(67) Rabie, H. R.; Vera, J. H. *Langmuir* **1996**, *12*, 3580-3584.

Chapter 4

Cosurfactant Impact on Probe Molecule Location in Reverse Micelles

Elizabeth M. Corbeil and Nancy E. Levinger

Submitted to the Journal of Physical Chemistry

Elizabeth M. Corbeil collected and analyzed all of the quaternary reverse micelle data presented in this chapter. Dr. Ruth Riter collected and analyzed all of the ternary reverse micelle data. Elizabeth M. Corbeil wrote the manuscript.

Abstract: A wide variety of probe molecules have been used to characterize the environment found within reverse micelles. This manuscript reports on results from steady-state and time-resolved spectroscopies of the probe molecule Coumarin 343. The steady-state spectra for the probe molecule in ternary and quaternary systems is nearly identical. However, the time-resolved studies clearly indicate substantial differences in the probe sensed by the probe molecule. Implications of these results for the interpretation of spectroscopy of probe molecules in confined media are discussed.

† permanent address: Department of Chemistry, Agnes Scott College, 141 East College Ave., Decatur, GA 30030

* corresponding author email: Nancy.Levinger@colostate.edu

I. Introduction.

Reverse micelles have recently garnered significant attention as model systems to explore the effects of confinement. Confined environments occur naturally in many biologically important systems as well as a range of physically interesting materials such as porous glasses. The beauty of the reverse micelle is that it is easily created, shows substantial stability and provides a well-characterized nanoscopic water pool for a range of chemistries.

The branched double chained surfactant Aerosol OT (AOT, sodium di(2-ethylhexyl) sulfoccinate), see Figure 4.1, has been the surfactant of choice for creating monodisperse reverse micelles and is therefore very well characterized.[1] The size of the reverse micelles is usually given by

$$w_0 = \frac{[H_2O]}{[AOT]}. \qquad (4.1)$$

AOT reverse micelles can be formed from w_0=1 up to w_0=70 in a range of nonpolar solvents. Many studies have shown that AOT reverse micelles formed in ternary solutions of water, AOT and nonpolar solvent display a spherical form.[2-9] Because the water defines the volume while the AOT surfactant defines the surface area, for spherical reverse micelles w_0 is directly proportional to the micellar radius.

One common method to interrogate interior of a reverse

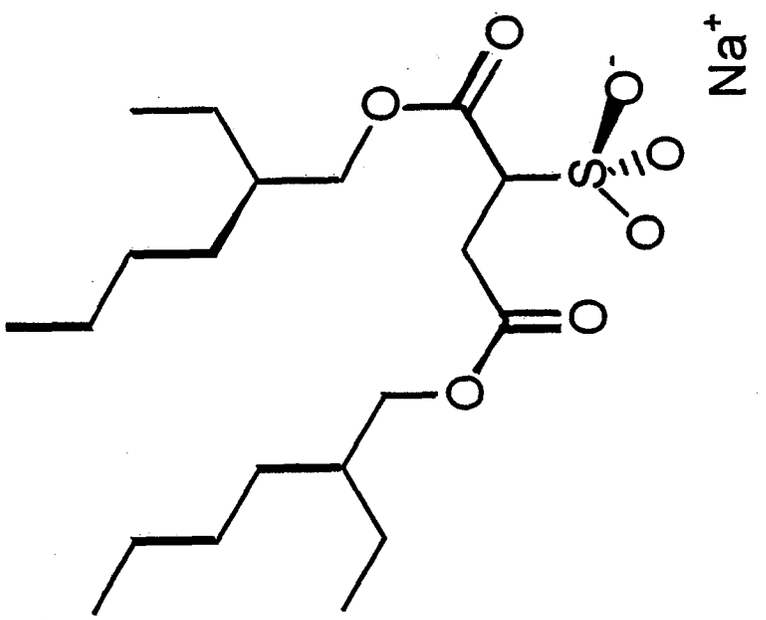

Figure 4.1. Structure of Aerosol-OT (AOT).

micelle is to follow the spectroscopic characteristics of a probe molecule solubilized in the solution forming reverse micelles.[10] A solute can occupy a variety of locations in reverse micelles, for example in the oil phase, in the water pool or near the interface of the reverse micelle.[11] Several spectroscopic studies have investigated the microenvironment of the probe molecule.[10,12] Many studies gauge the environment of the probe by its changing spectroscopy. For example, Correa et al. have used standard micropolarity probe molecules to measure the polarity inside reverse micelles.[13] Gupta et al. report acidity of reverse micellar interiors based on the various spectral signatures of the indicator dye, acridine orange.[14]

Dynamical measurements have also been used to probe the microenvironment of solute molecules in reverse micelles .[15-24] These studies have all found that micellar water behaves more restricted than bulk water. The auramine O probe that Hasegawa et al. used to measure the microviscosity of AOT reverse micelles[19] allowed them to gauge viscosity changes at the inner micellar interface. They found that the microviscosity decreased rapidly for w_0<10 and then decreased more gradually for larger reverse micelles. Altamirano et al. investigated the fluorescence quenching of pyrene derivatives in AOT reverse micelles.[22] They found the fluorescence quenching increased as w_0 increased for

probes located in the water pool, while fluorescence quenching at the interface was much lower than that of water. They attributed this result to the high microviscosity of the interface. Sarker et al. measured nanosecond components of the water solvation motion.[18] These results indicated that water in AOT reverse micelles moves more slowly than bulk water.

Recently, we have explored ultrafast solvation dynamics of water in AOT reverse micelles.[15,16,25] Polar solvation dynamics is the measure of the polar solvent response to an instantaneous change of the charge distribution in a probe molecule. Solvation dynamics of a wide variety of bulk liquids have been well studied both experimentally and theoretically.[26-29] These studies have revealed two different types of solvent motion: an ultrafast time component attributed to an inertial solvent response (<100 fs), and a slower diffusive component (hundreds of femtoseconds to nanoseconds) due to the diffusive solvent motion in response to the probe's new charge distribution. In ternary AOT reverse micelles there is a time component on the femtosecond timescale and another time component on the nanosecond timescale.[15]

One effective method to measure solvation dynamics utilizes time-resolved-fluorescence-upconversion spectroscopy to monitor the time dependent emission spectrum of a fluorescent probe. When the probe is excited, the solvent reorganizes to lower its

free energy conforming to the change in charge distribution leading to an increasing red shift of its fluorescence. Measuring the time dependence of the emission frequency of the solute reveals the solvent's motion back to equilibrium and is quantified by the solvation response function (SRF), C(t), defined as

$$C(t) = \frac{\nu(t) - \nu(\infty)}{\nu(t) - \nu(0)} \qquad (4.2)$$

where $\nu(0)$, $\nu(t)$, $\nu(\infty)$ represent the frequency of fluorescence intensity maximum immediately after excitation, at some time *t* after excitation, and a time sufficiently long enough to ensure the excited solvent configuration is at equilibrium. Thus, one can monitor the interior motion of the microemulsion over time.

In comparison with the extensive information that is available about ternary solutions forming AOT reverse micelles, there are relatively few studies of quaternary AOT micellar systems, especially where an alcohol serves as cosurfactant.[8,30-33] Bardez et al. investigated the OH stretching region of water and found that it is quite sensitive to the polarization effects of the polar headgroups of the micelle surface and the presence of alcohol to the micellar system.[31] Nazario et al. investigated the effect of nonionic cosurfactants on AOT reverse micellar interface and micelle/micelle interactions. [8,32] These studies found that the addition of alkanol to the micellar system increases the percolation temperature, has little affect on the hydrodynamic

radius of the micelle, and decreases the fluidity of the interface. Finally, Plucinski et al. found that short chain alkanols accelerate the mass transfer of phenylalanine into reverse micelles while long chain alkanols inhibit this process.[33]

In the work presented here, we have explored how adding a cosurfactant to AOT reverse micelles impacts the location of a probe molecule by using steady state absorption and fluorescence spectroscopy and time-resolved fluorescence upconversion spectroscopy. We have measured solvation dynamics in quaternary solutions forming AOT reverse micelles and contrast the results with solvation studies in ternary solutions forming AOT reverse micelles. Through these experiments, we determine the effect the addition of a cosurfactant has on the dynamics in reverse micelles.

II. Experimental Methods.

IIA. Sample Preparation. To prepare reverse micellar solutions, the water content of AOT (sodium bis(2-ethylhexyl)sulfosuccinate, Aldrich) was first determined to be 0.43 water molecules per AOT headgroup with NMR. The AOT was then added to isooctane (Acros, ACS spectrophotometric grade) in concentrations ranging from 0.36 M to 0.17 M to which water was added to achieve w_0 values of 5, 10, 15, and 40. 1-heptanol (Fluka, 99% purity) was dried over molecular sieves and

added to the solution. A ratio of 1:5 or 3:5 1-heptanol:AOT was used to ensure that the reverse micelles maintained a spherical form. Reverse micellar radii were measured using dynamic light scattering (DLS, DynaPro, Protein Solutions). Micellar sizes measured using DLS showed that, as w_0 increases, the hydrodynamic radius also increases. This confirms that the micellar solutions swell as water is added to the systems. Also, radii for ternary and quaternary reverse micelles were similar for the same water content.

The anionic dye Coumarin 343 (C343, Exciton) was used without further purification. The dye was added in excess to each of the samples and allowed to sit overnight. The samples were then sonicated for a half hour and filtered to remove any excess dye. Absorption spectra were collected using a Hewlett Packard 8452A Diode Array Spectrophotometer and fluorescence spectra were collected using an ISA Fluorolog Fluorometer. From the absorption spectrum and information about AOT reverse micelle size and surface area [1,8] we estimate that the concentration of dye in the sample was 75 μM, which corresponds to approximately one dye molecule per every 100 micelles. The probability of finding one dye molecule in one micelle is 1/100, given by the binomial distribution; the probability of finding two dye molecules in one micelle is $1/4950=2.0\times10^{-4}$.[34] Thus the measured spectroscopy

and dynamics should arise from individual dye molecules rather than from aggregates.

IIB. Time-resolved studies. Time-resolved fluorescence Stokes shift experiments investigating solvation dynamics were performed via femtosecond fluorescence-upconversion. The experimental apparatus is similar to that reported earlier;[15] only the laser used for the experiment differs. Briefly, the excitation source is a mode-locked Ti:Sapphire laser (KM Labs) pumped by a CW intracavity doubled Nd:VO_4 laser (Verdi, Coherent) at 5 W. The Ti:Sapphire laser produces an output pulse with a 60 fs duration (fwhm assuming a Gaussian pulse shape) at an 80 MHz repetition rate. The spectrum of the pulse is centered at 805 nm. The beam is frequency doubled in a 0.5 mm beta barium borate (BBO) crystal. The frequency-doubled beam is separated from the fundamental beam using a dielectric beam splitter. The frequency doubled light traverses a half wave plate, and focuses onto a 1 mm flow cell through which the sample circulates. A small portion of the forward fluorescence is collected and refocused onto a second 0.5 mm BBO crystal using an ellipsoidal mirror. The fluorescence is upconverted with the residual fundamental beam that has been sent through a variable optical delay. All solvation dynamics measurements are made with the excitation beam polarization at 54.6° with respect to the gate beam to eliminate

effects from probe molecule rotation on the dynamics. The upconverted light is collimated, isolated from the gate and frequency doubled beams with an iris and focused through a UV-transmitting filter (340 nm, Opto-Sigma) into a 0.33 m single monochromator equipped with a 2400 groove/mm grating blazed at 400 nm. The instrument response is determined from the cross correlation of the excitation and gate pulses in the 0.5 mm upconversion crystal. The upconverted photons are detected using an photomultiplier tube at ambient temperature. A personal computer using LabVIEW collects signal from a photon counter as a function of the optical delay between the excitation and gate pulses. Fluorescence upconversion measurements are obtained by counting for one second at each delay. Scans are collected with high, medium, and low resolution in one scan, that is, 17 fs steps for the first 2.0 ps, followed by 200 fs steps for 58 ps, followed 2.5 ps steps for 453 ps for a total of a 512 ps scan. Data are collected at 8-10 different wavelengths to monitor the entire fluorescence spectrum.

We have measured fluorescence lifetimes for the C343 dye in all environments probed using time correlated single photon counting.[35] The lifetimes measured for the various systems are all within 10% of 3 ns, very similar to each other and essentially the same as the dye lifetime in bulk water.

IIC. Data Analysis. The spectral reconstruction method was used to determine the SRF's for water in various reverse micellar samples. This method is described in detail elsewhere.[15] The resulting time-resolved fluorescence upconversion decays were normalized to the steady-state spectrum and fit to multi-exponential functions. Time-resolved fluorescence spectra were constructed from the multi-exponential fits. The resulting spectra were fit to a log-normal function to determine the peak maximum ν(t). The peak maximum was used to calculate the SRF as shown in equation 4.2.

IID. Time-Resolved Fluorescence Anisotropy. Because time-resolved fluorescence anisotropy (TRFA)is an excellent method for tracking the degree and rate of rotation of the probe molecule,[36] we have employed this technique to gauge the location of the dye molecule in the reverse micellar water pool. TRFA measurements were collected utilizing the same system that is used for time-resolved fluorescence upconversion measurements. To determine the anisotropy of the dye molecule, the polarization of the excitation beam is either set to be parallel or perpendicular with respect to the gate beam. The fluorescence is then mixed with the residual gate pulse as in our fluorescence-upconversion experiment. The anisotropy r(t) was calculated via

$$r(t) = \frac{I_{\parallel}(t) - I_{\perp}(t)}{I_{\parallel}(t) + 2I_{\perp}(t)}. \qquad (4.3)$$

Here $I_{||}(t)$ and $I_{\perp}(t)$ are the time-dependent intensities of the signal from parallel and perpendicular excitation, respectively. The rotation of the dye coupled to the micelle should yield a substantially longer rotational correlation time than free dye. From a simple Debye-Stokes-Einstein analysis,[37]

$$\tau_{rot} = \frac{V_m \eta}{k_B T} \tag{4.4}$$

where V_m is the micellar volume, η is the viscosity of the supporting nonpolar phase and T is the temperature, we estimate that the rotational correlation time for a reverse micelle with w_0=5 is approximately 600 ns. Because we collect r(t) data only out to 500 ps, we cannot measure the micellar rotation but we can see if the dye rotation departs from its value in bulk solution indicating it is hindered.

III. Results

III.A. Steady State Spectroscopy. We have measured the steady-state absorption and fluorescence of C343 in a range of environments. Figure 4.2 displays absorption and fluorescence spectra of C343 in quaternary solutions forming AOT reverse micelles for varying hydration level, w_0. Because the steady-state absorption spectra of C343 follow the same trends as the fluorescence spectra, and because the time-resolved measurements are based on fluorescence, we show only the fluorescence spectra here. The C343 spectra shift to longer

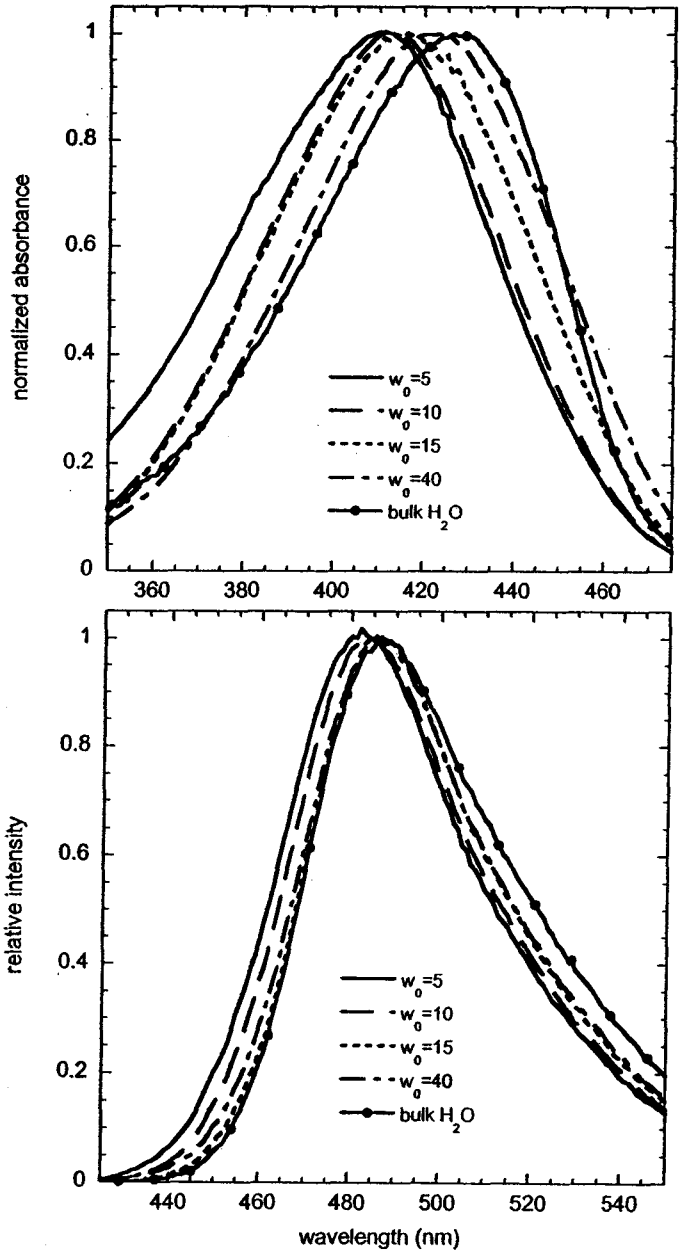

Figure 4.2. Steady-state absorption (a) and fluorescence (b) spectra of Coumarin 343 in water/1-heptanol/AOT/isooctane quaternary reverse micelles as a function of w_0.

wavelengths as w_0 increases, similar to our results for ternary solutions containing AOT reverse micelles.[15] However, even in the reverse micelles with the highest water loading, w_0=40, C343 spectra in the reverse micelles never overlay the spectrum in bulk water. We have measured the C343 spectrum in a range of environments where the dye could be found in the microemulsion samples, including bulk nonpolar solvent and in an alcohol/nonpolar solvent mixture. These spectra are shown in Fig. 4.3 along with the spectrum for C343 in quaternary reverse micelles with w_0=40 and bulk water. The spectra for C343 in the nonpolar solvent and alcohol/nonpolar mixture clearly differ significantly from the spectra of the dye in the reverse micelles. It is clear from the differences in these spectra that the dye resides in the interior of reverse micelles in the quaternary solutions containing reverse micelles. Figure 4.4 contrasts the spectrum of C343 in quaternary and ternary solutions forming reverse micelles with high water loading, w_0=40, and bulk water. At this w_0 level, there is a substantial the water pool formed inside the reverse micelles. We estimate that there a reverse micelle of this size should contain more than 100,000 water molecules,[4] which should be large enough to behave like bulk water. Steady-state infrared spectroscopy indicate bulk like hydrogen bonding characteristics for the water inside reverse micelles with w_0 >10,[38-45] but recent

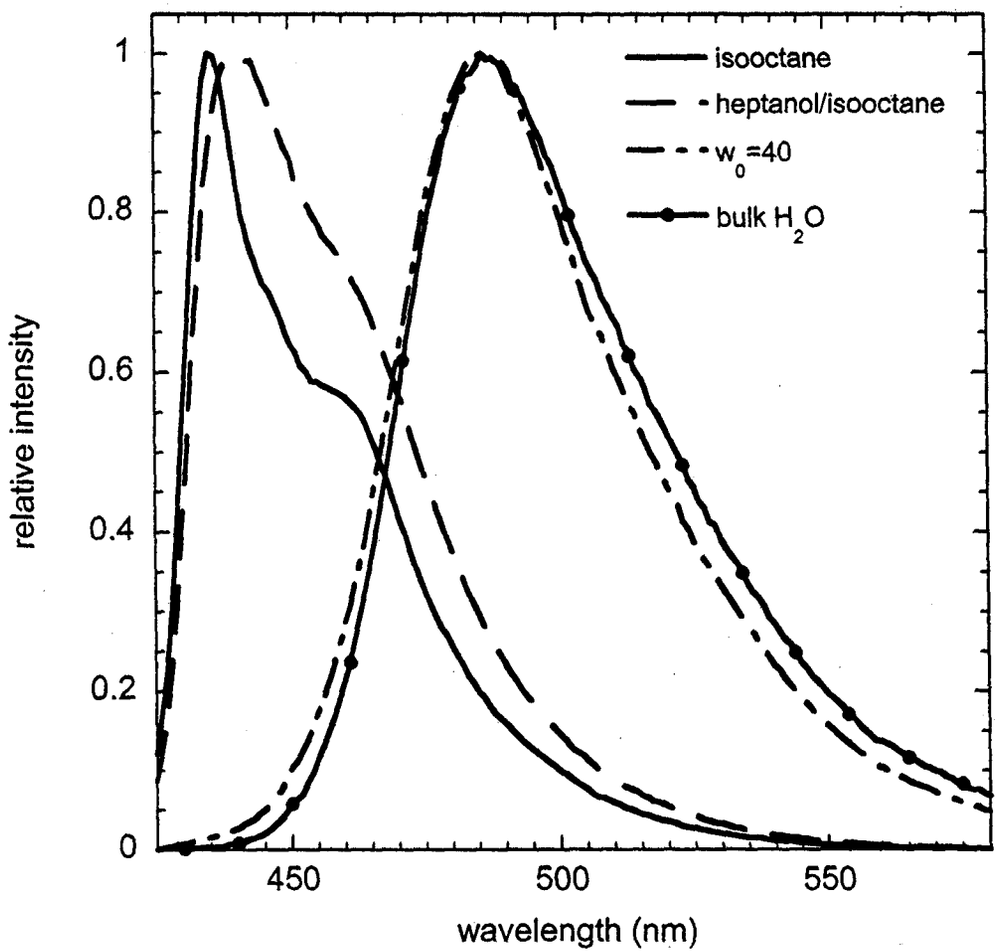

Figure 4.3. Steady-state absorption spectra of C343 in bulk isooctane (——), 1-heptanol-isooctane mixture (— —), ROH:AOT reverse micelles, w_0=40 (— - — -) and bulk water (—•—).

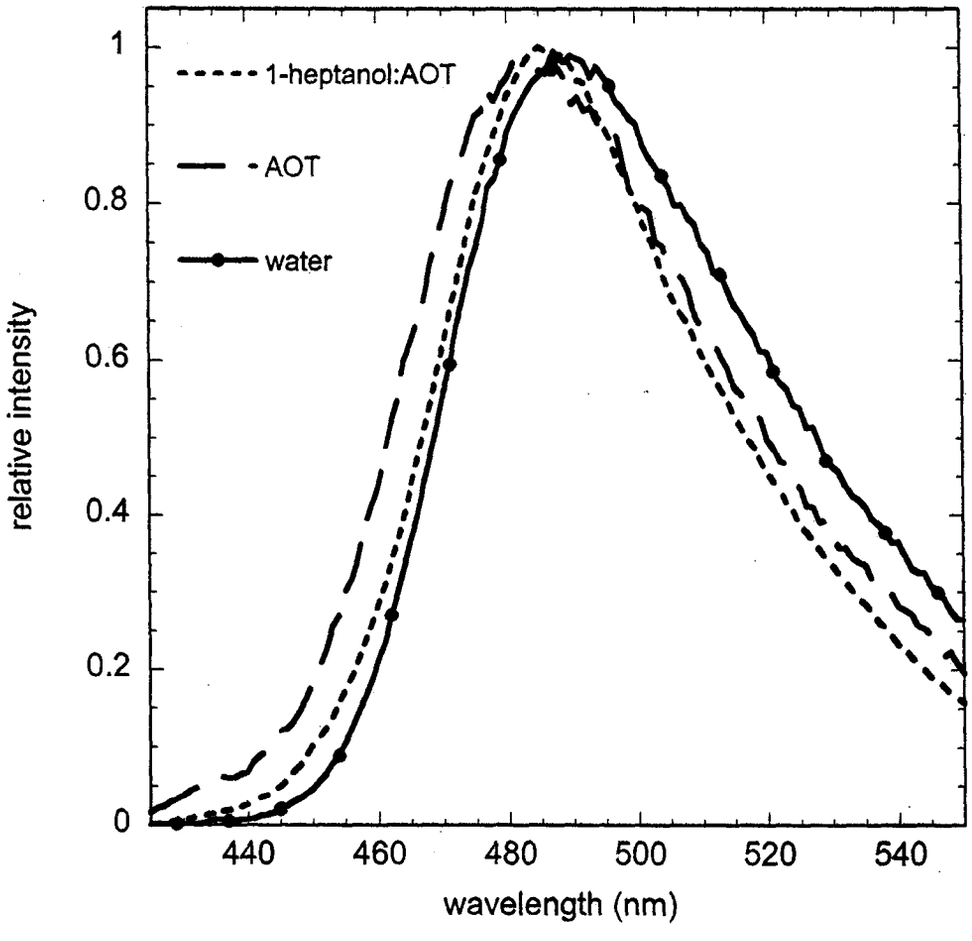

Figure 4.4. Steady-state fluorescence spectra of C343 in ternary AOT/isooctane/water w_0=40 (— —), quaternary AOT/1-heptanol/isooctane/water w_0=40 (- - -), and bulk water (——).

studies utilizing THz spectroscopy[46] have challenged the view that the reverse micellar water pool behaves bulk like even at very high water loading. While they are similar, the C343 spectra in the reverse micelles peak at shorter wavelength compared to the spectrum in bulk water. Also, the spectrum in the ternary system peaks at shorter wavelength and is slightly narrower than the quaternary system. These results indicate that the alcohol cosurfactant, while present in relatively small proportion compared to the AOT surfactant, impacts the environment sensed by the C343 probe molecule.

We have increased the relative heptanol concentration in the sample to explore its effect on the C343 spectroscopy in reverse micelles. Figure 4.5 shows the absorption spectra of C343 in quaternary reverse micelles where we increased the ratio of 1-heptanol: AOT from 1:5 to 3:5. Plotted on the same graph, these spectra nearly overlay the spectra collected for lower 1:5 cosurfactant:surfactant ratio. The similarity in the steady-state spectra for C343 in both quaternary reverse micellar environments suggests that adding more alcohol to the system does not change the local environment sensed by the dye.

III.B. Time Resolved Fluorescence Anisotropy. In addition to steady-state spectroscopy, we can gauge the local environment sensed by the dye through its rotational motion. Time-resolved

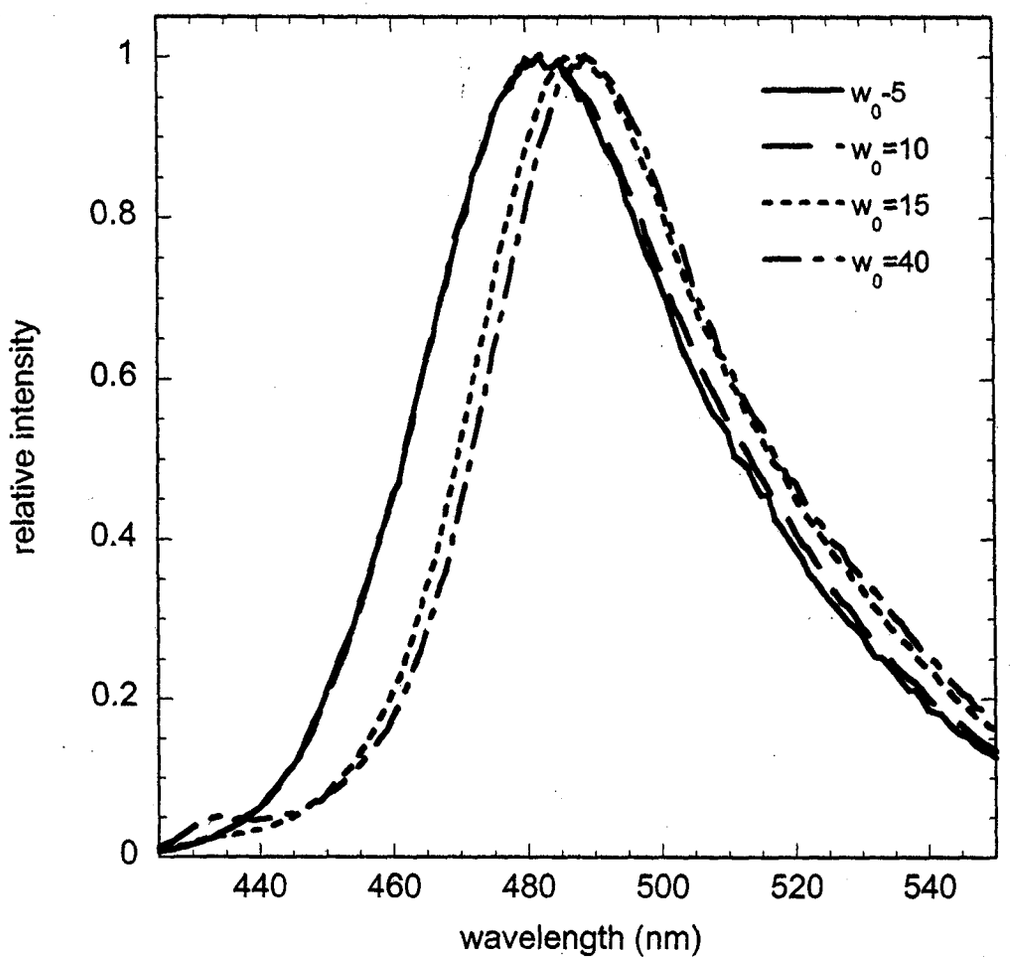

Figure 4.5. Steady-state absorption spectra of C343 in 1-heptanol:AOT 3:5 reverse micelles.

fluorescence anisotropy compares the decay of the fluorescence resulting from excitation with differing polarizations, hence can be used to measure rotational diffusion of a probe molecule as given in equation 4.3.[36] The anisotropy decay for the C343 dye in quaternary microemulsions is significantly slower than in bulk water, as shown in Fig. 4.6. For C343 in bulk solution, *r(t)* fits well to a single exponential decay with a relaxation time 87 ps.[15] In contrast, the anisotropy decay for C343 in AOT:1-heptanol 1:5 w_0=10 fits to a single exponential decay with a time constant of 430 ps plus a long time offset. Anisotropy decays we have measured in ternary solutions forming AOT reverse micelles with $w_0 \geq 7.5$ display biexponential behavior;[15] because the short time component of those decays was similar to the value for the dye in bulk water, we interpreted the results as indicative of the C343 dye residing in a range of locations from the interface to the water pool. The core of a spherical reverse micelle with a water content of w_0=10 should present some water with bulk like characteristics.[47,48] The single 430 ps rotational correlation time measured for the quaternary reverse micelles here indicates that that the dye environment is not like bulk water. As discussed in Section IID, the overall rotation time for the reverse micelles should be substantially longer than what can be measured with

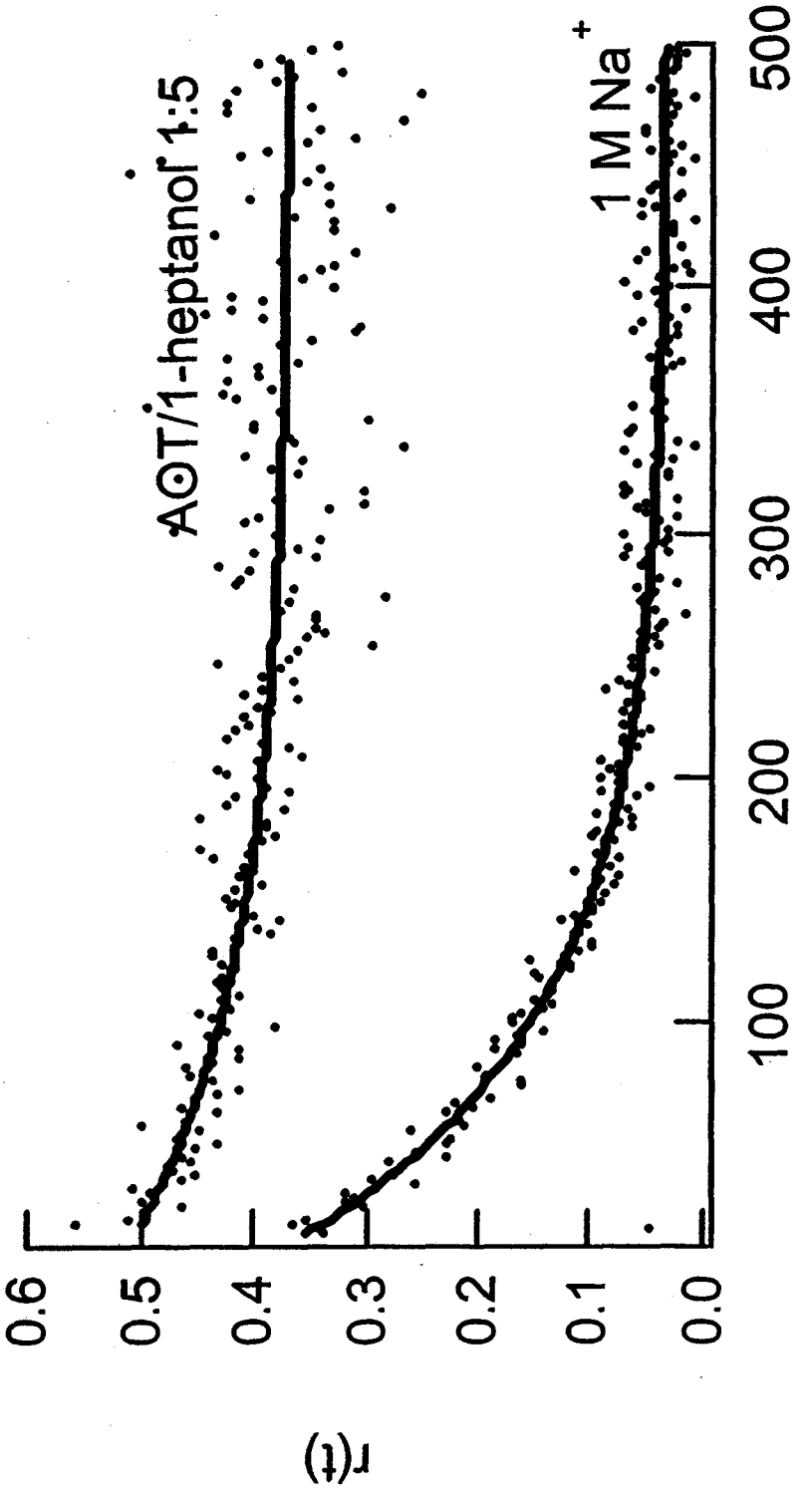

Figure 4.6. Time-resolved fluorescence anisotropy of 1 M Na^+ and AOT/1-heptanol/isooctane/water 1:5 w_0=10.

these experiments. The long time offset displayed by the data most likely arise from rotation of the micelle.

III.C. Solvation Dynamics. We have used our TRFSS measurements to create solvent response functions (SRF) from equation 4.2. The experimentally derived SRFs and fits to biexponential decays are shown as a function of w_0 in Fig. 4.7. To demonstrate the impact that the alcohol cosurfactant has on the solvation dynamics in the reverse micelles, we plot solvent response functions, including the predicted inertial response from time zero analysis,[49] for both ternary and quaternary solutions forming AOT reverse micelles in Fig. 4.7. Solvation relaxation times from multi-exponential fits to the data are given in Table 4.1 along with those for bulk water for comparison. Excluding the data point obtained from time zero analysis, the SRF's for quaternary AOT micellar systems fit well to a biexponential decays with time components of approximately 10 ps and 200 ps. Excluding the inertial component, the solvent response functions for ternary AOT systems require a bi-exponential decay for adequate fitting with time components are on the 200 fs and 3 ps timescale for all hydration levels as seen in Table 4.1.

To explore the role of the heptanol cosurfactant on the solvation dynamics, we measured the SRF in AOT reverse micelles with w_0=5 for differing alcohol fractions, that is, in

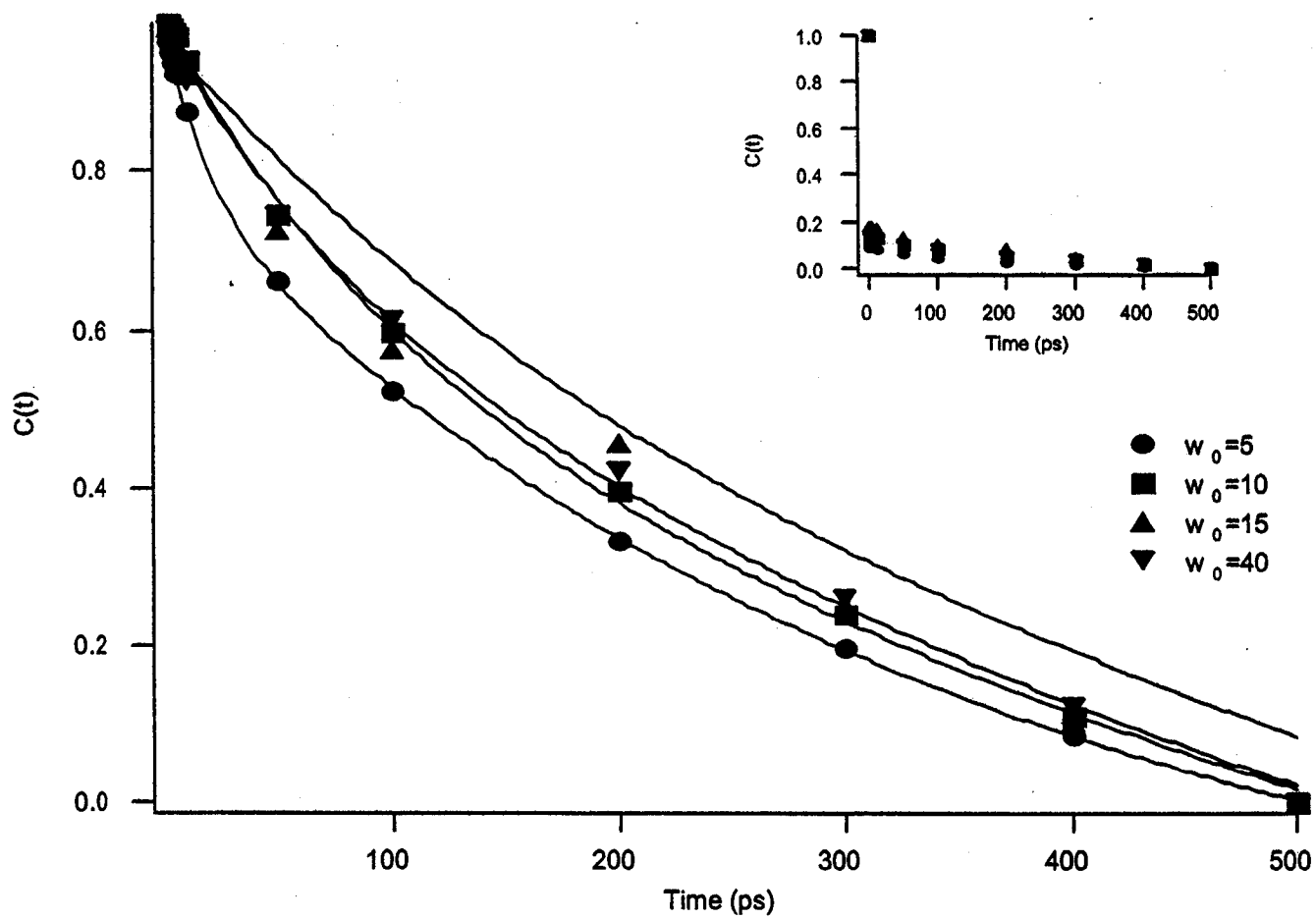

Figure 4.7a. Solvent correlation function, C(t), and multiexponential fits for AOT/1-heptanol/isooctane/water 1:5. Inset. Solvent correlation function including point obtained from time zero analysis.

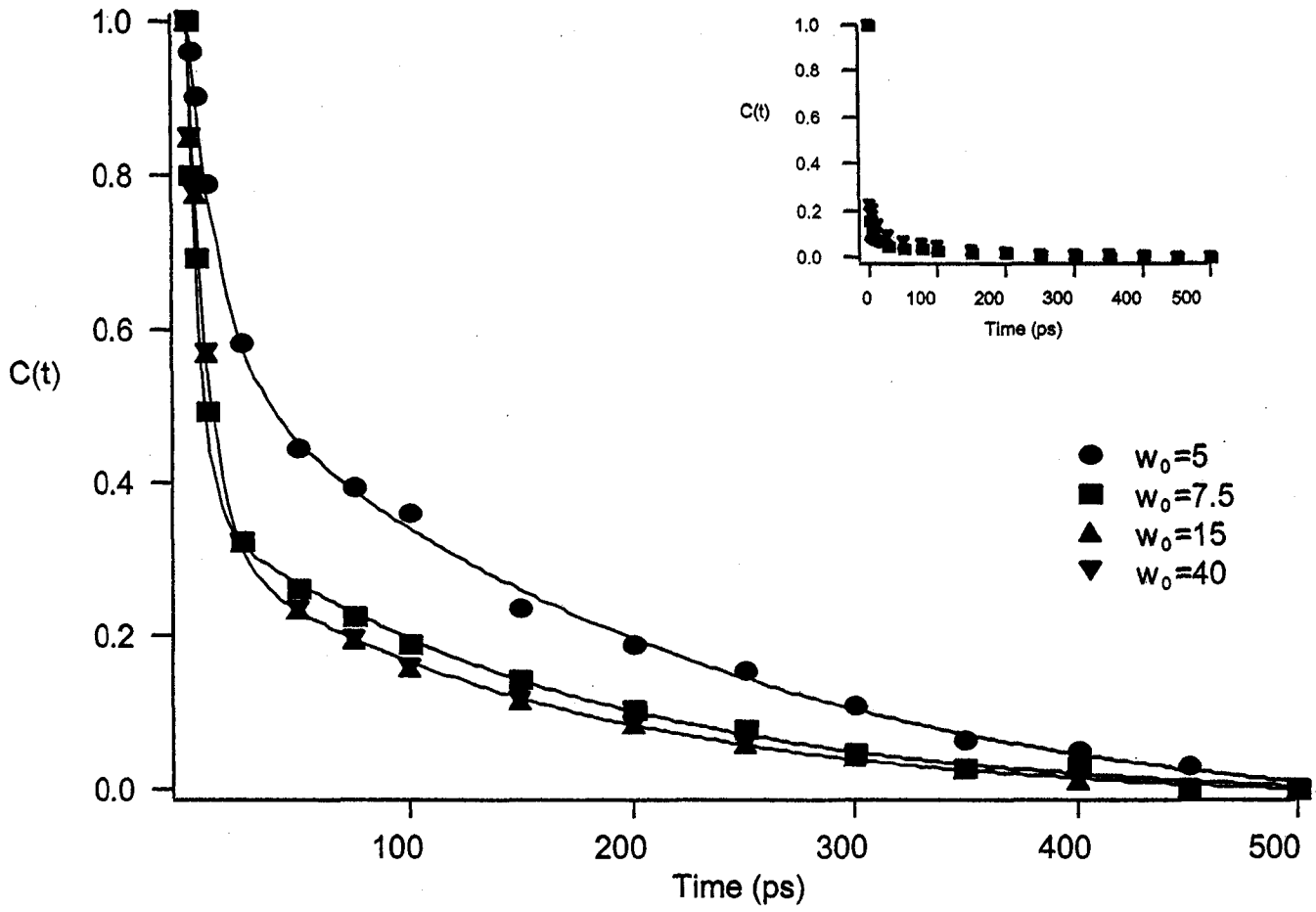

Figure 4.7b. Solvent correlation function, C(t), and multiexponential fits for AOT/isooctane/water. Inset. Solvent correlation function including point obtained from time zero analysis.

systems with the AOT:alcohol ratio equal to 1:5 and 3:5. Similar to the solvation response in the quaternary reverse micelles with lower alcohol content, when we exclude the point from the time zero analysis, the data fit well to a biexponential decay; parameters for the fit are given in Table 4.1. The response seen in this system is quite similar to the time components of the solvent response in the quaternary AOT micellar systems with the lower cosurfactant:surfactant molar ratio of 1:5 (see Table 4.1). The addition of a cosurfactant to AOT micellar systems has an enormous effect on the observed solvation dynamics. Unlike ternary systems we have studied, the time resolved fluorescence traces for quaternary solutions forming AOT micelles lack a decay component occurring on the hundreds of femtosecond to ones of picoseconds time scale.

While the transients from quaternary solutions containing reverse micelles shown in Fig. 4.7 lack diffusive relaxation on a sub-picosecond or picosecond time scale, we predict a large inertial response in the quaternary reverse micelles when we apply the time zero analysis. Thus, it appears that there is a significant portion of the solvent response that occurs on a timescale significantly shorter then we can measure. Reanalysis of ternary AOT micellar systems with time zero analysis reveals that the inertial component also comprises a significant part of the

Sample	1-heptanol:AOT	w_0	r (nm)	Stokes shift (cm^{-1})	r (nm)	C(t) A_1	τ_1 (ps)	A_2	τ_2 (ps)
AOT	1:5	5	3.7	3845	3.7	0.13	11	0.08	200
	1:5	10	4.3	2895	4.3	0.01	21	0.13	210
	1:5	15	4.7	2555	4.7	0.15	0.16	0.16	230
	1:5	40	14.3	2666	14.3	0.008	0.13	0.13	230
AOT	3:5	5	2.5	4022	2.5	0.001	8	0.05	190
AOT[a]	-	5				0.04	0.25	0.05	3.3
	-	7.5				0.13	0.11	0.06	3.0
	-	15				0.18	0.17	0.07	2.8
	-	40				0.15	0.16	0.10	2.3

Table 4.1. Fit parameters of the ultrafast components of the solvent correlation functions for water in various micellar environments.

relaxation, approximately 90% of the total solvent response. Thus, even though we observe solvent motion on the 2 ps time scale in the ternary systems containing AOT micelles, we also miss a large portion of the solvent response occurring on the sub 100 femtosecond time scale.

IV. Discussion

It is clear from the data presented above that the dynamics recorded by the C343 probe molecule in the quaternary solutions forming reverse micelles differ drastically from both ternary AOT reverse micelle systems and from bulk water despite the similarities in the steady-state spectra. Because the steady-state spectra shift as a function of water content, w_0, we expected that the TRFSS response would be similar to our results for ternary solutions containing reverse micelles. While we have observed changing solvation dynamics as a function of w_0 for ternary solutions forming AOT reverse micelles,[15] the solvation dynamics in the quaternary reverse micelles appear relatively insensitive to the amount of water solubilized in the micellar interior, as shown in Fig. 4.7. In addition, in both ternary and quaternary reverse micellar systems we predict an enormous ultrafast response, significantly higher than what is observed for bulk water. At the same time, the timescale for diffusive relaxation in the quaternary

reverse micelles is substantially slower than it is for the ternary reverse micelles. This strongly suggests that the alcohol cosurfactant present in the quaternary reverse micelles plays a substantial role in determining the solvation dynamics. However, the concentration of heptanol in the AOT micellar systems does not appear to have a strong impact of the solvation dynamics.

Because the alcohol cosurfactant affects the observed solvation dynamics, we considered the possibility that that the solvation dynamics merely reflect bulk alcohol relaxation. Indeed, longitudinal relaxation times from dielectric relaxation studies suggest that the solvation dynamics observed in 1-heptanol should have a characteristic relaxation time of ~150 ps.[28,50-52] Previous reports in the literature show that alcohol molecules added to solutions containing reverse micelles associate with the self assembled structures rather than existing dispersed or as aggregates in the supporting nonpolar solvent, especially in systems such as the ones presented here where the overall concentration of alcohol in the reverse micellar solutions is quite low compared to other components, particularly the surfactant. In addition, the steady-state fluorescence spectrum of C343 in a mixture of heptanol dissolved in alkane solvent possesses a distinctly different shape from the steady state spectra measured in samples containing reverse micelles, as shown in Fig. 4.3.

Hence, it is highly unlikely that the dynamics observed arise from solvation by the heptanol alone.

In another possible scenario, the heptanol molecules would aggregate in to "rafts" at the reverse micellar interface. In the smallest reverse micelles we measure, we estimate only 15 heptanol molecules per micelle. Aggregates of heptanol molecules in the reverse micellar interface would cause the micellar surface curvature to change leading to ellipsoidal rather than spherical droplets. We measure similar particle sizes and polydispersities for reverse micelles in ternary and quaternary solutions of a given w_0 value, which shows that the added heptanol does not cause significant changes in micelle shape. Thus, it is unlikely that the heptanol cosurfactant present in these reverse micelles exists aggregated in the interface. We are confident that the long time relaxation component observed for the reverse micelles formed in quaternary systems is not due to solvation by bulk heptanol or by heptanol aggregates in the micellar interface.

Because the diffusive relaxation observed does not vary substantially and shows essentially no dependence on the water content inside the reverse micelles, one possible way that the addition of alcohol could influence the measured solvation dynamics would be by facilitating the C343 dye probe to partition

into the reverse micellar interface. This should provide a reasonably similar environment for the dye regardless of w_0 value. If the dye were embedded in the interface, the environment experienced by the dye in the interface could be similar to the environment present in an ordered liquid crystal. Rau et al. report solvation dynamics experiments performed in alkylcyanobiphenyl liquid crystal solutions.[53] They observe multiple timescales for the solvation dynamics, ranging from tens of ps to ns. They attribute the dynamics occurring on the tens of ps timescale as characteristic of the liquid crystalline interactions. Saielli et al. measured solvation dynamics in a nematic liquid crystal mixture.[54] Their results suggest that the local environment rather than long range order dominates the observed dynamics. The results presented here do not resemble results of either liquid crystal work suggesting that the environment sensed by the C343 dye probe is not like a liquid crystal. In addition, while the solvation dynamics show no dependence on w_0, the steady state spectra do reflect water content in the reverse micelles. Thus, it seems unlikely that the dye resides intercalated into the micellar interface. Addition of an alkanol such as heptanol to AOT reverse micelles has been shown to increase the rigidity of the interface.[8,33] Researchers hypothesize that this results from the alcohol partitioning into the alkyl chain region increasing the curvature of

the interface. Increased interfacial rigidity should reduce the propensity for the dye to intercalate into the interfacial region. However, it is possible that increasing rigidity of the interface induces the interfacial water to move significantly differently from bulk water.

Interfacial microviscosity can be estimated from time resolved fluorescence anisotropy. Our results from time-resolved fluorescence anisotropy of C343 in water/AOT/heptanol/isooctane reverse micellar systems yield a single rotational correlation time with a time constant significantly longer than what we measure in bulk aqueous solution.[15] Our previous measurements of time-resolved fluorescence anisotropy in ternary solutions forming AOT reverse micelles showed a bimodal response for the dye, with one component similar in time scale to the dye in bulk solution and one that was much slower. We interpreted these data as suggesting the dye resided in a range of locations within the reverse micelles, sometimes at the inner interface (but not embedded) and sometimes diving into the micellar core.[15] In contrast, the anisotropy decay we observe in the quaternary solutions forming AOT reverse micelles displays only a single, long time component and a baseline offset. Furthermore, the decay time matches neither the rotation time for C343 in water nor the rotation time of the reverse micelle. This suggests that the

rotation of the dye molecule is hindered. Comparing the results for the rotation of C343 in bulk water and using the Debye-Stokes-Einstein treatment, equation 4.4, we predict that the local viscosity sensed by the dye is nearly 5 times that of bulk water. Andrade et al. suggest that microviscosity inside the reverse micelles is six to nine times lower than in bulk water.[55]

Various solvation dynamics studies have considered the relation of solvent viscosity and solvation dynamics or dielectric friction. Recently, researchers measuring polar solvation dynamics in ionic liquid solutions have found a direct connection between viscosity and the observed dynamics.[56-61] In particular, Maroncelli and coworkers observe a slower component of the solvation dynamics relaxing on the 100s of picoseconds time scale, that tracks the viscosity of the ionic solution and a very fast component, shorter than 5 ps, that is too fast for them to resolve.[56,57] They interpret the slow component of the observed relaxation as due to translational motion of molecules in the ionic liquid and the fast, unresolvable motion as due to small local fluctuations that effectively relax the local environment. The slow response we observe in our reverse micelles that is interdependent of micelle water content could reflect increased solvent viscosity at the micellar interface. Abuin et al. measured the impact of adding alcohol cosurfactants to AOT reverse

micelles through the spectroscopy of several molecular probes. [62] They observed decreasing fluorescence lifetimes for fluorescent probe molecules solubilized in AOT when alcohol cosurfactants, such as hexanol, were added to the reverse micelles. Comparisons of micropolarity and fluorescence lifetime data led Abuin et al. to suggest that the interfacial microviscosity increases upon alcohol cosurfactant addition to the AOT reverse micelles.[62] The similarity of the dynamics observed in ionic liquids to what we observe for solvation dynamics in the quaternary solutions containing reverse micelles, evidence of increased interfacial viscosity from other experiments on reverse micelles, and our own time-resolved fluorescence anisotropy experiments leads us to hypothesize that the solvation dynamics reported by the C343 probe molecule reflects a viscous environment that has characteristics similar to ionic liquids. Given the high concentration of ion pairs expected at the interface, it is not surprising that the interfacial region resembles an ionic liquid. At the same time, it is interesting that adding heptanol to the interfacial region appears to impact the interfacial viscosity and also causes the probe molecule to reside in this region of increased viscosity. Garcia-Rio et al. report that addition of alkanol to the interface causes the interface to become more hydrophobic as alkanol molecules replace water molecules

at the interface.[63] For our solvation dynamics experiments, this should create a more favorable environment for C343.

In the measurements reported here, we miss a large portion of the solvation dynamics because our apparatus cannot resolve dynamics on a time scale shorter than 100 fs. We predict a substantial portion of the relaxation occurs on this time scale. Ultrafast relaxation at lipid interfaces has been observed in other systems. Most specifically, Bursing et al. observed a substantial 9 fs component to the relaxation in three pulse photon echo spectroscopy measurements at the surface of phospholipids vesicles.[64] Apparently, small amplitude, very fast fluctuations present at the interface are sufficient to relax the nonequilibrium milieu created when the probe molecule is promoted to the excited state.

Finally, these studies indicate the importance of multiple measurements to characterize a system. In order to assess the environment of a probe molecule in a heterogeneous system, coupling steady-state experiments with dynamical studies can help to fully understand the local environment of a probe molecule. A perusal of our steady-state spectroscopy data alone might cause one to conclude that the dye molecule migrates into the free water pool as the hydration level increases. This hypothesis is further supported by the IR spectroscopic results by

Bardez et al. that shows three distinct types of water in quaternary solutions forming AOT reverse micelles for which the probe molecule to reside.[31] In addition, our steady-state spectroscopy results suggest that there is a change in micropolarity of the dye molecule as a function of w_0 in direct opposition to the dynamical results that show that the micropolarity as well as the microviscosity of the dye environment does not change with water loading.

V. Conclusion.

These experiments reported here show how the addition of heptanol to AOT reverse micelles significantly slows solvent reorganization in the reverse micelles suggesting that the probe molecule, C343, is located in a highly viscous environmentat the reverse micellar interface regardless of w_0. In addition, the solvation dynamics in these quaternary systems exhibit no bulk like water diffusive relaxation as previously observed in the ternary systems.[15] While steady-state absorption and fluorescence spectra of C343 in the quaternary solutions forming AOT reverse micelles show similar red shifts as a function of increasing w_0 as do the steady-state spectra of C343 in the ternary solutions forming AOT reverse micelles, dynamical measurements clearly show that the dye molecule samples significantly different environments in the related microemulsion systems. Hence,

steady-state spectroscopy alone may not be sufficient when using a molecule to probe properties in these heterogeneous systems.

Acknowledgements: This material is based upon work supported by the National Science Foundation under Grant Number 0075266. RER gratefully acknowledges support for a sabbatical leave from Agnes Scott College.

References:

(1) De, T. K.; Maitra, A. *Advances in Colloid and Interface Science* **1995**, *59*, 95.

(2) Nave, S.; Eastoe, J.; Heenan, R. K.; Steytler, D.; Grillo, I. *Langmuir* **2000**, *16*, 8741.

(3) Caponetti, E.; Magid, L. J.; Hayter, J. B.; Johnson, J. S. *Langmuir* **1986**, *2*, 722.

(4) Zulauf, M.; Eicke, H. F. *Journal of Physical Chemistry* **1979**, *83*, 480.

(5) Borkovec, M. *Journal of Chemical Physics* **1989**, *91*, 6268.

(6) Carlstrom, G.; Halle, B. *Journal of Physical Chemistry* **1989**, *93*, 3287.

(7) Dunn, C. M.; Robinson, B. H.; Leng, F. J. *Spectrochimica Acta Part. A- Molecular Biomolecular Spectroscopy* **1990**, *46*, 1017.

(8) Nazario, L. M. M.; Hatton, T. A.; Crespo, J. *Langmuir* **1996**, *12*, 6326.

(9) Kinugasa, T.; Kondo, A.; Nishimura, S.; Miyauchi, Y.; Nishii, Y.; Watanabe, K.; Takeuchi, H. *Colloid Surfaces A-Physicochemical and Engineering Aspects* **2002**, *204*, 193.

(10) Silber, J. J.; Biasutti, A.; Abuin, E.; Lissi, E. *Advances in Colloid and Interface Science* **1999**, *82*, 189.

(11) Pileni, M. P. *Journal of Physical Chemistry* **1993**, *97*, 6961.

(12) Chaudhuri, R.; Sengupta, P. K.; Mukherjee, K. K. R. *J. Photochemistry and Photobiology A- Chemistry* **1997**, *108*, 261.

(13) Correa, N. M.; Biasutti, M. A.; Silber, J. J. *Journal of Colloid and Interface Science* **1995**, *172*, 71.

(14) Gupta, S.; Mukhopadhyay, L. *Indian J. Chem. Sect A-Inorg. Phys. Theor. Anal. Chem.* **1997**, *36*, 31.

(15) Riter, R. E.; Willard, D. M.; Levinger, N. E. *Journal of Physical Chemistry B* **1998**, *102*, 2705.

(16) Riter, R. E.; Undiks, E. P.; Levinger, N. E. *Journal of the American Chemical Society* **1998**, *120*, 6062.

(17) Riter, R. E.; Undiks, E. P.; Kimmel, J. R.; Levinger, N. E. *Journal of Physical Chemistry B* **1998**, *102*, 7931.

(18) Sarkar, N.; Das, K.; Datta, A.; Das, S.; Bhattacharyya, K. *Journal of Physical Chemistry* **1996**, *100*, 10523.

(19) Hasegawa, M.; Sugimura, T.; Kuraishi, K.; Shindo, Y.; Kitahara, A. *Chemical Letters* **1992**, 1373.

(20) Zhang, J.; Bright, F. V. *Journal of Physical Chemistry* **1991**, *95*, 7900.

(21) Cho, C. H.; Chung, M.; Lee, J.; Nguyen, T.; Singh, S.; Vedamuthu, M.; Yao, S. H.; Zhu, J. B.; Robinson, G. W. *Journal of Physical Chemistry* **1995**, *99*, 7806.

(22) Altamirano, M. S.; Borsarelli, C. D.; Cosa, J. J.; Previtali, C. M. *Journal of Colloid and Interface Science* **1998**, *205*, 390.

(23) Hazra, P.; Chakrabarty, D.; Sarkar, N. *Chemical Physics Letters* **2003**, *371*, 553.

(24) Hazra, P.; Chakrabarty, D.; Sarkar, N. *Langmuir* **2002**, *18*, 7872.

(25) Willard, D. M.; Riter, R. E.; Levinger, N. E. *Journal of the American Chemical Society* **1998**, *120*, 4151.

(26) Barbara, P. F.; Walker, G. C.; Kang, T. J.; Jarzeba, W. **1990**, *1209*, 18.

(27) Maroncelli, M.; Macinnis, J.; Fleming, G. R. *Science* **1989**, *243*, 1674.

(28) Horng, M. L.; Gardecki, J. A.; Papazyan, A.; Maroncelli, M. *Journal of Physical Chemistry* **1995**, *99*, 17311.

(29) Stratt, R. M.; Maroncelli, M. *Journal of Physical Chemistry* **1996**, *100*, 12981.

(30) Perez-Casas, S.; Castillo, R.; Costas, M. *Journal of Physical Chemistry B* **1997**, *101*, 7043.

(31) Bardez, E.; Giordano, R.; Jannelli, M. P.; Migliardo, P.; Wanderlingh, U. *Journal of Molecular Structure* **1996**, *383*, 183.

(32) Nazario, L. M. M.; Crespo, J.; Holzwarth, J. F.; Hatton, T. A. *Langmuir* **2000**, *16*, 5892.

(33) Plucinski, P.; Reitmeir, J. *Colloid Surfaces A-Physicochemical and Engineering Aspects* **1995**, *97*, 157.

(34) Lindgren, B. W.; McElrath, G. W.; Berry, D. A. *Introduction to Probability and Statistics*; Macmillan Publishing Co., Inc.: New York, 1978.

(35) Corbeil, E. M.; Levinger, N. E. *Langmuir* **2003**, *19*, 7264.

(36) Lakowicz, J. R. *Principles of Fluorescence Spectroscopy*; Plenum Press: New York, 1983.

(37) Debye, P. J. W. *Polar Molecules*; Chemical Catalog Co.: New York, 1929.

(38) Chattopadhyay, A.; Mukherjee, S.; Raghuraman, H. **2002**, *106*, 13002.

(39) Freda, M.; Onori, G.; Paciaroni, A.; Santucci, A. *Physical Chemistry Chemical Physics* **2002**, *101*, 55.

(40) Li, Q.; Li, T.; Wu, J. G. *Journal of Physical Chemistry B* **2000**, *104*, 9011.

(41) D'Angelo, M.; Fioretto, D.; Onori, G.; Santucci, A. *Physical Review E* **1998**, *58*, 7657.

(42) Novaki, L. P.; El Seoud, O. A. *Journal of Colloid and Interface Science* **1998**, *202*, 391.

(43) Temsamani, M. B.; Maeck, M.; El Hassani, I.; Hurwitz, H. D. *Journal of Physical Chemistry B* **1998**, *102*, 3335.

(44) Dangelo, M.; Fioretto, D.; Onori, G.; Santucci, A. *Journal of Molecular Structure* **1996**, *383*, 157.

(45) Moran, P. D.; Bowmaker, G. A.; Cooney, R. P.; Bartlett, J. R.; Woolfrey, J. L. *Langmuir* **1995**, *11*, 738.

(46) Boyd, J. E.; Briskman, A.; Sayes, C. M.; Mittleman, D.; Colvin, V. *Journal of Physical Chemistry B* **2002**, *106*, 6346.

(47) Faeder, J.; Ladanyi, B. M. *Journal of Physical Chemistry B* **2000**, *104*, 1033.

(48) Faeder, J.; Ladanyi, B. M. *Journal of Physical Chemistry B* **2001**, *105*, 11148.

(49) Fee, R. S.; Maroncelli, M. *Chemical Physics* **1994**, *183*, 235.

(50) Laitinen, E.; Salonen, K.; Harju, T. *Journal of Chemical Physics* **1996**, *104*, 6138.

(51) Laitinen, E.; Korppi Tommola, J.; Linnanto, J. *Journal of Chemical Physics* **1997**, *107*, 7601.

(52) Moog, R. S.; Maroncelli, M. *Journal of Physical Chemistry* **1991**, *95*, 10359.

(53) Rau, J.; Ferrante, C.; Deeg, F. W.; Brauchle, C. *Journal of Physical Chemistry B* **1999**, *103*, 931.

(54) Saielli, G.; Polimeno, A.; Nordio, P. L.; Bartolini, P.; Ricci, M.; Righini, R. *Journal of the Chemical Society- Faraday Transactions* **1998**, *94*, 121.

(55) Andrade, S. M.; Costa, S. M. B. *Photochemical and Photobiological Science* **2002**, *1*, 500.

(56) Arzhantsev, S.; Ito, N.; Heitz, M.; Maroncelli, M. *Chemical Physics Letters* **2003**, *381*, 278.

(57) Ingram, J. A.; Moog, R. S.; Ito, N.; Biswas, R.; Maroncelli, M. *Journal of Physical Chemistry B* **2003**, *107*, 5926.

(58) Chakrabarty, D.; Harza, P.; Chakraborty, A.; Seth, D.; Sarkar, N. *Chemical Physics Letters* **2003**, *381*, 697.

(59) Karmakar, R.; Samanta, A. *Journal of Physical Chemistry A* **2003**, *107*, 7340.

(60) Karmakar, R.; Samanta, A. *Journal of Physical Chemistry A* **2002**, *106*, 6670.

(61) Karmakar, R.; Samanta, A. *Journal of Physical Chemistry A* **2002**, *106*, 4447.

(62) Abuin, E.; Lissi, E.; Ceron, A.; Rubio, M. A. *Journal of Colloid and Interface Science* **2003**, *258*, 363.

(63) Garcia-Rio, L.; Herves, P.; Mejuto, J. C.; Perez-Juste, J.; Rodriguez-Dafonte, P. *Journal of Colloid and Interface Science* **2000**, *225*, 259.

(64) Bursing, H.; Kundu, S.; Vohringer, P. *Journal of Physical Chemistry B* **2003**, *107*, 2404.

Chapter 5

Conclusion

The overall goal of this work was to investigate solvent motion in quaternary reverse micelles. Specifically, we first investigated the effects cationic versus anionic surfactants have on solvent motion in reverse micelles. We then investigated the effects different alkanol chain lengths have on solvent motion in CTAB reverse micelles. In these studies, we discovered that the motion was significantly reduced in quaternary reverse micelles relative to both ternary reverse micelles and bulk water. The solvent responses of these systems had a significant inertial portion that was much larger than that found in bulk water but similar to that in ternary AOT reverse micelles. Also in all of the systems studied we observed a diffusive component, which is an order of magnitude slower than in ternary reverse micelles.[1]

These experiments are the first experiments that explore solvent motion in quaternary reverse micelles. Originally, we anticipated that solvent motion in quaternary micellar systems would be similar to ternary reverse micelles. Contrary to expectation, we found that as the hydration of the reverse micelle increased there was no change in the probe environment in CTAB reverse micelles. We also discovered that increasing the alkanol chain length in CTAB/cyclohexane micellar systems has no

change in the probe environment. The solvent response in these systems found to be independent of w_0 as well as alkanol chain length. We then explored how changing the surfactant affects the solvent response in quaternary reverse micelles. The solvent response in SDS reverse micelles was slightly faster then that observed in CTAB reverse micelles. Still, the solvent response was much slower than that observed in ternary reverse micelles. From all of these studies, we concluded that the probe is located near the interface and thus collective motion of the interface is responsible for the solvent response.

Upon the startling discovery that the solvent response is independent of hydration, alkanol chain length, and surfactant, we explored solvent motion in AOT reverse micelles. AOT was chosen because this surfactant can form both ternary and quaternary reverse micelles. Steady-state spectroscopy for ternary and quaternary AOT micellar systems revealed the migration of the probe molecule into the free water pool as hydration increased. However, time-resolved fluorescence spectroscopy studies indicated that the solvent motion in quaternary reverse micelles was drastically different from ternary micellar systems. In both of the systems studied, we observed an enormous inertial component that is much faster than we are capable of observing. In quaternary AOT micellar systems, we

observed a diffusive response that was on the order of several hundred picoseconds. This time component was also observed in both CTAB and SDS reverse micelles indicating that the dye molecule is probing the interfacial region in all of the micellar systems explored.

Surprisingly, we observe similar relaxation components for all the quaternary reverse micelles we examined. In general, we found a large femtosecond component due to inertial solvation dynamics and a several hundred picosecond diffusive component. These components vary to some extent between systems. However, the greatest variation arises from the relative amplitudes associated with each component. We also attribute some variation in solvent response from anionic and cationic surfactants. These results are surprising because they suggest that in general the solvent response is independent of hydration level, chain length, and surfactant. Hence, we conclude that we are observing the solvent response due to collective motion of the interface. We were unable to conclude if alkanol was solely responsible for the solvent response because there was no change in the solvent motion in when we increased the alkanol concentration in AOT micellar systems. We were also unable to attribute the solvent response to frozen or partially bound water because the solvent response was independent of hydration.

From the results of this study, we suggest a number of possible research directions. First of all, due to the limitations of our experimental setup, the observed dynamics were limited to approximately 150 fs, which was the instrumental response. As we have shown with time zero analysis, we are missing approximately 80% to 90% of the solvent response. Three photon echo experiments provide a different way to explore the solvent response. Secondly, it would be interesting to explore secondary and tertiary alkanols in quaternary reverse micelles. This is because the tails of the alkanols could spread out similar to AOT and create a more fluid interface. Thus we would expect much faster solvation dynamics at the interface.

Finally, the solvation dynamics at the interface of these quaternary reverse micellar systems should be investigated using a probe molecule that has been covalently bonded to the surfactant headgroup. These experiments would potentially reveal if the solvent motion is from collective motion of the interface or if the solvation dynamics is due to frozen or partially bound water molecules. As a result, these proposed studies will lead to a better understanding of the fluidity of the interface.

Reference:

(1)Riter, R. E.; Willard, D. M.; Levinger, N. E. *Journal of Physical Chemistry* **1998**, *102*, 2705-2714.

Appendix 1

Data Analysis

This section describes how to analyze single wavelength fluorescence transients to generate the solvent response function, C(t). The data analysis involves first fitting the time resolved fluorescence transients to an exponential decay convolved with a Gaussian. We then normalize the time resolved fluorescence transients to the steady-state fluorescence spectrum. After this, we reconstruct the time resolved fluorescence transients and from this we are able to construct the time evolving fluorescence spectrum. The data analysis process involves many different processes. Fitting the time resolved fluorescence transients is most easily done in RFGraph (Fayer Group), but it can also be done in Igor (WaveMetrics), or in Origin (OriginLab). Most of the mathematical manipulation is easily done in a data base management program such as Excel (Microsoft) or Origin (OriginLab). Finally, the other fitting processes that are required for data analysis can be done in KaleidaGraph (Synergy), Igor (Wavemetrics), or Origin (OriginLab).

1. Set the baseline of a time resolved fluorescence transient to the signal before the fluorescence appears:

$$I = I_t - I_{\min} \qquad \text{(A.1)}$$

where I_t is the fluorescence intensity at time, t, and I_{min} is the minimum fluorescence intensity (before the fluorescence appears) for the fluorescence transient.

2. Normalize the fluorescence transient using the following equation:

$$I_n = I / I_{\max} \qquad \text{(A.2)}$$

where I_n is the normalized fluorescence transient, I is the fluorescence intensity from step 1 and I_{max} is the maximum fluorescence intensity, after background subtraction, for a given fluorescence transient.

3. After normalizing the fluorescence transient, fit the fluorescence transient to an exponential decay convolved with a Gaussian:

$$y = \exp(-x^2 / 2s^2) \otimes \sum a_n \exp(-x / t_n) \qquad \text{(A.3)}$$

where a_n is the amplitude for the exponential fit, t_n is the time component for the exponential fit, and s is the width of the Gaussian. The first 3 steps can easily be done in RFGraph (Fayer Group).

4. Repeat this procedure for all of the fluorescence transients

5. Reconstruct the time resolved fluorescence transients by imputing values for x in the exponential fit obtained in step 3 (ignore the Gaussian portion of this fit). Use time components, x, ranging from 33 fs to the longest time component of the time resolved fluorescence transient. This procedure is shown in Table A.1.
6. Normalize the steady-state fluorescence spectrum and fit the spectrum to a lognormal function:

$$F(\nu) = h\exp(-\ln(2) + (\ln(1 + (2\gamma(\nu - \nu_t)/\Delta))/\gamma)^2) \qquad \text{(A.4)}$$

where h is the height of the fluorescence spectrum, γ is the asymmetry parameter, ν_t is the peak frequency and Δ is the width parameter. This can be done in any fitting program such as KaleidaGraph (Synergy), Igor (WaveMetrics), or Origin (OriginLab).
7. Set the intensity for the longest time component of a fluorescence transient for a given wavelength equal to the intensity of the steady-state fluorescence spectrum for that wavelength as shown below

$$c_\lambda = \frac{I_{\lambda ss}}{I_{\lambda t}} \qquad \text{(A.5)}$$

where c_λ is a constant for a given wavelength, $I_{\lambda t}$ is the fluorescence intensity of the longest time component at a given wavelength, and $I_{\lambda ss}$ is the fluorescence intensity of

Wavelength (nm)	0.033	0.067	0.1	1	2	3	4	5	10	50	400	500
440	0.99	0.99	0.99	0.99	0.98	0.98	0.97	0.96	0.93	0.75	0.35	0.32
450	1.19	1.19	1.18	1.16	1.14	1.11	1.09	1.07	0.99	0.76	0.37	0.33
460	1.50	1.50	1.50	1.49	1.48	1.47	1.46	1.46	1.42	1.17	0.60	0.55
470	0.99	0.99	0.99	0.99	0.99	0.99	0.99	0.99	0.98	0.93	0.62	0.56
480	0.89	0.89	0.89	0.89	0.89	0.89	0.89	0.89	0.88	0.86	0.68	0.63
490	0.81	0.81	0.81	0.81	0.81	0.81	0.81	0.81	0.81	0.80	0.71	0.68
500	0.89	0.89	0.89	0.89	0.89	0.89	0.89	0.89	0.89	0.89	0.78	0.74
510	0.88	0.88	0.88	0.87	0.87	0.87	0.87	0.87	0.87	0.86	0.73	0.69
520	0.65	0.65	0.65	0.65	0.65	0.65	0.65	0.66	0.66	0.70	0.85	0.85
530	0.44	0.44	0.44	0.44	0.45	0.45	0.45	0.46	0.47	0.59	0.80	0.80

Table A.1. Reconstruction of the time resolved fluorescence transients.

the steady-state fluorescence spectrum at a given wavelength. This step is illustrated in Fig. A.1.

8. Repeat step 7 for all of the fluorescence transients. Hence, you should have a c_λ for every wavelength for which a fluorescence transient was collected.
9. Multiply c_λ obtained from step 7 by the reconstructed fluorescence transients obtained in step 5.
10. The time evolving fluorescence spectrum can now be calculated as shown in Table A.2 and Fig. A.2.
11. Fit the time resolved fluorescence spectra to a lognormal function.
12. The solvent response function, C(t), is calculated via the following equation

$$C(t) = \frac{\nu(t) - \nu(\infty)}{\nu(t) - \nu(0)} \qquad \text{(A.6)}$$

where $\nu(t)$ is the peak frequency obtained from step 11 for a given time, $\nu(0)$ is obtained from time zero analysis as described in chapter 2, and $\nu(\infty)$ is the peak frequency of the steady-state fluorescence spectrum obtained in step 6.

13. Fit the solvent response function to an exponential as shown:

$$y = \sum a_n \exp(-x/t_n) \qquad \text{(A.7)}$$

An example solvent response is shown in Fig A.3

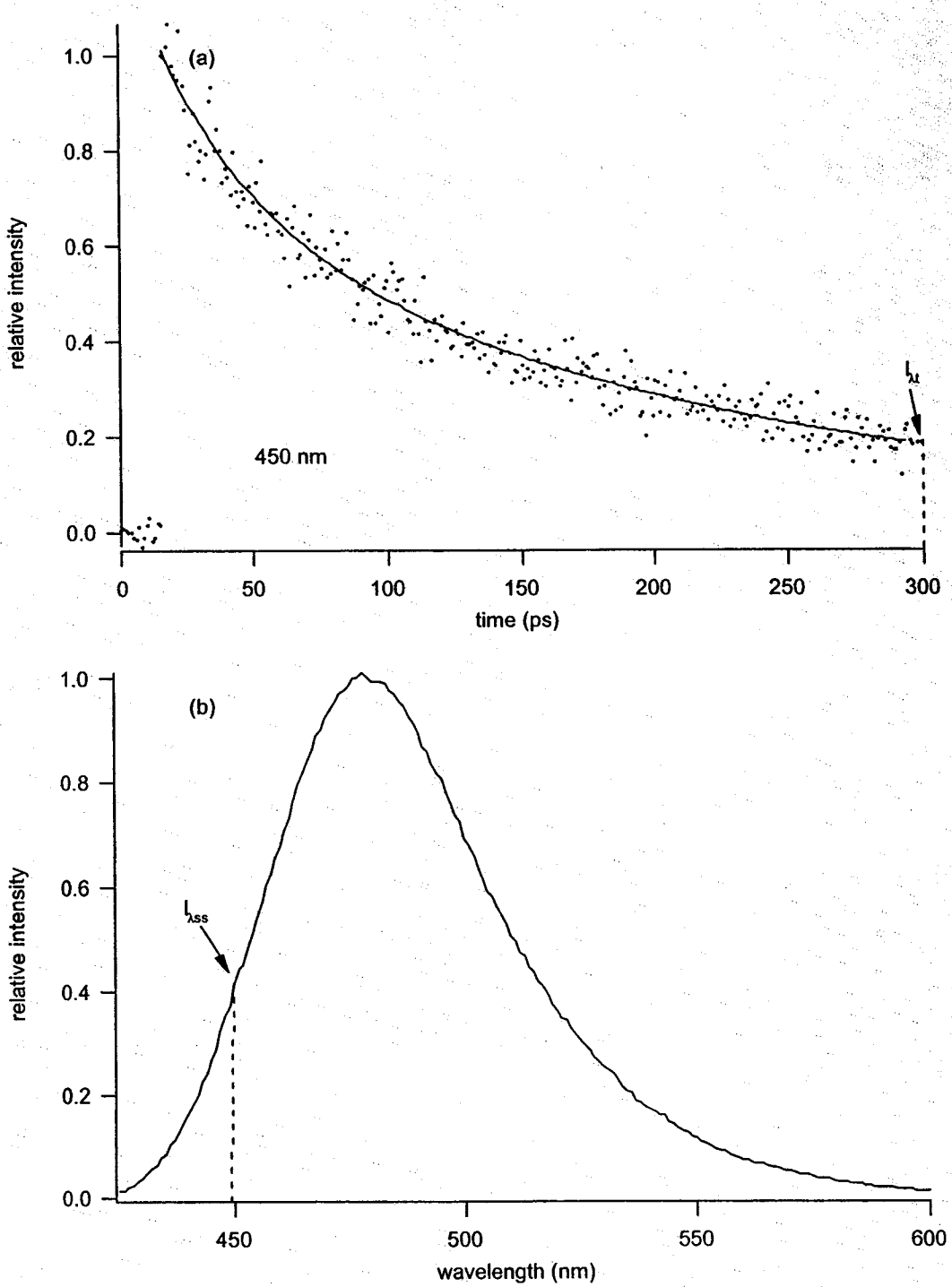

Figure A.1. (a). 450 nm time resolved fluorescence transient. (b) steady-state fluorescence spectrum.

Wavelength (nm)	0.033	0.067	0.1	1	2	3	4	5	10	50	100	500	$C_{\lambda t}$	$I_{\lambda ss}$
440	2.08	2.07	2.05	1.67	1.35	1.12	0.94	0.80	0.49	0.34	0.27	0.14	0.45	0.14
450	1.11	1.11	1.11	1.10	1.10	1.09	1.08	1.08	1.05	0.90	0.79	0.39	1.18	0.39
460	1.80	1.80	1.80	1.79	1.78	1.77	1.76	1.75	1.70	1.45	1.22	0.68	1.24	0.68
470	1.61	1.61	1.61	1.60	1.60	1.60	1.60	1.59	1.58	1.49	1.39	0.90	1.60	0.90
480	1.38	1.38	1.38	1.37	1.37	1.37	1.37	1.37	1.36	1.29	1.24	0.95	1.50	0.95
490	0.98	0.98	0.98	0.98	0.98	0.98	0.98	0.98	0.98	1.00	0.98	0.85	1.24	0.85
500	0.78	0.78	0.78	0.78	0.78	0.79	0.79	0.79	0.79	0.80	0.79	0.67	0.90	0.67
510	0.59	0.59	0.59	0.59	0.59	0.59	0.59	0.59	0.59	0.60	0.59	0.48	0.70	0.48
520	0.26	0.26	0.26	0.26	0.26	0.26	0.26	0.26	0.26	0.27	0.28	0.32	0.38	0.32
530	0.14	0.14	0.14	0.14	0.15	0.15	0.15	0.15	0.15	0.15	0.18	0.21	0.26	0.21

Table A.2. Numerical values for spectral reconstruction.

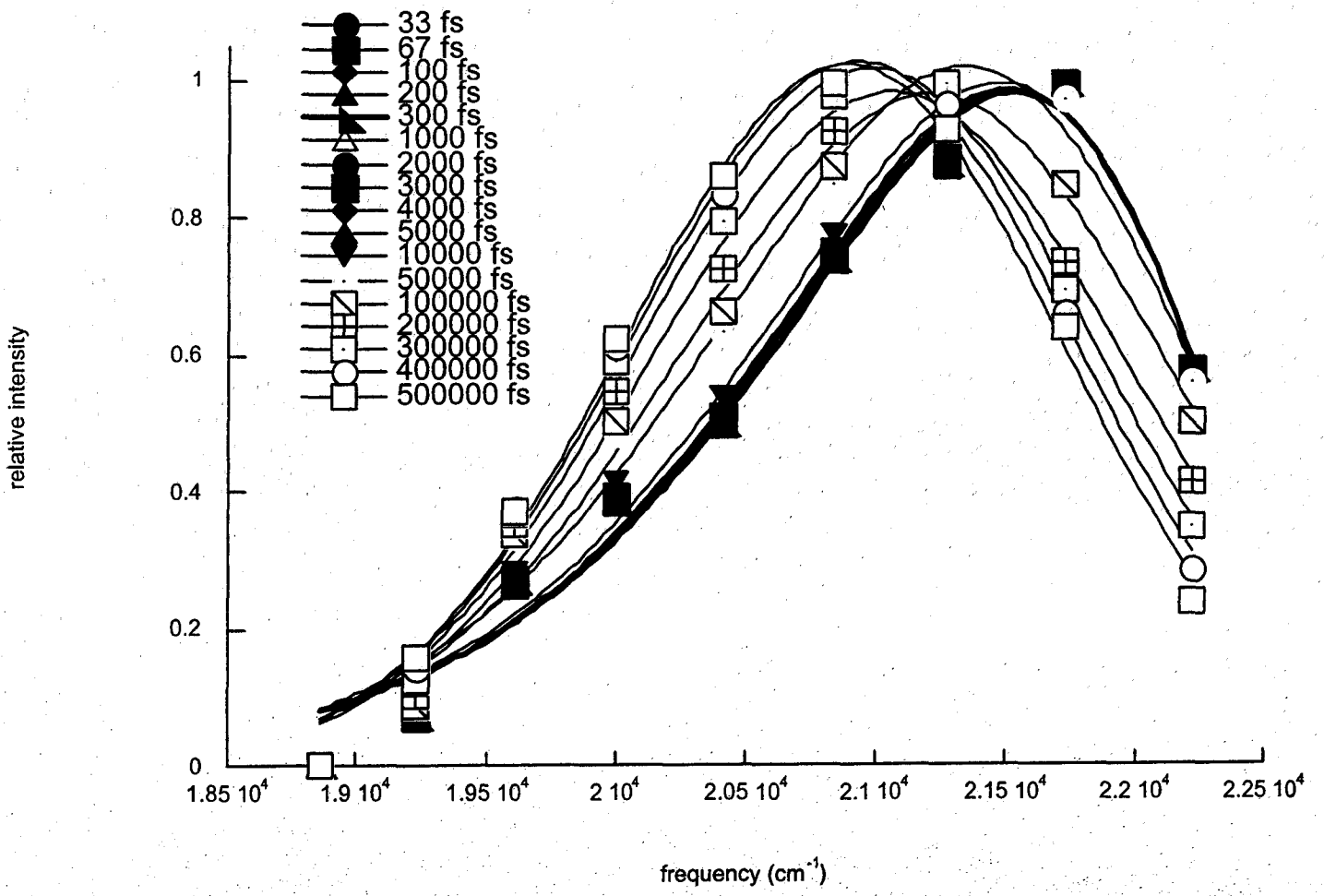

Figure A.2. Time resolved spectra for CTAB/1-heptanol/cyclohexane/water $w_0=10$.

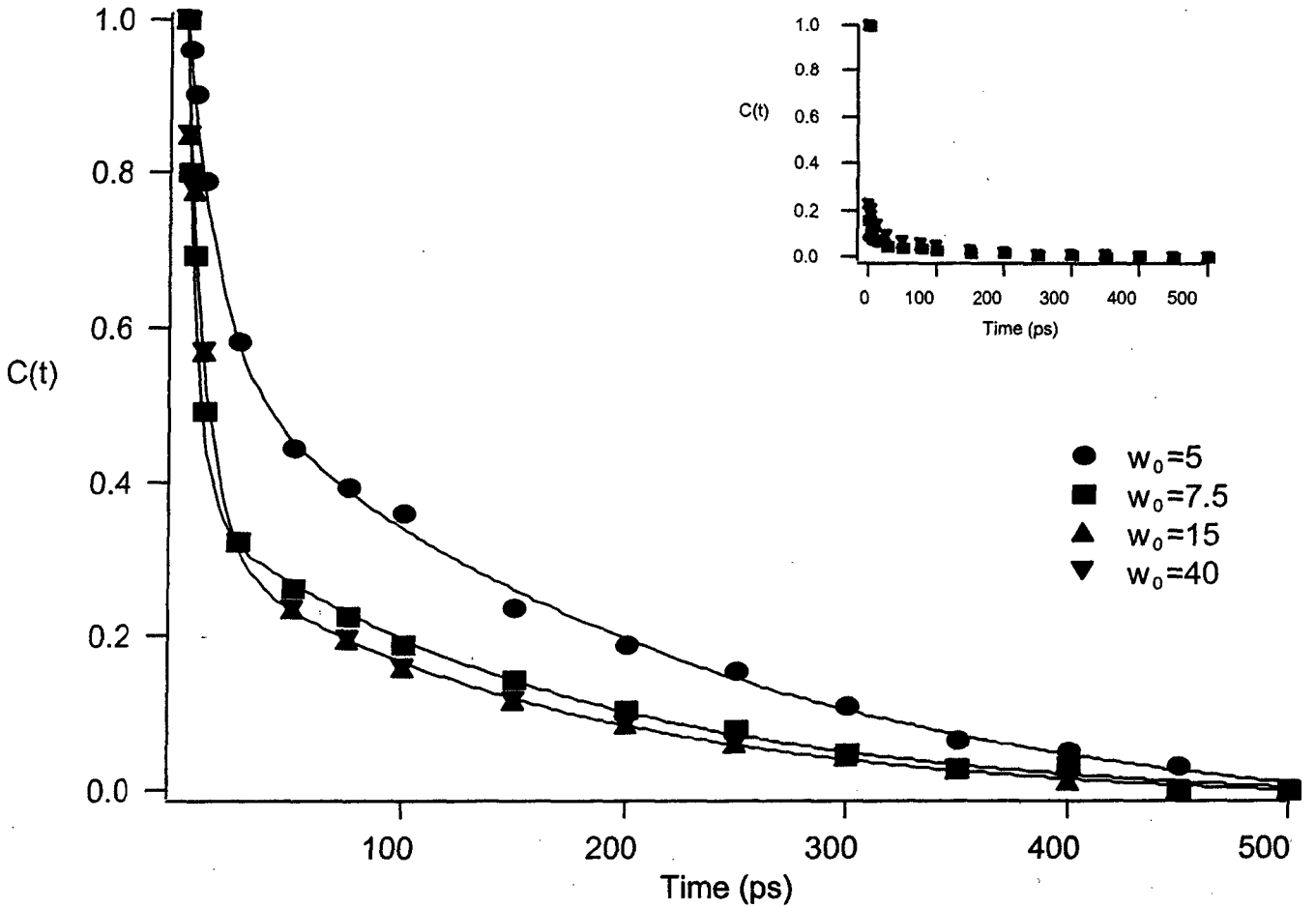

Figure A.3. Solvent correlation function, C(t), and multiexponential fits for AOT/isooctane/water. Inset. Solvent correlation function including point obtained from time zero analysis.